Fetal splanchnic arteries

A longitudinal study and hemodynamic relations to common Doppler parameters

Cathrine Ebbing

Dissertation for the degree philosophiae doctor (PhD)

at the University of Bergen

2008

ISBN 978-82-308-0565-7
Bergen, Norway 2008

Printed by Allkopi Ph: +47 55 54 49 40

Fetal splanchnic arteries

A longitudinal study and hemodynamic relations to common Doppler parameters

Cathrine Ebbing

Clinical Fetal Physiology Research Group, Department of Clinical Medicine, University of Bergen

and

Department of Obstetrics and Gynecology, Haukeland University Hospital, Bergen, Norway

Contents

Acknowledgements

This work has been carried out at the Section for Fetal Medicine and Ultrasound Diagnostics, Department of Obstetrics and Gynecology, Haukeland University Hospital and the Department of Clinical Medicine, University of Bergen. I have received a research fellowship from the Western Norway Regional Health Authority from March 2005 to June 2008. I thank the L. Meltzer Høyskolefond and the Norwegian Society for Perinatal Medicine for financial support.

My primary supervisor, Professor Torvid Kiserud, introduced me to fetal medicine. His genuine curiosity, vast knowledge, impressive enthusiasm and creativity inspired me to enter clinical research. I am greatly indebted to him for his constructive criticism, support and encouragement during these years.

Professor Svein Rasmussen, my second supervisor, generously and patiently shared his skills and insight into advanced statistics. His contributions to this work have been invaluable.

My collaborators and co-authors at the Centre for Developmental Origins of Health and Disease in Southampton, United Kingdom, Mark A. Hanson and Keith M. Godfrey, brought new valuable aspects into the discussions and shared their expertise in the publication process.

Through the years, my colleagues Synnøve Lian Johnsen and Jörg Kessler backed me up when needed, shared their experience and offered their sincere friendship.

I acknowledge my colleagues at the Section for Fetal Medicine and Ultrasound Diagnostics and Department of Obstetrics and Gynecology for taking the time and effort to inform me about eligible participants and for their positive attitude towards my work.

The Department of Obstetrics and Gynecology, Haukeland University Hospital provided excellent infrastructure and working conditions for me in course of the study.

The friendly staff at the Section for Fetal Medicine and Ultrasound Diagnostics made the everyday logistics function smoothly.

I am indebted to all the pregnant women who unconditionally and enthusiastically participated in the study, allowing me to use several hours of their time.

I am privileged to have a family and loyal friends who take an interest in my work but, more importantly, take me as I am. Thank you all!

My dearest Peter, Thea and Jacob; you are the joy of my life!

Bergen, February 2008

Cathrine Ebbing

Abbreviations

CA	celiac artery
CI	confidence interval
CCO	combined cardiac output
D	diameter
DV	ductus venosus
h	velocity profile factor
HA	hepatic artery
HABR	hepatic artery buffer response
IUGR	intrauterine growth restriction
IVC	inferior vena cava
LPV	left portal vein
max	maximum
MCA	middle cerebral artery
PI	pulsatility index
PV	portal vein
Q	volume of blood flow
SA	splenic artery
SD	standard deviation
SMA	superior mesenteric artery
UA	umbilical artery
UV	umbilical vein
V_{ps}	peak systolic velocity
V_{tamx}	time-averaged maximum velocity

Abstract

Although the arterial splanchnic circulation is known to be dynamic and of clinical interest during postnatal life, little is known about its prenatal development and function. We hypothesised that current ultrasound technology allows standardised techniques and reference ranges to be established and the dynamics of this section of the fetal circulation to be studied.

Aims: The aims of the study were 1) to establish reproducible ultrasound techniques for assessing the fetal celiac, hepatic, splenic and superior mesenteric arteries and longitudinal reference ranges for flow velocity and pulsatility index, 2) to address the hemodynamic relationships between these arteries and the umbilical liver perfusion under physiological conditions and how these arteries are related to the cerebral and umbilical circulation and 3) to establish longitudinal reference ranges for the middle cerebral artery and the cerebroplacental ratio.

Material and methods: We recruited 27 women with low-risk pregnancies to the pilot study establishing insonation techniques and a further 161 for a longitudinal study, all after we obtained written consent. In the longitudinal study, we scheduled the participants for ultrasound examinations 3–5 times during the second half of pregnancy, each session lasting a maximum of 1 hour. The Doppler assessment included the middle cerebral and umbilical artery, the celiac, hepatic, splenic and superior mesenteric arteries, the left portal vein, the umbilical vein and the ductus venosus. We carried out fetal biometry each time. The ductus venosus peak velocity represented the port-caval pressure gradient, and the velocity in the left portal vein reflected the distribution of umbilical blood within the fetal liver. Means and centiles were constructed using multi-level modelling. We assessed the relationships between splanchnic arteries using Pearson's correlation coefficients, and the relationship with the umbilical liver perfusion and the pulsatility index of the cerebral and umbilical arteries was assessed using deviance statistics.

Results: We established the interrogation of the left branch as our standard for the Doppler assessment of the hepatic artery since this technique minimised interference from neighbouring vessels and established longitudinal reference ranges. We showed that low port-caval pressure was associated with low impedance in the hepatic artery, supporting the assumption that the hepatic artery buffer response also operates in the fetus (Article I). We also established longitudinal reference ranges for the celiac and splenic arteries and provided terms for conditional ranges for repeat measurements. Splenic and celiac arteries showed compensatory mechanisms supporting the portal perfusion of the fetal liver: low umbilical perfusion and port-caval pressure were linked to splenic and celiac artery vasodilation (Article II). Along the same lines, we established longitudinal reference ranges for the superior mesenteric artery and demonstrated a link to the port-caval pressure and venous liver perfusion (Article III). However, there was limited correlation between the pulsatility index of the branches from the celiac artery and the pulsatility index of the superior mesenteric artery, suggesting largely independent local regulation (Articles II and III). The longitudinal reference ranges established for the middle cerebral artery and cerebroplacental ratio differed from those derived from cross-sectional data (Article IV). Further, the conditional ranges assigned for serial measurements are narrower and shifted compared with the ranges for the entire population (Articles II–IV). The covariation of the umbilical and cerebral arteries with the celiac, splenic and superior mesenteric arteries indicates additional common determinants for these circuits (Articles II and III).

Conclusions: We provide longitudinal reference ranges for the upper splanchnic and middle cerebral arteries and the cerebroplacental ratio and terms for conditional mean and ranges suitable for serial measurements. The development of these ranges indicates increased perfusion of the splanchnic tissues towards the end of pregnancy. Our study suggests that the hepatic artery buffer response is operating in the fetus and that the splenic and superior mesenteric arteries, by feeding the portal vein through a distended vasculature, also support the fetal liver perfusion. Although locally these splanchnic arteries operate independently, they also seem to be under common influence with the cerebral and umbilical circulation.

What is already known on this topic	What this study adds
Article I	
During postnatal life the portal vein is the only source of venous liver perfusion; prenatally, 80 % is of umbilical origin.	A standardised measurement technique for Doppler assessment of the fetal hepatic artery. Reference ranges for the left hepatic artery flow velocities and pulsatility index.
The hepatic artery buffer response is important in maintaining liver perfusion in postnatal life.	The hepatic artery buffer response seems to operate in the human fetus: low arterial impedance is seen at low venous perfusion and port-caval pressures.
Studies of growth restricted fetuses have shown increased hepatic arterial involvement.	
Article II	
The celiac artery gives of branches to supply the liver, spleen, pancreas and proximal gut.	A standardised measurement technique for the celiac artery, longitudinal reference ranges for the celiac and splenic artery Doppler assessment, and conditional terms for serial measurements in the fetal surveillance. The hepatic and splenic branches from the celiac artery seem to be largely independently regulated in non-compromised fetuses. The celiac and splenic artery hemodynamics is functionally linked to the port-caval pressure gradient and umbilical venous liver perfusion: low arterial impedance is seen at low port-caval pressures and perfusion. The celiac and splenic artery hemodynamics co-varies with the cerebral and umbilical circulation, suggesting common hemodynamic determinants.
The spleen grows linearly throughout gestation, is involved in hematopoiesis and has a high degree of adrenergic innervation.	
Studies of fetuses with intrauterine growth restriction show a low pulsatility index in the splenic artery, whereas high systolic velocity in the splenic artery is predictive of anemia.	
After birth drainage of the splenic vascular bed is a major contributor to portal flow.	
Article III	
In postnatal life, the superior mesenteric artery is an important and responsive section of circulation. Increased impedance and low flow velocity prenatally seems to increase the risk of necrotising enterocolitis.	Longitudinal reference ranges for the fetal superior mesenteric artery Doppler assessment. The superior mesenteric artery is functionally linked to the port-caval pressure gradient as well as the internal distribution of umbilical blood in the fetal liver. The hemodynamics of the superior mesenteric artery covaries with the cerebral and umbilical circulation, suggesting influence of general circulatory determinants. The local regulation of the celiac branches and the superior mesenteric artery seems largely independent from each other, all aimed at maintaining an even hepatic perfusion in the fetus.
Portal flow increases throughout gestation, and the superior mesenteric artery vascular bed is an important contributor to the portal venous flow.	
Current cross-sectional reference ranges for the pulsatility index in the fetal superior mesenteric artery are based on few observations.	
Article IV	
Doppler assessment of the middle cerebral artery is used in the hemodynamic surveillance of fetuses at risk for anemia or growth restriction. The combined cerebroplacental pulsatility ratio predicts perinatal outcome better that the pulsatility index in the umbilical or middle cerebral artery alone.	Longitudinal reference ranges for middle cerebral artery flow velocities and pulsatility index, and the cerebroplacental pulsatility ratio. Terms for conditional mean and ranges suitable for serial measurements in clinical monitoring.

List of articles

This dissertation is based on the following articles:

I: Ebbing C, Rasmussen S, Godfrey KM, Hanson MA, Kiserud T. Hepatic artery hemodynamics suggest operation of a buffer response in the human fetus. *Reproductive Sciences* 2008;15:166–178.

II: Ebbing C, Rasmussen S, Godfrey KM, Hanson MA, Kiserud T. Fetal celiac and splenic artery flow velocities and pulsatility index: longitudinal reference ranges and evidence for vasodilation at a low porto-caval pressure gradient. In press, *Ultrasound in Obstetrics and Gynecology*.

III: Ebbing C, Rasmussen S, Godfrey KM, Hanson MA, Kiserud T. Fetal superior mesenteric artery: longitudinal reference ranges and evidence of regulatory link to portal liver circulation. Submitted 2008.

IV: Ebbing C, Rasmussen S, Kiserud T. Middle cerebral artery blood flow velocities and pulsatility index and the cerebroplacental pulsatility ratio: longitudinal reference ranges and terms for serial measurements. *Ultrasound in Obstetrics and Gynecology* 2007;30:287–296.

1. Introduction

A short history of fetal physiology

The discipline of modern fetal physiology started in the 1920s with studies of fetal sheep. In the 1930s, the problem of the course of the fetal circulation was solved by using radiological methods (Barclay et al. 1945). The first studies were performed on exteriorised fetuses, and fetal and placental growth, development and composition were the main issues explored. In the 1950s, fetal physiologists started to cooperate with clinicians in the field of perinatal medicine. The discovery that the growth of the trunk and limbs occurred independently of growth hormone secreted from the central nervous system was the beginning of fetal endocrinology, and fetal intraperitoneal infusion of red cells for treating rhesus disease was the beginning of fetal medicine (Dawes 1994).

During the 1960s and 1970s, Rudolph and colleagues measured systemic blood flow and cardiac output using isotope-labeled microspheres in fetal lambs (Rudolph and Heymann 1967). Their findings were corroborated recently by Doppler-ultrasound studies, allowing studies of the human fetus in its protected environment. Although newer research increasingly details the human version of fetal physiology, experimental animal studies have provided a substantial body of understanding. Nevertheless, these results may not always be transferable to human physiology. The present study is another contribution to the human fetal research in this field.

Everyday clinical perinatal medicine applies in practice the results of fetal physiology research, such as continuous positive airway pressure, dexamethasone, Doppler and ultrasound monitoring. The last decade has shown that the fetal environment influences the risk of disease later in life: individuals with low birth weight are at increased risk of cardiovascular disease and type 2 diabetes (Barker and Hanson 2004). The developmental origin of health and disease hypotheses has brought new aspects to the research in fetal physiology.

1.1 Fetal splanchnic development

1.1.1 Gut

The gastrointestinal tract develops from the primitive digestive tube, which is derived from the dorsal intraembryonic portion of the yolk sac. The primitive digestive tube consists primarily of endodermal cells. Three major arteries supply the digestive tube: the celiac artery (CA) supplies the foregut (oropharynx - duodenum), the superior mesenteric artery (SMA) the midgut (distal duodenum -distal third of the colon transversum) and the inferior mesenteric artery the hindgut (distal colon and rectum) (Figure 1). The midgut opens ventrally into the yolk sac, and the cranial end of the midgut elongates more rapidly than the embryonic body itself, which leads to a physiological umbilical herniation. The apex of the loop entering the yolk sac is directly in line with the mesenteric artery (the omphalomesenteric duct) (Sadler 1985a). Following the ventral herniation, a counterclockwise rotation around the SMA begins, and at 10 weeks the bowel starts its return to the embryonic abdominal cavity. The prearterial segment enters first and consequently posterior to the SMA, while the cecum and colon enters last and in front of the SMA (Clark and Munshi 2004).

At 10–11 weeks of gestation, swallowing begins. Ingestion of amniotic material is important for the growth and development of the gastrointestinal tract. The fetus ingests 300–1000 ml of amniotic fluid per day, and it is suggested that 60–70% of the protein in the amniotic fluid is turned over every day, which accounts for 15–20% of total body protein deposition in fetal sheep (Trahair 2001). The gut tissues derive a significant part of their nutrition from locally absorbed substances, but global fetal growth is also reduced by the obstruction of fetal digestion (Cozzi and Wilkinson 1969). When the composition of the swallowed fluid is altered, body allometry is also changed (Trahair and Sangild 2000), indicating that ingestion is also

important before birth. The entire surface of the intestines is constantly being shed and replaced in 3- to 5-day cycles, and the fetal enterocyte uptake and transport of luminal material are crucial for the local metabolism.

Towards the end of pregnancy, the gut must be prepared to face the change in diet, and the hypothalamic-pituitary-adrenal axis, which is involved in the complex cascade leading to parturition, is also involved in the maturation of the enterocytes (Burrin 2004).

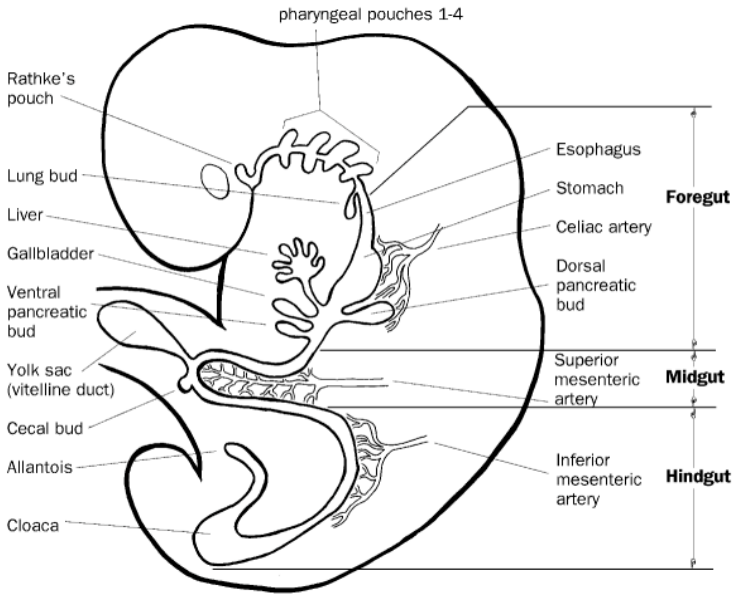

Figure 1. The primitive digestive tract. Source: www.med.umich.edu/lrc/coursepages/M1/embryology/embryo/10digestivesystem.htm, with kind permission from Professor Tom Gest.

1.1.2 Liver

During the third or fourth week of gestation, a liver bud constituting of proliferative tissue originates from the ventral foregut (Figure 1). In the liver bud, hepatoblasts differentiate into either hepatocytes or cholangiocytes, and these cells are intermingled by precursors of endothelial cells. The endothelial cells, hematopoietic cells and connective tissue of the liver are derived from the mesoderm of the septum transversum, which later forms part of the diaphragm. The Kuppfer cells originate from the yolk sac and bone marrow (Lobritto 2004).

The vitelline veins that drain the yolk sac fuse to form a plexus around the proximal bowel and are the initial sources of sinusoidal blood. This plexus later becomes the portal vein (PV). The vessels developing in the connecting stalk to the chorionic plate are the umbilical veins (UV). Initially (<5 weeks) they pass on each side into the liver, where they communicate with the vitelline sinusoids. At a later stage (7 weeks) the right UV atrophies and disappears and the left UV remains patent throughout gestation and carries blood from the placenta (chorion) and empties into the hepatic sinusoids. The UV and vitelline vein are connected to the hepatic sinusoids through veins that develop into the intrahepatic PV. The left branch of the PV connects to the UV via the portal sinus.

The PV enters the liver and branches into smaller and smaller vessels that travel along with small branches of the hepatic artery (HA) and the bile ducts in the portal tracts, eventually emptying into the hepatic sinusoids (Sadler 1985b).

The current hypothesis for hepatic development and vasculogenesis is that vessel anatomy does not follow a predetermined pattern but is instead guided by local needs and flow dynamics during gestational weeks 10–25, controlled by vascular endothelial growth factors. Recent reports (Weinstein 2002; Lammert et al. 2003) show that endothelial cells induce essential steps in organ formation and cell differentiation. Vascular differentiation results in the development of the arteries and capillaries on the arterial side and PV and hepatic sinusoids on the venous side. After 25 weeks, only small changes in vascular architecture and differentiation are observed (Gouysse et al. 2002).

In contrast, the cellular architecture of the liver develops until 5 years of age (Horst and Karpen 2004). The functional unit of the liver is the hepatic lobule with one central vein. Portal triads consisting of a PV, HA and bile duct form the corners of the hexagonal lobule, and each lobule contains plates of hepatocytes and between them the hepatic sinusoids that carry a mixture of blood of portal and arterial origin and drain into the central vein. The direction of blood flow in the lobule is toward the

central vein, which eventually empties into the hepatic veins, while the direction of bile flow in the lobule is the opposite, toward the bile duct.

The fetal liver has a prominent role in regulating growth (Tchirikov et al. 2001, 2002). Its blood supply is unique since it derives from three sources: the UV and PV and the HA. The fetal liver differentiates from being an essential hematopoietic organ to a hepatopoietic organ during the second trimester (Nava et al. 2005). It is the main site for hematopoiesis until the end of the second trimester, when a shift to the bone marrow occurs (Mikkola et al. 2005). Both liver growth and hematopoiesis seem to be affected by its perfusion (McLellan et al. 1995; Rocheleau et al. 1999; Tchirikov et al. 2001, 2002; Kunisaki et al. 2006).

1.1.3 Spleen

During the fifth week of gestation, a mesodermal primordium of the spleen appears posterior to the developing stomach. Similar to the liver, differentiation of the constituents in the fetal spleen is closely related to the development and differentiation of the vascular tree. A characteristic organ structure becomes evident from 15 weeks onwards when the splenic lobules are formed. Each lobule has a central artery, and the red pulp develops in the periphery of these lobules (Vellguth et al. 1985).

Erythrocytes, their precursors and numerous thrombocytes are recognized in the red pulp of the spleen, which is involved in clearing the blood and possibly erythropoiesis or hematopoiesis. Later (gestational weeks 17–24), the white pulp develops around the central arteries and increases in size at the expense of the red pulp until the compartments are of equal size at 24 weeks (Vellguth et al. 1985). In contrast, the red pulp comprises 75–80% of the volume of the postnatal spleen.

The white pulp is the lymphoid compartment of the spleen, and during the third trimester immunoglobulin G and M are synthesised there.

Recent data on the ontogeny of intrinsic innervation in the human fetal spleen describe a mainly sympathetic noradrenergic innervation with a perivascular distribution of the nerves, increasing in density during gestation. This suggests an increasing role of the sympathetic nervous system in blood flow control, lymphocyte traffic and maturation of the immune system (Anagnostou et al. 2007).

The spleen functions in the interface of the circulatory and the immune systems, and it grows linearly in the second half of pregnancy (Aoki et al. 1992; Oepkes et al. 1993). After birth, it has dual roles in maintenance and adaptation to stress and disease. The red pulp filters and removes senescent or defective red blood cells and antibody-coated bacteria in the circulation. The white pulp is the lymphoid compartment, produces antibodies against invading pathogens and releases platelets and neutrophils in response to bleeding or infection.

The adult spleen is also a site for extramedullary hematopoiesis when the bone marrow cannot fulfil the demand in times of stress and disease, whereas the fetal spleen as a site for hematopoiesis has been debated (Wolf et al. 1983; Vellguth et al. 1985; Chadburn 2000). However, newer studies have concluded that the major site of hematopoiesis transitions from the fetal liver to the spleen and bone marrow late in fetal development (Christensen et al. 2004; Cumano and Godin 2007). Hematopoietic stem cells circulate from the fetal liver to the spleen, and hematopoietic differentiation occurs there (Cumano and Godin 2007).

1.2 Fetal circulation

General aspects

The fetal circulation displays specific features: the placental circuit with the umbilical arteries (UA) and vein(s) connecting the fetus and the placenta and the three fetal shunts, the ductus venosus (DV), the foramen ovale and the ductus arteriosus (or rather the aortic isthmus)).

The UA originate from the fetal internal iliac arteries and return one third of the cardiac output (one fifth after 32 weeks) to the placenta (Rudolph et al. 1971; Sutton et al. 1991; Kiserud et al. 2006a). The placental vasculature is compliant and relatively non-responsive, and the placental compartment constitutes a large blood volume.

The right and left sides of the fetal heart work in parallel, and the right ventricular output, supplying the lungs, placenta and lower part of the body, is larger than the left cardiac output (supplying the heart, brain and upper body) (Mielke and Benda 2001; Kiserud et al. 2006a). The combined cardiac output (CCO) increases throughout gestation but is unchanged when normalised for fetal weight (Mielke and Benda 2001; Kiserud et al. 2006a). There is no pressure difference between the ventricles, and the ventricular pressure increases during gestation (Johnson et al. 2000).

The ductus arteriosus connects the pulmonary trunk with the descending aorta. Low-oxygenated blood from the right ventricle enters the descending aorta to mix with blood from the left ventricle. The aortic isthmus is located between the origin of the left subclavian artery and the aortic end of the ductus arteriosus and establishes communication between the aortic and pulmonary arches (Fouron 2003).

Arterial pressure is an important determinant of blood flow. The systolic and diastolic pressure increases linearly throughout gestation (Johnson et al. 2000), mean arterial pressure from 15 mmHg at mid-gestation to 40–50 mmHg at term. The blood pressure and ability to change it depend on such cardiac features as size and myocardial contractility but also peripheral vascular resistance. Resistance to flow depends on vessel diameter and blood viscosity, especially in the segments of the circulation with low flow velocity.

1.2.1 The umbilical and left portal vein and the ductus venosus

The UV returns nutrient-rich oxygenated blood from the placenta to the fetal body, and the fetal liver has the highest priority, taking 75–80% of it (Bellotti et al. 2000; Kiserud et al. 2000).

The DV is a shunt connecting the UV to the inferior vena cava (IVC) close to the atrial inlet and directs oxygenated UV blood towards the foramen ovale and the central circulation. Thirty percent of the umbilical flow (20% near term) is shunted through the DV (Bellotti et al. 2000; Kiserud et al. 2000). The DV flow is influenced by blood viscosity and pressure, stimulation by alpha-adrenergic substances or endothelin induces DV constriction, while beta-adrenergic stimulation, nitrogen monoxide and prostaglandins induce vasodilation of the DV (Coceani and Olley 1988; Kiserud et al. 2000; Tchirikov et al. 2003, 2005). During experimental hypoxia and hypovolemia, the DV shunting fraction increases (Edelstone et al. 1980), and an increased degree of shunting is seen in fetuses with placental compromise and intrauterine growth restriction (IUGR) (Tchirikov et al. 1998; Bellotti et al. 2004; Kiserud et al. 2006b).

The umbilical pressure in the human fetus is 2–11 mmHg, and the portal perfusion pressure has been calculated to vary between 0.5 and 3.5 mmHg during the heart cycle (Kiserud et al. 1994a; Ville et al. 1994). The blood flow velocity in the DV connecting the intra-abdominal UV to the IVC is an indicator of the port-caval pressure gradient that perfuses the liver tissue. The simplified Bernoulli equation is suggested for estimating the pressure gradient (Δp: in mmHg) based on the peak systolic velocity in the DV (V_{DVps}) and the maximum velocity in the UV (V_{UVmax}) (Kiserud et al. 1994a):

$$\Delta p = 4((V_{DVps})^2 - (V_{UVmax})^2).$$

The left portal vein (LPV) connects the umbilical with the portal circulation (Figure 5), and the flow velocity in the LPV directly reflects UV supply to the right

liver lobe (Kessler et al. 2007a). The flow is orthograde during the second half of pregnancy, but reversal is a normal phenomenon during fetal respiratory movements.

The oxygen saturation in the UV blood is 80–90% at mid-gestation and approximately 70% at term (Weiner 1990). Oxygenated blood is shunted through the DV from the UV and runs through the foramen ovale to the left atrium, left ventricle and aortic arch, ensuring a steady supply of highly oxygenated blood to the heart and brain. Spillover of the shunted UV blood to the foramen ovale and low oxygen extraction in the liver makes the difference in oxygen saturation between the right and left ventricle relatively small (10–12%) (Rudolph 1985).

1.2.2 Arterial circulation

The most fundamental principle of cardiovascular regulation has traditionally been that it should match each tissue's blood flow to its metabolic demands. Blood flow in the various organs is mainly regulated by altering vessel diameter, mediated by pressure or neural, hormonal or metabolic influence on the vascular musculature. The capacity to sustain the perfusion of an organ when blood pressure or cardiac output is altered depends on the ability for autoregulation and the responses to neural and hormonal stimuli. These responses and capacities are a function of the gestational maturation of the various vascular beds.

The sympathetic nervous system is the main mediator of the neural control of blood vessels (arterioles). Increased sympathetic tone induces vasoconstriction in peripheral beds such as the skin, carcass and gut. In contrast, it causes vasodilation and increased blood flow in the heart, brain and adrenal glands. The change in the distribution of the cardiac output to the various vascular beds is called redistribution.

Local control of the circulation, autoregulation, has two functions: keeping the blood flow constant in the face of changes in blood pressure and adapting blood flow in the organ to local changes in metabolism independently of the blood pressure. The mechanisms of autoregulation are: myogenic effect (vasoconstriction response to an

increase in blood pressure), local metabolic (vasodilator response to low O_2 and increased concentration of metabolites) and vasoactive substances (Despopoulos and Silbernagl 1986; Greisen 2005). Local control may include changes in the microcirculatory bed to enhance oxygen extraction (local redistribution).

Adaptation to acute hypovolemia and hypoxia is distinguished from responses to chronic challenges. Increased adrenergic tone (α- and β-adrenergic) is both an acute and a chronic response, while the humoral agents are likely to be more important in the response to prolonged hypoxia. The ability to regulate may be impaired after sustained hypoxia or hypovolemia (Bristow et al. 1985).

The heart, brain, intestine and kidney have highly efficient autoregulation mechanisms, and splanchnic organs and kidneys have extensive autonomic innervation. Recent experimental research has revealed that the liver has a highly specialized system for regulating intrahepatic blood volume and flow. The portal perfusion is a key component in the intrinsic regulation of the HA (Lautt 2007).

1.2.3 Umbilical arteries

The UA coil around the UV in a clockwise manner (90%) to enter the placenta (Figure 2). In 95% of the cases, the UA communicate near the placental end through the Hyrtl anastomoses. This communication is likely to equalize pressure and blood flow of the two UA (Raio et al. 2001).

The UA return deoxygenated blood from the fetus to the placenta. In the human fetus, the umbilical/CCO flow fraction is estimated to be approximately 30% (Rudolph et al. 1971; Sutton et al. 1991) before 32 weeks and declines to 20% beyond 32 weeks (Kiserud et al. 2006a). This implies an increased degree of recirculation of blood within the fetal body towards term (Kiserud et al. 2006a).

The UAs are readily assessable for Doppler interrogation. In the placenta, increased vascularization (through increased number and reduced size of the placental villi) decreases the downstream impedance of the UA towards term. This is reflected

in the linear decline in the pulsatility index (PI) of the UA through gestation (Gudmundsson and Marsal 1988; Acharya et al. 2005a). The PI is a measure of the systolic-diastolic differential of the velocity pulse:
PI = peak systolic velocity - end diastolic velocity/ time averaged maximum velocity) (Gosling and King 1975).

The blood flow velocities increase towards term and is positively correlated with the volume of blood flow as measured in the UV (Acharya et al. 2005b). Especially the diastolic flow velocity rises as gestation advances (Stuart et al. 1980), resulting in the observed decline in PI towards term.

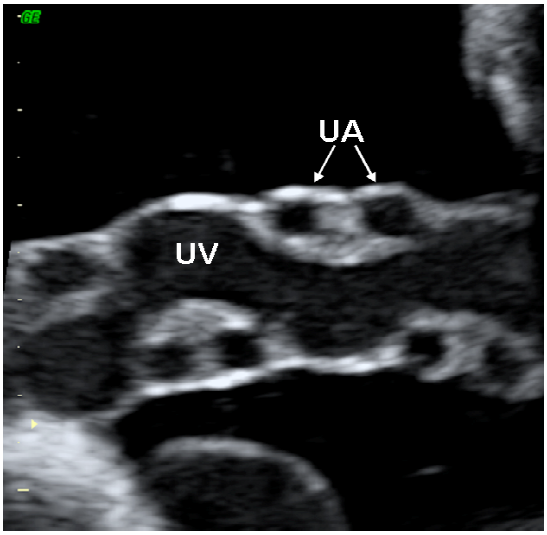

Figure 2. Ultrasound image of the umbilical cord. UA: umbilical arteries (arrows). UV: umbilical vein.

If placental growth and vascularisation is impaired, resulting in fetal growth restriction, an increase in resistance in the placental capillary bed and, accordingly, an increase in downstream impedance of the UA (increased PI) reflect the degree of pathology. A decline in UA diastolic velocity is seen when the capillary bed is reduced by 30%, and UA diastolic velocity is absent or reversed when the capillary bed is reduced by more than 50% (Figure 3) (Giles et al. 1985). Solid evidence indicates that Doppler assessment of the fetoplacental circulation via the UA is an important clinical monitoring tool for high-risk pregnancies (Alfirevic and Neilson 1995).

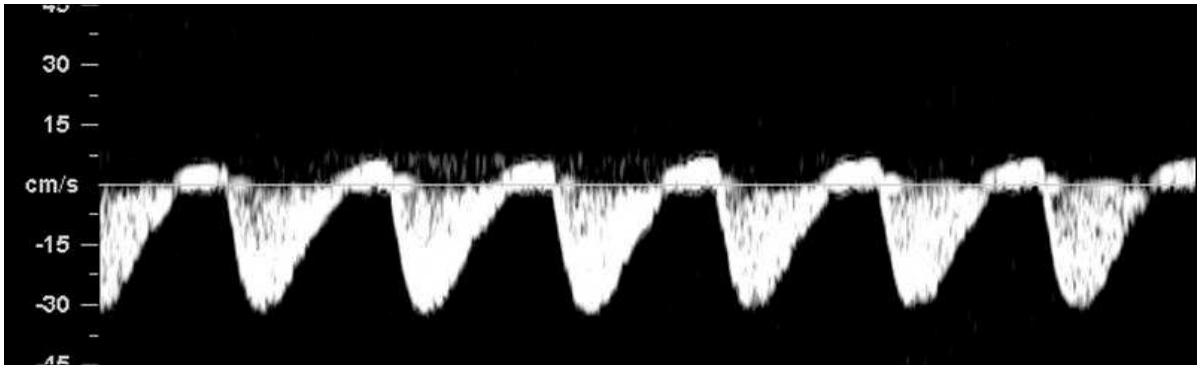

Figure 3. Doppler recording in the umbilical artery of a fetus (gestational age 29 weeks) with intrauterine growth restriction showing reversed diastolic velocity.

1.2.4 Middle cerebral artery

The middle cerebral artery (MCA) supplies 80% of the cerebrum, and under normoxic conditions near term 16% of the CCO is directed to the brain in monkeys (Behrman et al. 1970) versus only 3% in fetal sheep near term (Jensen et al. 1991). Autoregulation of cerebral blood flow is developed early in gestation (at 0.6–0.7 gestation in the fetal sheep) (Kurth and Wagerle 1992). Acute hypoxia promotes adenosine release, which causes vasodilation and depresses cerebral oxygen consumption (Pearce 2006). The vasodilator response to hypoxia varies with gestational age and is also heterogeneous among different brain regions.

Redistribution to the cerebral circulation is seen as a response to hypoxia (Jensen et al. 1991), and low PI_{MCA} is associated with low fetal pO_2 (Vyas et al. 1990). The effect is termed “brain-sparing”; an increase (especially) in the diastolic flow velocity and consequently reduced downstream vascular impedance (PI_{MCA}) as assessed by Doppler ultrasound (Wladimiroff et al. 1986). The brain-sparing effect has been shown to be transient in animal studies and preterminal human fetuses, presumably caused by the development of brain oedema (Richardson et al. 1989; Konje et al. 2001). Redistribution combined with IUGR is associated with an increased risk of brain lesions (Habek et al. 2004) and suboptimal nervous system development (Scherjon et al. 2000). The term brain-sparing may therefore be

misleading, as it is not only a beneficial adaptation but a necessary compensatory mechanism that may have long-term detrimental effects. A recent study showed that the cerebral resistance gradual declines with reduced growth, also before the stage of apparent growth restriction (Verburg et al. 2008).

The MCA is the cerebral vessel of choice for Doppler assessment (Figure 4). It is also suitable for assessing absolute velocity, since it may regularly be interrogated with an accurate insonation according to the direction of the vessel. Assessment of the flow velocity and PI of the MCA has become an integrated part of the monitoring of fetuses with placental compromise (Mari and Deter 1992) or anemia (Mari 2000). The peak systolic velocity of the MCA (V_{MCAps}) increases significantly and consistently in anemic fetuses. Reduced blood viscosity and increased cardiac output are thought to result in hyperkinetic circulation, while oxygen tension and partial pressure of CO_2 may also modify flow velocity by local vascular regulation (Pickelsheimer et al. 2007). In fetuses at risk for anemia, the V_{MCAps} correlates well with fetal hemoglobin obtained at cordocentesis, and the method has reduced the need for invasive testing for fetal anemia (Zimmermann et al. 2002). After 35 weeks of gestation, however, the method is not effective in predicting fetal anemia (Zimmermann et al. 2002) and V_{MCAps} has low predictive accuracy for anemia in IUGR fetuses (Makh et al. 2003). Other physiological adaptations may also result in high V_{MCAps}; it has been reported to predict poor outcome in IUGR fetuses (Hanif et al. 2007; Mari et al. 2007).

Assessing the PI_{MCA} in combination with the PI_{UA} in a common index (PI_{MCA}/PI_{UA}= cerebroplacental ratio) gives simultaneous information on fetal adaptation to placental circulation and has been shown to predict adverse outcome better than PI_{MCA} and PI_{UA} alone (Gramellini et al. 1992). A cerebral vasodilator response to increased placental resistance results in a shift between the right and left ventricular output in favour of the left caused by increased afterload of the right ventricle.

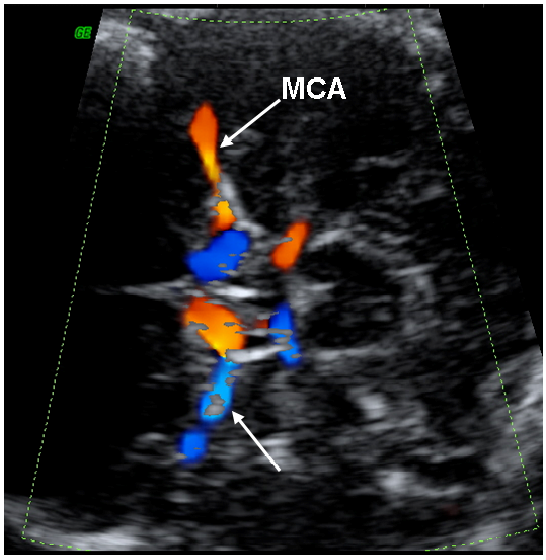

Figure 4. Colour Doppler image of the fetal circle of Willis (gestational age 29 weeks). Middle cerebral arteries (MCA) arrows.

1.2.5 Splanchnic arteries

The arterial blood supply to the gastrointestinal system has extra- and intramural components. The intramural systems have specialisation's (in the liver, spleen and intestine) adapted to the functions of these organs, and branches of the arteries form rich anastomotic systems (Geboes et al. 2001). There is more variation in the development of the venous drainage than in the arterial tree of the splanchnic organs. Experimental data suggest that, after birth, multiple interrelated mechanisms involving the splanchnic and renal circuits act to maintain central hemodynamics, portal pressure and liver perfusion (Lautt 2007).

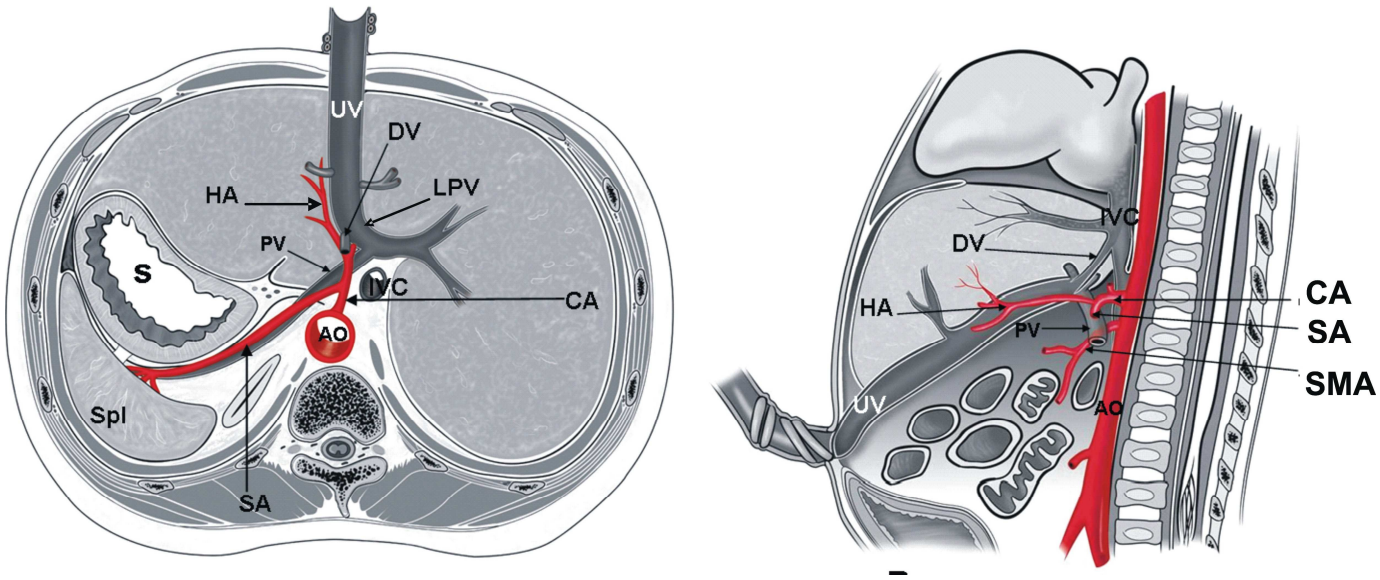

Figure 5. ***Left****. Oblique horizontal section of the upper fetal abdomen.* ***Right****. Sagittal section of the fetal trunk. AO: aorta; CA: celiac artery; IVC: inferior vena cava; SA: splenic artery; HA: left hepatic artery; SMA: superior mesenteric artery; DV: ductus venosus; UV: umbilical vein; PV: portal vein; LPV: left portal vein; Spl: spleen; S: stomach.*

Celiac and splenic arteries

The CA is a short and relatively large vessel arising from the aorta between the crura of the diaphragm (Figure 5). It passes horizontally forward and divides into three branches: the common HA, SA and left gastric artery (this study did not assess the latter). About 2% of humans have a common celiomesenteric trunk, and variation in vascular anatomy is common (Geboes et al. 2001; Ferrari et al. 2007). The celiac plexus of the autonomic nervous system covers the origin of the CA.

Experimental data (in pigs) show different responses to dobutamine in the CA and HA, indicating operation of different regulatory mechanisms (Brander et al. 2006). The hemodynamics of the fetal CA has not been explored.

The SA courses on the cranial border of the pancreas to the spleen. It supplies the pancreas, stomach and spleen and is a major contributor to hepatic portal flow. Stress induces splenic contraction (Aoki et al. 1992), and in adults this is considered to be a compensatory mechanism to increase the venous return from the spleen to the central circulation during stress (Froelich et al. 1988). Fetal alloimmunization or fetal

growth restriction (respectively) affect the flow velocity and PI of the fetal SA, and Doppler assessment of the SA provides information on the risk of adverse outcome in high-risk pregnancies (Abuhamad et al. 1995; Capponi et al. 1997; Bahado-Singh et al. 2000). Reference ranges based on cross-sectional data have been established for the flow velocity and PI of the fetal SA (Abuhamad et al. 1995; Capponi et al. 1997; Bahado-Singh et al. 2000). The relationships between fetal SA and local or general hemodynamics have not been explored.

Hepatic artery

The HA arises from the CA in most cases (18% from the SMA) (Michels 1966). Where the gastroduodenal artery branches off, it becomes the hepatic proper artery. This artery enters the portal tract, where it divides into the left, right and middle HA. The right HA supplies the right liver lobe, the middle HA supplies the medial segments of the left lobe (the quadrate lobe) and the left HA supplies the left lobe. We focused on the latter in the present study. Variation in the pattern of HA supply is common. When the HA branches have penetrated the hepatic parenchyma, they arborize in the portal tracts and form two plexuses (one around small PV and one around the bile ducts) before delivering blood to the hepatic sinusoid. The sinusoids drain slowly into the terminal hepatic veins, eventually emptying in the IVC just below its junction to the right atrium.

The arterial contribution to the fetal liver perfusion is not known, but fetal sheep data suggest <10% (Edelstone et al. 1978), while postnatally the contribution is 25% (Greenway and Stark 1971).

Maintaining hepatic blood flow is essential for the homeostatic roles of the liver in postnatal life, and experimental studies show that liver perfusion is ensured through several hemodynamic compensatory mechanisms (Lautt 1996). One, the hepatic artery buffer response (HABR), is activated instantaneously upon reductions in portal flow. Adenosine, a potent vasodilator, is secreted at a constant rate into the space of Mall surrounding the terminal branches of the hepatic arterioles and portal

venules before they drain into the hepatic sinusoids. Its concentration is regulated by the washout to the portal blood: reduced portal flow reduces washout and accumulates adenosine, which dilates the HA, thus buffering the reduced portal flow. A similar mechanism accounts for the autoregulation of the HA, whereby increased HA flow leads to increased washout of adenosine and subsequently constriction of the HA (Ezzat and Lautt 1987).

Studies of adults have confirmed the function of the HABR (Iwao et al. 1996; Gulberg et al. 2002), and studies of growth-restricted fetuses have observed reduced vascular impedance and an increase in flow velocity in the HA (Kilavuz and Vetter 1999; Dubiel et al. 2001).

Superior mesenteric artery

The embryonic vitelline arteries fuse to form the superior mesenteric trunk. The terminal branches of this trunk supply the yolk sac, and these branches obliterate when the ileum separates from the yolk sac (Sadler 1985b). Rapid growth of the intestine requires proportional growth of the corresponding circulation. Experimentally, it has been shown that the capacity to autoregulate intestinal flow is a function of gestational maturation (Rouwet et al. 2000).

During hypovolemia and hypoxia, blood flow is dramatically redistributed away from the gut, kidney and carcass to the brain, adrenal glands and heart mediated by sympathetic activity (α-adrenergic receptors) (Jensen and Hanson 1995; Bennet et al. 2000; Quaedackers et al. 2004). The mesenteric hemodynamic response to circulatory shock redistributes blood away from the intestinal capacitance vessels, resulting in an “autotransfusion” of up to 30% of the circulatory blood volume to the systemic circulation (Ceppa et al. 2003). Under these conditions, although there is some degree of vasoconstriction in other peripheral systems, it is disproportionately greater within the mesenteric vascular bed. The strong mesenteric constrictor response is caused by a five-fold affinity for angiotensin II in the mesenteric vascular smooth muscle (Gunther et al. 1980). To deal with low supply, the vascular bed of the gut is

capable of redistributing locally (intramurally) and increasing oxygen extraction to prevent ischemic injury.

Sustained hypoxia resulting in hypoperfusion of the fetal intestines is associated with neonatal gastrointestinal morbidity (Robel-Tillig et al. 2002; Bennet et al. 2006), and preterm neonates with high resistance patterns of flow velocity of the SMA on the first day of life are at increased risk of developing necrotizing enterocolitis (Murdoch et al. 2006).

Studies of neonates show that flow velocity in the SMA rises and resistance declines during the first postnatal days (Martinussen et al. 1994) and that the severity of IUGR negatively influences flow velocity in the SMA (Martinussen et al. 1997). In fetal sheep, 4% of the cardiac output is directed to the gastrointestinal tract, not including the spleen and liver (Itskovitz-Eldor and Israel 2005), while splanchnic circulation receives 20% of the postnatal cardiac output and shows great flexibility, increasing 30–130% during digestion (Perko 2001). A study of healthy adults found that the flow velocity of the SMA depends on changes in central hemodynamics (Perko et al. 1996).

Inferior mesenteric artery

The inferior mesenteric artery arises from the aorta at the level of the third lumbar vertebra. It supplies the distal third of the colon and the rectum. The venous drainage of the colon is mainly through the inferior mesenteric vein that empties into the splenic vein. The hemodynamics of the inferior mesenteric artery is not the topic of the present study and hence is not addressed further.

2. Ultrasound

Sound with a frequency above 20 kHz is inaudible to the human ear and is known as ultrasound. The frequencies commonly used for medical diagnostics are 2–10 MHz. The resistance of a medium to sound transmission is called acoustic impedance. The acoustic impedance of soft tissues is relatively low, whereas bone has higher impedance. The boundaries between tissues with different properties of acoustic impedance are called acoustic interfaces, and reflection occurs there. The magnitude of the reflected wave is proportional to the magnitude of the difference in impedance at the interface (Maulik 2005). The progressive decline of a propagating ultrasound wave is known as attenuation. Many factors influence attenuation, such as the impedance of the penetrated tissue, scattering and reflection and transmitting frequency; the higher the frequency, the greater the attenuation. This limits the use of high-frequency transducers for interrogation of deep structures. Tissue absorption is an important source of attenuation, whereby ultrasound energy is converted to heat energy.

The resolution of an image is the smallest distance between two targets that can be discriminated (Angelsen 2000). A high frequency shortens the pulse duration and narrows the beam width, which increases the resolution, but tissue penetration is low. The operator can use insonation angle, gain, focusing of the ultrasound beam and choice of frequency to optimise image quality.

2.1 Doppler ultrasound

Christian A. Doppler, an Austrian physicist and mathematician, first described the Doppler effect in 1842. It is defined as the observed changes in the frequency of transmitted waves when relative motion exists between the source of the wave and the observer. The principle is applicable to all forms of wave propagation, and the shift in frequency is proportional to the speed of movement between the source and receiver.

In diagnostic Doppler ultrasound, the red blood cells act as moving receivers and as moving sources.

The Doppler equation:

$f_D = 2 * f_t * v/c$

f_D represents the Doppler frequency shift, f_t the frequency of the incident beam (transducer frequency), v the velocity of the scatterer (reflector) in a given direction, and c the propagation speed of sound in the medium. If the direction of the incident beam is at an angle θ to the direction of flow (Doppler angle), the equation includes the cosine of the angle θ.

$f_D = 2 * f_t * \cos \theta \; v/c$

and the velocity of the moving scatterer may be calculated as:

$v = f_D * c/2 * f_t * \cos \theta$

That is, the velocity of the reflector is proportional to the cosine of the Doppler angle. If the Doppler angle is 90°, the reflector is moving perpendicular to the ultrasound beam and the detected Doppler shift is zero. Knowledge of the insonation (Doppler) angle is essential in evaluating absolute velocity, and uncertainty in peak velocity increases as the Doppler angle approaches 90°. At 20° of insonation, an error of 5° corresponds to a 3.6% error in velocity. At 80° of insonation, the velocity error is 99%.

Different Doppler techniques may be applied in diagnostic ultrasound, such as pulsed-wave Doppler, colour Doppler, continuous-wave Doppler and power Doppler. The pulsed-wave Doppler and colour Doppler techniques will be discussed here since these modes were applied in this study.

Pulsed-wave Doppler

Pulsed-wave Doppler provides the ability to select Doppler signals from specific depths. Short pulses of ultrasound are sent out and received. Each Doppler signal is sampled once for every pulse transmission, and the time interval for the pulse transmission and reception determines the distance or range of the target area from the transducer.

The rate at which a pulse is generated is called the pulse repetition frequency. If the pulse repetition frequency is less than twice the frequency of the maximal Doppler signal frequency ($2f_D$), aliasing will occur, known as the Nyquist limit (pulse repetition frequency equals $2f_D$). To eliminate aliasing, the operator should adjust the frequency scale on the spectral Doppler display and, secondly, adjust the baseline.

Spectral analysis is a quantitative analysis showing the distribution of frequencies (that is, velocities) to be presented as a function of time.

The three-dimensional region in the path of the transmitted ultrasound beam from which the frequency shift signals are obtained is called the Doppler sample volume. The operator can control the axial dimensions, while the transverse dimensions are determined by the ultrasonic beam width, which approximates the diameter of the transducer face in the near field and broadens in the far field (Maulik 2005).

Colour Doppler

Colour flow imaging combines data from moving reflectors (the Doppler shifts) with grey-scale images and provides anatomical details along with information on flow (high or low velocity and direction). The limitation of this display is that the image rate tends to be slower. To improve the frame rate, the operator may reduce the size of the imaged field in colour mode.

2.2 Safety

Ultrasound may react with tissues by 1) thermal effects (tissue heating) and 2) non-thermal mechanical effects (cavitation). (We do not discuss other mechanical effects here, as their biological significance is unclear.)

When ultrasound penetrates tissue, the tissue absorbs a portion of its energy and converts it to heat. The rate of heat generation depends on the characteristics of the transmitted ultrasound and on the tissue. The elevation of temperature in tissue also depends on factors that control the dissipation of heat in the tissue, such as perfusion. B-mode (grey-scale) ultrasound operates at acoustic outputs that are incapable of producing harmful temperature rises. The extent of heating for pulsed Doppler is higher than other ultrasound modes, which require the operator to be aware, especially when examining sensitive tissue such as a fetus.

Experimental studies in animals provide evidence of biological effects from ultrasound in fetuses. These studies show that developmental injury requires a temperature rise of at least 1.5°C above normal body temperature, and exposure that elevates temperature in situ above 41°C for more than 5 minutes should be considered hazardous (Ziskin and Barnett 2001). Since bone tissue has the highest acoustic impedance, it carries the highest likelihood of thermal effects. Since the brain is enclosed in bone, it is vulnerable to bone-related heating, and experimental data confirm that the greatest brain heating occurs close to the bone and correlates with gestational age and bone mineralization (Barnett 2001). A study on monkeys reported a peak temperature rise of 0.6°C after Doppler exposure of the brain vessels, suggesting that the presence of tissue perfusion may play a protective role by dissipating heat (Tarantal et al. 1993). In contrast, studies on guinea pigs showed that cerebral blood perfusion had a negligible effect on cooling (Barnett 2001).

The mechanical biological effects of ultrasound exposure include cavitation, which is the formation, growth, oscillation and collapse of bubbles in a liquid. The mechanism of bubble formation seems to depend on the presence of a tissue–gas

interface, and this is why this effect is less likely to be implicated in the ultrasound exposure of the fetus.

Human epidemiology studies fail to show adverse outcome in fetuses exposed to ultrasound (Itskovitz-Eldor and Israel 2005), but studies of biological effects face methodological obstacles. Modern ultrasound devices have higher output than older equipment, and data are limited for elucidating a dose–response relationship of prenatal ultrasound exposure and adverse effects (Salvesen 2007). The epidemiological evidence shows no association between ultrasound exposure and childhood malignancies, adverse effects on growth or brain development (Itskovitz-Eldor and Israel 2005).

Modern ultrasound equipment provides a real-time output display showing the thermal indices for soft tissue, bone and cranial bone and mechanical indices that serve to alert the operator to potential biological effects. The thermal indices estimate the rise in tissue temperature in °C that is possible during the relevant ultrasound exposure, while the mechanical indices estimate the potential for producing non-thermal biological effects in the tissue (worst-case situations). However, these indices have some limitations, as the potential effects may be underestimated (Marsal 2005). The international guidelines based on the ALARA (as low as reasonably achievable) principle underscore the operators' responsibility to use ultrasound prudently.

3. The present study

Reports of serial measurements in the monitoring of fetuses at risk have used reference ranges based on cross-sectional data (Hecher et al. 2001; Bilardo et al. 2004; Baschat et al. 2007). We expected an increasing use of serial measurements in the clinical management of individual pregnancies and therefore chose a longitudinal study design, as temporal changes cannot be appropriately considered in a cross-sectional manner (Royston 1995). A longitudinal study provides the necessary terms for calculating conditional ranges, which we believe are more appropriate in repeat assessments as they take into account the individual hemodynamic state, assuming that this is an important determinant for subsequent development.

The motivation and hypotheses that initiated the study were as follows.
We assumed that we could identify the necessary details and landmarks to establish a reliable method of studying major splanchnic arteries in the human fetus: CA, HA, SA and SMA.

We anticipated that these techniques could be used to construct longitudinal reference ranges describing the normal development during the second half of pregnancy and suitable for monitoring fetal Doppler parameters.

We hypothesised that, although 85% of the venous liver perfusion is of umbilical origin during prenatal life (Kessler et al. 2008), the HA, SA and SMA are involved in maintaining the liver perfusion and can be traced under physiological conditions.

3.1 Aims of the study

- To establish a standardised, reproducible ultrasound examination technique and longitudinal reference ranges for the HA flow velocity and PI.

- To determine the blood velocity pattern in the HA at various states of port-caval pressure gradient and venous liver perfusion, and the relationship with MCA and UA hemodynamics.

- To establish longitudinal reference ranges for flow velocity and PI in the CA, SA and SMA.

- To assess the blood velocity pattern of the CA, SA and SMA at various states of liver perfusion and port-caval pressure gradient, and the relationship with the hemodynamics of the MCA and UA.

- To determine the hemodynamic relationship between the CA and its branches (SA and HA), and between the CA branches and the SMA.

- To establish longitudinal reference ranges for the MCA flow velocity and PI and the cerebroplacental pulsatility ratio.

3.2 Material and methods

3.2.1 Study design

Reference ranges should be constructed from prospectively collected data in a population selected for the purpose; thus, we chose a prospective observational longitudinal design.

3.2.2 Study population

Women attending the ultrasound department for routine second trimester scans between gestational week 17-20 were invited to participate in the study, which we conducted during 2004-2006. The regional Committee for Research Ethics approved the study protocol (REK-Vest no. 203.03). During the pilot study, 27 women were examined 1–3 times, giving a total of 43 examinations. After gestational age had been

assessed by head biometry at routine ultrasound scan in the second trimester (Johnsen et al 2004), another 161 healthy pregnant women with singleton pregnancies were recruited.

The reasons for not being enrolled were fetal anomaly, any maternal chronic disease and a history of pregnancy-induced hypertension, fetal growth restriction, placental abruption or delivery before 37 weeks. We obtained informed written consent from the participants before enrolment. We aimed at examining each participant four times at 3- to 5-week intervals.

We collected information from the medical records on birth weight, gender, placental weight, Apgar score, duration of gestation at delivery, congenital anomalies, mode of delivery and transfer to the neonatal intensive care unit.

In the study of the hemodynamics of the HA (Article I), three clinical cases were included to illustrate the potential clinical use of Doppler assessment of the HA.

3.2.3 Measurements

We used a 2-5, 2-7 or 4-8 MHz abdominal transducer (Voluson 730 Expert; GE Medical Systems, Kretz Ultrasound, Zipf, Austria) with colour Doppler and pulsed Doppler facilities. The high-pass filter was set as low as possible, at 70 Hz. The mechanical and thermal indices were below 1.1 and 0.9, respectively, in most of the sessions, and were always kept below 1.9 and 1.5.

At each session we aimed at measuring blood flow velocity in the 1) MCA, 2) UA, 3) CA, 4) left HA, 5) SA, 6) SMA, 7) DV, 8) intra-abdominal UV and 9) LPV. We measured three biometric parameters three times at standard sections (head and abdominal circumference and femur length) (Johnsen et al. 2006), noted a mean for each and used these data to calculate the estimated fetal weight according to the formula of Combs et al. (1993). For estimating the volume of UV blood flow, we measured vessel diameter (D)(inner edges in a perpendicular insonation to the vessel

wall at least three times) in the intra-abdominal UV distal to the first hepatic branches (Figure 6). Diameter was measured repeatedly to reduce random error (Kiserud and Rasmussen 1998). Flow velocity in the intra-abdominal UV was recorded in an axial direction of the vessel, and the volume of blood flow in the UV (Q_{UV}, ml/min) calculated as:

$$Q_{UV} = \pi * (D/2)^2 * v_{max} * h * 60$$

where h is velocity profile factor and $h = 0.5$ for the UV (Kiserud et al. 1994b).

We applied standardized techniques for assessing the MCA, DV and LPV (Kiserud et al. 1991; Mari et al. 2005; Kessler et al. 2007a) and performed the UA recordings in a free-floating section of the umbilical cord. Each examination did not last more than 1 hour, and we placed the women in a semirecumbent position.

We videotaped one examination session and timed the use of the different ultrasound modes. The total examination time was 50 minutes, frozen time was 8:10 minutes (16.3%), grey-scale time 16:18 minutes (32.6%), colour Doppler 20:04 (40.1%) and pulsed Doppler 5:28 minutes (10.9%).

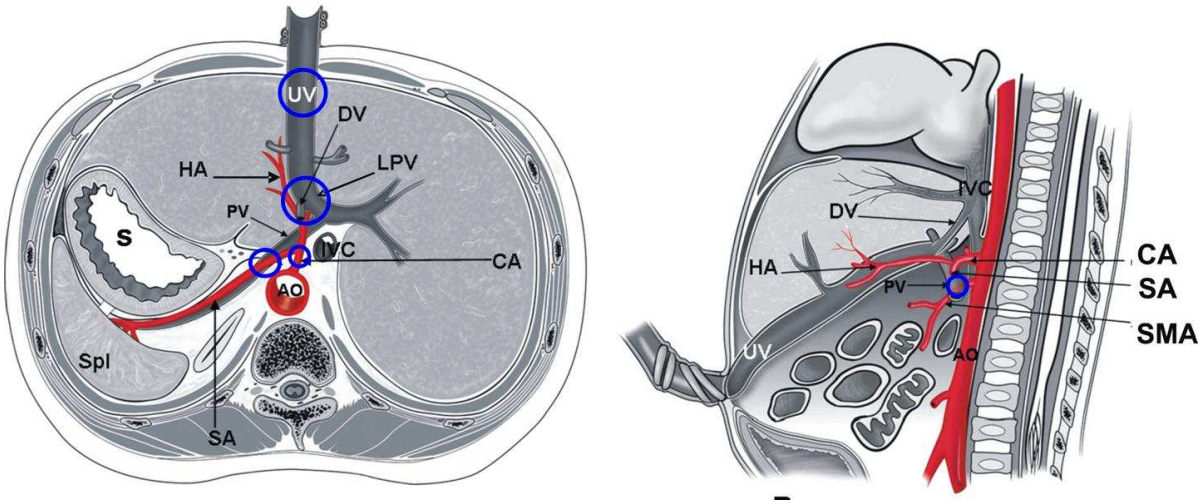

*Figure 6. Schematic drawing of the fetal abdomen with vessels of interest in this study. **A**. Horizontal view. **B**. Sagittal view. The measurement points (encircled): UV: umbilical vein; DV: ductus venosus; LPV: left portal vein; SA: splenic artery; CA: celiac artery; HA: hepatic artery left branch; SMA: superior mesenteric artery; PV: portal vein; Spl: spleen, S: stomach.*

In the pilot study, we sought to visualize the branches from the CA directed to the fetal liver using colour Doppler. The CA branches off from the abdominal aorta into the left gastric artery, SA and common HA. In contrast to the renal arteries that branch off directly from the aorta, the SA has its origin from the CA in front of the aorta (Figure 6). The SA was regularly identified as it traverses behind the stomach to the hilum of the spleen, cranial to the splenic vein, while the common HA was less obvious running along the PV before dividing into the left and right HA (Figure 6). We did not identify the middle HA in this study.

Flow in the common HA and right branch has the same direction as the neighboring main PV and right PV, causing interference in the pulsed Doppler recording, and was therefore less suitable for the assessment (Figure 7). However, the left branch of the HA could be visualized free of the PV as it approached the DV to continue distally to the left of the intra-abdominal UV. Since blood flow in the left branch of the HA has the opposite direction to that in the neighboring DV and UV, the Doppler recordings at this point can mostly be analyzed without interference, and we chose this as the standard technique for the study.

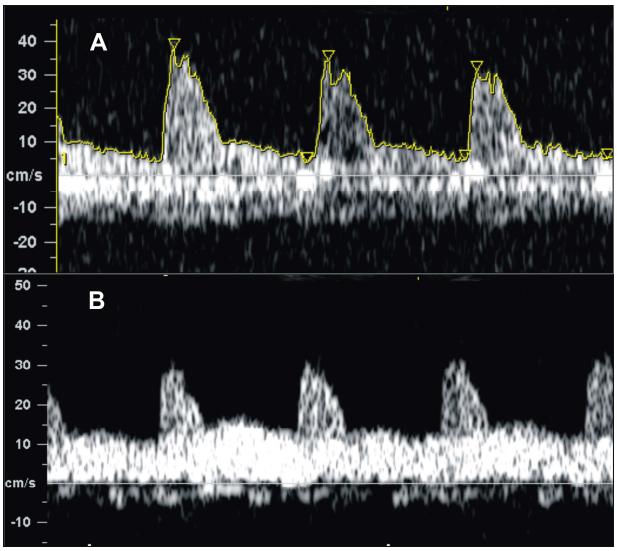

*Figure 7. Doppler recordings of the hepatic artery waveform. **A**. Recording from the left branch. **B**. Recording from the common hepatic artery with interference from the neighbouring portal vein (gestational age 35 weeks).*

The CA was assessed close to the aorta in a sagittal or horizontal view of the fetal abdomen (Figures 6 and 8). The SA was visualized in a horizontal insonation and the sample volume placed over the proximal part of the vessel (Figure 9). The left HA was assessed in a horizontal or a sagittal view of the fetal abdomen and measured as described above.

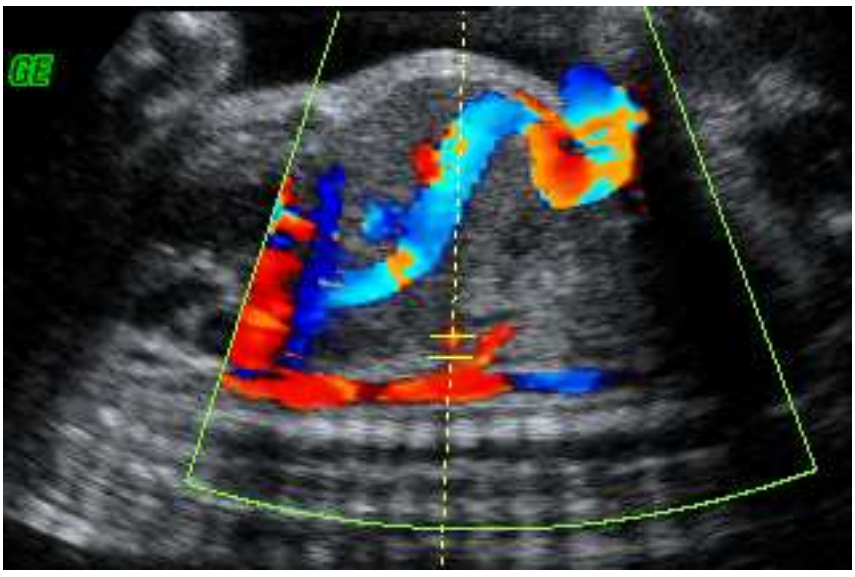

Figure 8. The celiac artery, the first anterior branch from the descending aorta below the diaphragm, here assessed in a sagittal view of the fetal abdomen. The Doppler gate is placed over the proximal part of the vessel (gestational age 28 weeks).

The SMA is the second anterior branch from the abdominal aorta. It leaves the aorta at the level of the kidney arteries, is directed anterior and caudal into the mesentery. We assessed the SMA in a sagittal or horizontal insonation and placed the sample volume over the proximal part of the vessel (Figures 6 and 10).

For all Doppler assessments, we performed the insonation along the direction of the vessels, keeping the angle of insonation as low as possible: always ≤10° for the MCA and ≤30° for all other vessels. We acquired the recordings in fetal quiescence and over at least three heart cycles. We traced the Doppler waveforms automatically or manually, determined the systolic peak and time-averaged maximum velocity and calculated the PI (Gosling and King 1975).

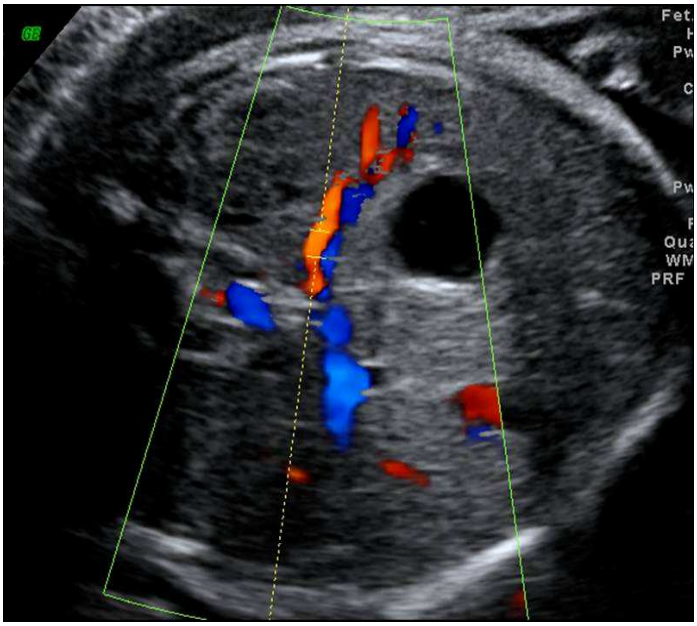

Figure 9. Colour Doppler image of the splenic artery in horizontal view of the fetal abdomen, traversing posterior to the stomach. The Doppler gate is placed over the proximal part of the vessel (gestational age 34 weeks).

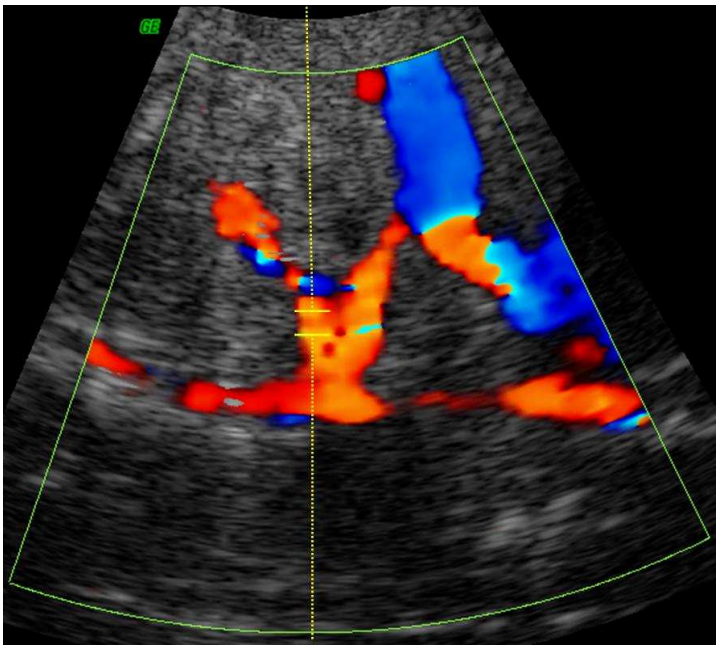

Figure 10: Colour Doppler image of the superior mesenteric artery. The Doppler gate is placed over the proximal part of the vessel (gestational age 38 weeks).

3.2.4 Statistics

Power calculations

Longitudinal data can be used to provide the terms to evaluate temporal changes, that is for calculating the expected value and reference ranges based on a previous measurement (Royston 1995; Royston and Wright 1998). Experience from cross-sectional studies suggests that about 15 observations per gestational week (N_c) are necessary for calculating reliable centiles (Royston and Altman 1995; Kiserud et al. 2000). The corresponding number for a longitudinally designed study (N_l) is N_c/D, where D is the design factor, which has been calculated as 2.3 in studies on fetal size (Royston and Altman 1995). Thus, observations over 20 weeks correspond to $N_c = 300$ and $N_l = 130$. An anticipated overall success rate of 80% for Doppler measurements increased the study group to 160 participants.

Construction of mean and centile curves

We used multilevel modelling to calculate mean and centiles for the variables according to gestational age. The first level was the variance between measurements of the same fetus and the second was the variance between the participating women. The MlWin program (MlWin, Centre for Multilevel Modelling, University of Bristol, UK) and SPSS (SPSS Inc., Chicago, IL, USA) were used for the statistical analysis.

To test for normal distribution of the outcome variables and the power in which the dependent variables were transformed, we used Box-Cox power transformation. Fractional polynomial regression models were fitted to the data as one fixed and one random component.

We calculated the 2.5th, 5th, 10th and 25th centiles by subtracting 1.96 standard deviations (SD), 1.645 SD, 1.282 SD and 0.674 SD from the mean, respectively. The 97.5th, 95th, 90th and 75th centiles were calculated by adding the respective multiples of the SD to the mean. We derived the 95% confidence interval (CI) of the mean and 5th and 95th centiles from the standard error of the regression lines. To obtain approximate standard error around the 5th and 95th percentiles, transformed observations ± 1.645 SD were regressed against gestational age.

Further regression analysis

To assess the possible effect of fetal variables (such as gender, estimated fetal weight, V_{DVps}, Q_{UV}, normalized Q_{UV} per kilogram of body weight and V_{UVmax}) on the outcome variables (velocity and pulsatility index in the HA, SA, CA and SMA), we included these possible determinants as indicator variables in the multilevel regression models, which describe the mean of the outcome variables. We included the determinants in three categories (<10th centile, 10th to 90th centile and >90th centile) in the regression model since we assumed that responses would occur more commonly in extreme conditions. Indicator variables with significant improvement in the goodness of fit to the models, as assessed by the deviance statistics (χ^2 with $p < 0.05$), were considered to influence the outcome variables.

Reproducibility

Intra- and interobserver variations for the flow velocity and PI of the MCA were calculated with a paired sample *t*-test and limits of agreement (Bland and Altman 1986). We calculated the variations of the splanchnic arteries with a paired sample t-test and intra- and interclass correlation coefficients based on repeat observations (Bland and Altman 2003).

4. Results

4.1 Study population

Table 1 presents the characteristics of the study population. Since the aims of the study were to establish longitudinal reference ranges for cerebral and splanchnic arteries and to study hemodynamic relationships in physiological pregnancies, we recruited healthy women with no history of pregnancy complications. According to the prospective design of the study (that is, the outcome was not known at enrolment), we decided not to exclude participants who developed complications. Since the birth weight (Skjaerven et al. 2000) and caesarean rate did not differ from those of the local population (local caesarean rate: 11.8%), we believe that the ranges may be applied to the general population and that the information we provide on hemodynamic relationships can be applied to physiological pregnancies.

One woman had one set of measurements, 2 women had two, 18 had three, 126 four and 14 had five. No participant withdrew from the study after enrolment. All except three were Caucasians. Four smokers were included. Three neonates (1.9%) were transferred to the neonatal intensive care unit (one because of supraventricular arrhythmia and two after operative delivery).

Clinical cases (Article I)

Case 1. Fetomaternal bleeding following maternal abdominal trauma at 30 weeks. A healthy girl 3400 g had a normal delivery at 40.3 weeks. Case 2. Non-immune fetal hydrops caused by human parvovirus B19 infection was diagnosed at 24 weeks, and had one intrauterine transfusion for anemia at 24.6 weeks. A boy 2680 g (<10th centile) was delivered normally at 37.3 weeks. Case 3. IUGR at term, a girl 2550 g (<5th centile) was delivered by acute caesarean because of fetal distress at 40.3 weeks.

Table 1. Characteristics of the study population (*n* = 161)

Characteristics	**Median (range) or %**
Maternal age at inclusion (years)	29 (20–40)
Parity	1 (0–5)
Birth order one (%)	48.4
Body mass index (kg/m^2) at first visit	22.9 (18.1–40.8)
Gestational age at delivery (weeks)	40.4 (35.4–42.6)
Caesarean section (%)	10.6
Male baby (%)	50.3
Placental weight (g)	720 (350–1200)
Birth weight (g)	3700 (2260–4980)
Apgar score, 5 min, <7 (%)	0.62

4.2 Success rate

The total number of sessions during the study was 633, and median 4 (range 1–5) examinations per participant (Table 2). The reasons for not achieving measurements were fetal position, fetal movements and time constraints. We gave the highest priority to measuring the splanchnic arteries.

Table 2. Success rate for flow velocity measurements in the different vessels related to the total number of examinations (n = 633)

Vessel	Number of observations	Success rate (%)
Middle cerebral artery	604	95.4
Umbilical artery	611	96.5
Cerebroplacental ratio	550	86.9
Hepatic artery	176	27.8
Celiac artery	510	80.6
Splenic artery	521	82.3
Superior mesenteric artery	589	93.0
Ductus venosus	596	94.1
Left portal vein	282	44.5
Umbilical vein	598	94.5

4.3 Reproducibility

The intra- and interobserver analysis showed that reproducibility was acceptable for clinical use in the MCA, CA, SA and SMA (clinically acceptable limits of agreement and intra- and interclass correlation coefficients >75%). For the HA study we found lower intra- and interclass correlation. This may be explained by the physiological properties of the HA (rapid changes are expected (Lautt 2007)) and technical difficulties.

4.4 Middle cerebral and umbilical arteries and the cerebroplacental ratio

Middle cerebral artery

Serial monitoring commonly used in monitoring fetuses at risk ideally requires reference ranges based on longitudinal data. Reference ranges published for clinical use are based on cross-sectional data (Figure 11) (Mari and Deter 1992; Kurmanavicius et al. 2001; Bahlmann 2002; Baschat 2003). A few longitudinal studies have been published, but these are small or lack ranges for commonly used parameters (Arstrom et al. 1989; Meerman et al. 1990; Harrington et al. 1995). Our reference ranges (based on 566 observations) differ somewhat from the published cross-sectional ranges, but all the curves compared for the PI of the MCA have similar values for the last weeks of pregnancy (Figure 11).

We established longitudinal reference ranges for the MCA and cerebroplacental ratio and provided terms for calculating conditional reference intervals, i.e. the calculation of expected mean and ranges based on a former observation in the same fetus (Figure 12). Our suggestion is to calculate the conditional ranges based on the first observation in a series of observations. The conditional ranges are narrower and shifted in the same direction as the index value compared with the ranges for the entire population.

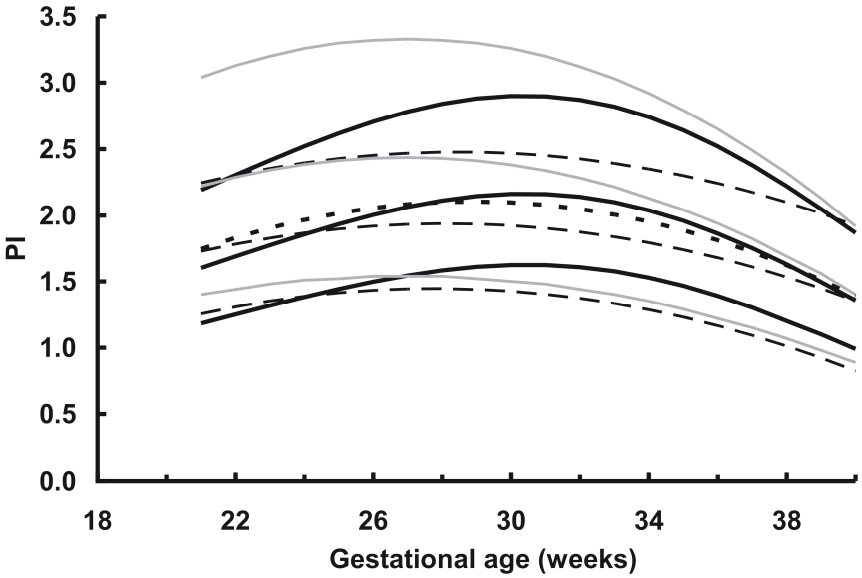

Figure 11. Reference ranges (5th, 50th and 95th centiles) for the pulsatility index (PI) based on 566 observations in our longitudinal study (continuous black lines) compared with those from cross-sectional studies: — —: Bahlmann (2002); continuous grey lines: Mari and Deter (1992); and - - - (mean): (Baschat 2003).

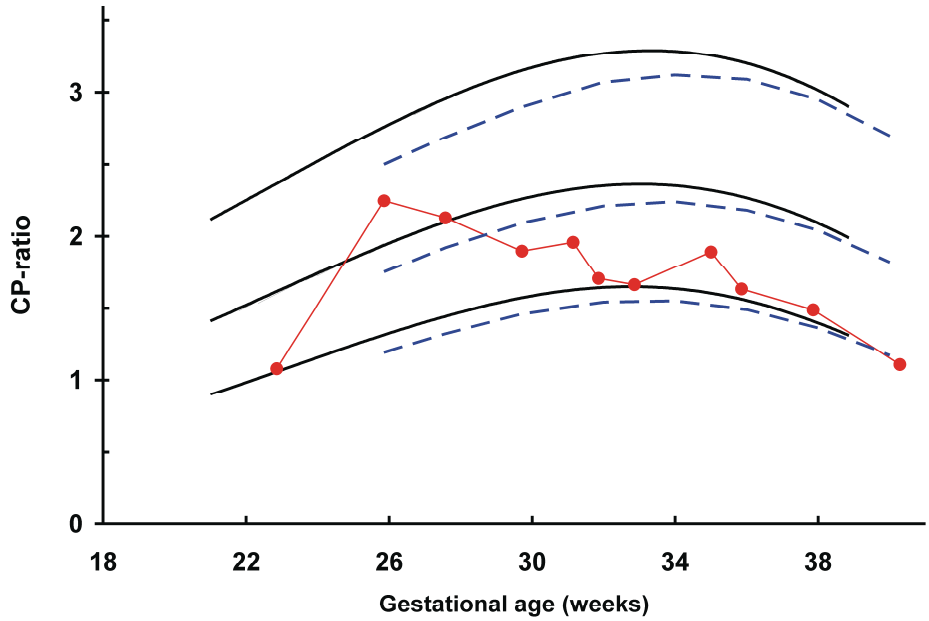

Figure 12. Serial measurements of the cerebroplacental ratio (CP-ratio) in a pregnancy at risk for IUGR (red). The conditional ranges (blue broken lines) are calculated from the observation at GA 22.9. Reference ranges 5th, 50th and 95th centiles (continuous black lines).

Umbilical artery

The UA was measured 611 times in a free-floating loop of the umbilical cord. The velocity and PI were entered into the statistical analysis and for the calculation of the cerebroplacental ratio. We compared our results with those of another study with corresponding design (Acharya et al. 2005a) and found minor differences (Figure 13).

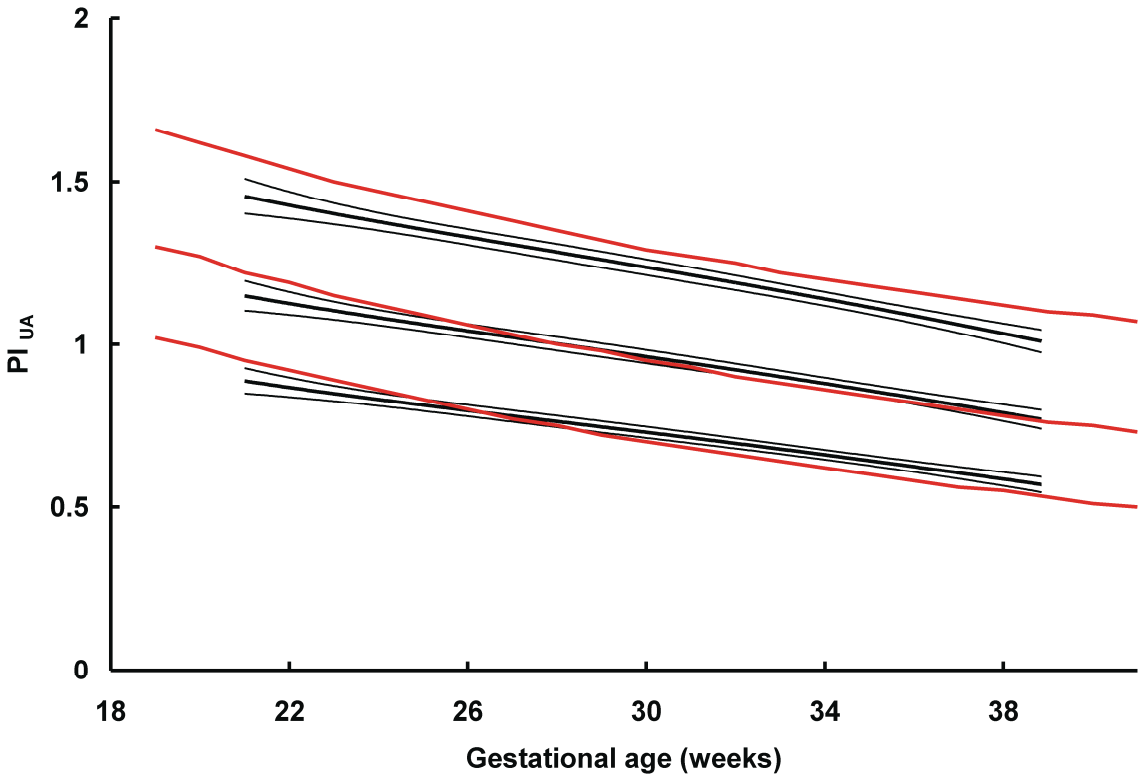

Figure 13. Pulsatility index of the umbilical artery (PI_{UA}) with 5th, 50th and 95th centiles (thick black lines) and their 95% CI (thin black lines) based on 611 observations in 161 low-risk pregnancies compared with the corresponding centiles from another study (Acharya et al. 2005a) (red lines)

4.5 The umbilical and left portal vein and the ductus venosus

Umbilical vein flow has been studied extensively. All studies show increasing flow ($ml \cdot min^{-1}$) but decreasing normalized flow ($ml \cdot min^{-1} \cdot kg^{-1}$) through gestation (Bellotti et al. 2000; Kiserud et al. 2000; Acharya et al. 2005c). Our findings are in accordance with this (using maximum flow velocity for estimating UV flow) (Figure

14). For the regression analysis, we constructed centiles for the maximum UV flow velocity, flow (ml · min^{-1}) and normalised flow (ml · min^{-1} · kg^{-1}).

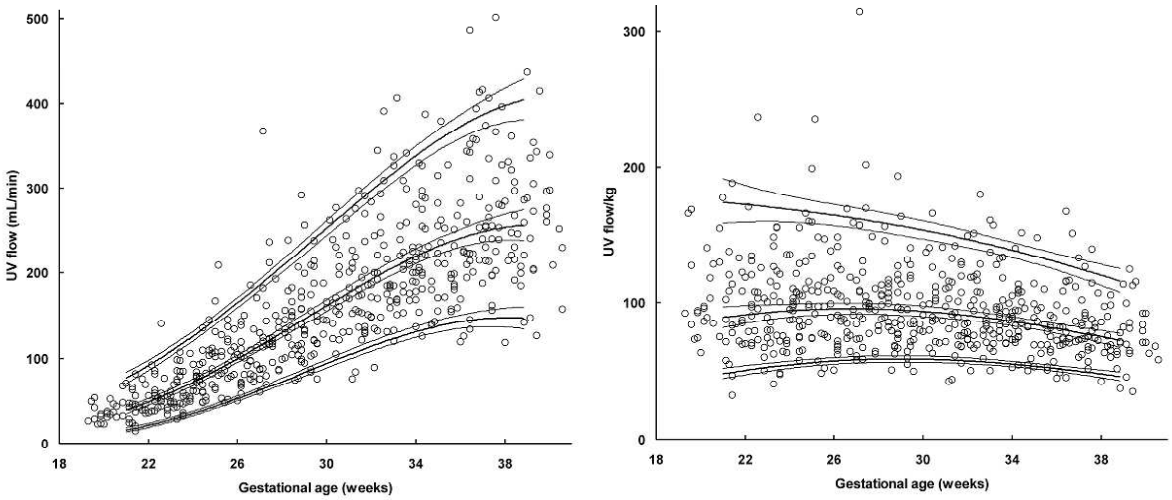

Figure 14. ***Left****. Umbilical flow (ml/min) with 5th, 50th and 95th centiles and 95% CI (thin lines) based on 568 observations.* ***Right****. Normalised umbilical flow (ml · min^{-1} · kg^{-1}) based on 553 sets of observations of estimated fetal weight, UV diameter and UV maximum velocity in 161 low-risk pregnancies.*

The flow velocity in the LPV is a direct reflection of umbilical venous supply to the right liver lobe (Kessler et al. 2007a). Thus, low velocity indicates a shift towards less oxygenated blood and relatively more oxygen-depleted PV blood to the right liver lobe. We constructed centiles for the further regression analysis.

In our study V_{DVps} was used as a surrogate measure for portal perfusion pressure (Kiserud et al. 1994a). We used a standardized technique (Kiserud et al. 1991) and constructed centiles for use in the regression analysis.

4.6 Hepatic artery

We established a standardised technique (Figure 6) and reference ranges (Figure 15) for measuring blood velocity and PI in the HA. We found the left HA suitable for Doppler interrogation. Flow velocities in the left HA increase during the second half of pregnancy (from mean V_{HAps} 18 to 33 cm/s), while the mean PI_{HA} increases from

1.49 at 21 weeks to 1.88 at 32 weeks when a plateau is reached (week 38 mean = 1.83). Although the Doppler measurements of the HA were increasingly successful as the study developed, our overall success rate was low (Table 2). This may be explained by difficulty in anatomical identification, low flow and interference from neighbouring veins. We expect that pathological low umbilical flow and portal perfusion pressure in clinical cases will provoke increased flow in the HA and enhance visualisation.

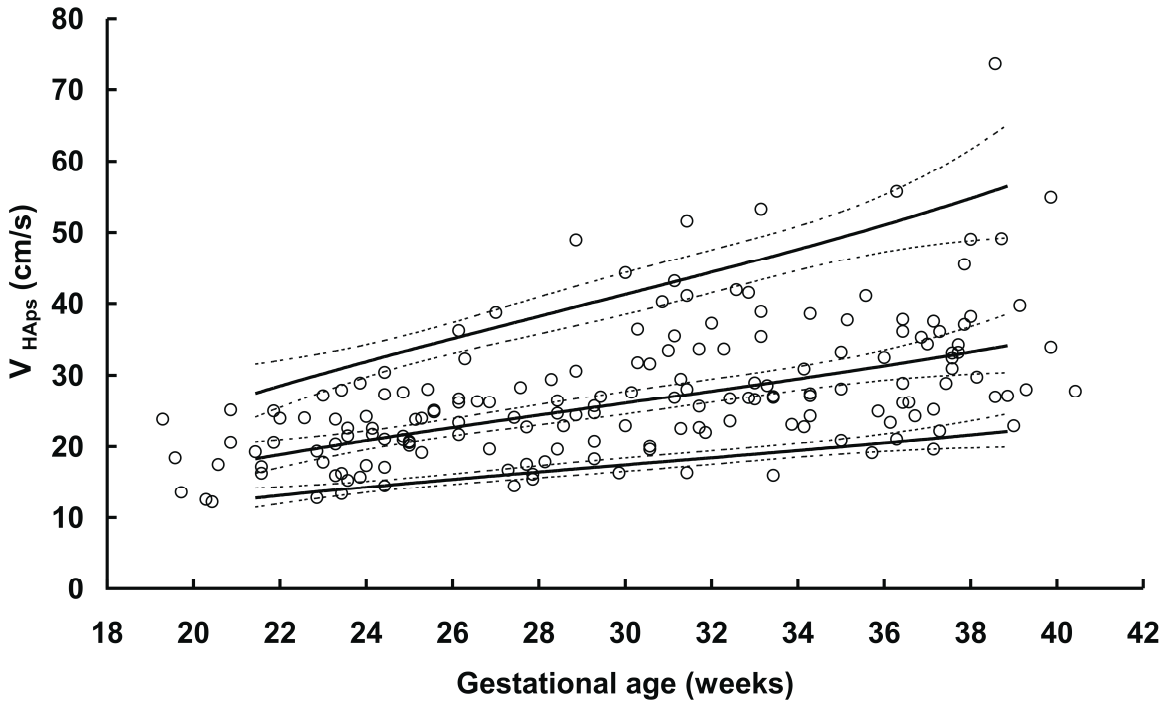

Figure 15. Peak systolic velocity of the left hepatic artery ($v_{HA\text{-}ps}$) 5th, 50th and 95th centiles and 95% CI for the centiles (thin broken lines) based on 176 observations

In the present study the regression analysis showed that high (>90th centile) UV and normalised UV flow were positively associated with PI_{HA}, and a low port-caval pressure gradient (V_{DVps}) was associated with a low PI_{HA}. This finding of a vasodilation in the HA at low UV perfusion and low port-caval pressure supports the hypothesis of an intrinsic regulation of the HA in the fetus similar to the postnatal HABR (Lautt 1996).

We found no significant association of the HA hemodynamics (PI) with the MCA and UA PI, indicating no common determinants for the HA, MCA and UA under unprovoked physiological conditions.

The clinical cases showed decreased pulsatility and increased peak velocity in the HA, indicating increased arterial contribution to liver perfusion in states of low venous perfusion or possibly increased hematopoietic demand (Kunisaki et al. 2006).

4.7 Celiac and splenic arteries

The CA feeds both the HA and SA that supply the fetal liver; the HA directly, and the SA indirectly via splenic venous drainage to the PV. To the best of our knowledge, a standardised insonation technique and reference ranges for the CA have not been available. Our reference ranges show that the flow velocities increases from a mean V_{CAps} of 26 to 50 cm/s and time-averaged maximum velocity (V_{CAtamx}) from 12 to 22 cm/s during 21–39 weeks of gestation, while the curve describing the mean PI_{CA} is parabolic, increasing from 1.73 to 2.10 at 29–30 weeks and declining to 1.81 at 39 weeks.

The SA is a major contributor to portal flow through the splenic vein. This vessel is anatomically readily assessable for Doppler evaluation in the fetus, also with an accurate insonation for evaluation of absolute velocities (Figure 8).

Similar to the CA, the SA velocity increases throughout the second half of pregnancy (V_{SAps} from 19 to 49 cm/s and V_{SAtamx}11 to 24 cm/s). The curve describing the mean PI_{SA} is lower than that of the PI_{CA} but is also parabolic and with a turning point (1.85) at the corresponding gestational weeks, decreasing to 1.58 at 39 weeks.

In the present study, we found weak correlations between PI_{HA} and PI_{CA} (r = 0.3, 95% CI 0.1 to 0.5) and PI_{HA} and PI_{SA} (r = 0.1, 95% CI –0.05 to 0.3), indicating largely independent local regulation of the branches from the CA. The correlation between PI_{CA} and PI_{SA} was stronger (r = 0.5, 95% CI 0.3 to 0.6). Thus, our

results suggest that the hemodynamics of the CA is more closely related to that of SA than HA.

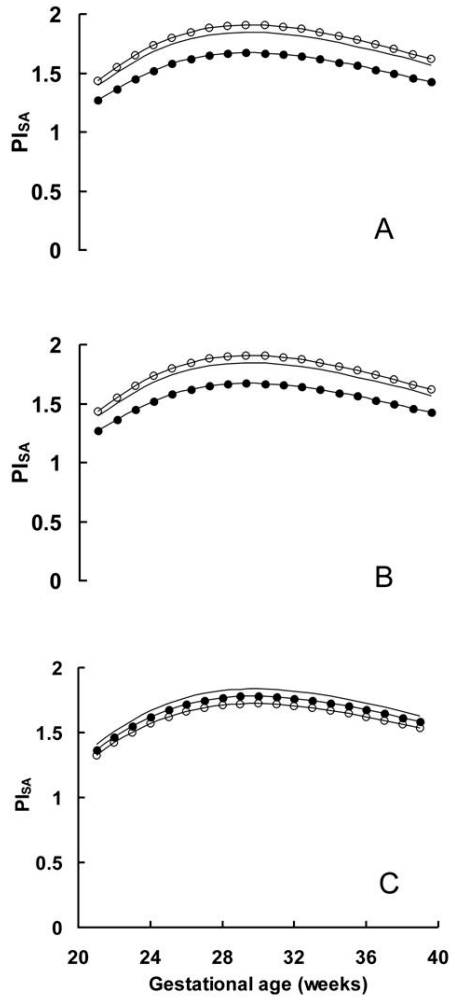

*Figure 16. The influence of port-caval pressure gradient expressed by the ductus venosus peak blood velocity (V_{DVps}) (**A**), umbilical venous distribution to the right liver lobe ($v_{LPVtamx}$) (**B**) and umbilical venous flow (Q_{UV}) (**C**) on splenic artery impedance (PI_{SA}) according to regression analyses. The difference between the lines represents the effect, all being significant (p<0.0001). Lines with closed circles: <10th centile for the variables; simple lines: 10th to 90th centiles; and lines with open circles: >90th centile.*

We tested the hypothesis that the port-caval perfusion pressure is a local determinant for CA and SA vasodilation. Regression analysis showed that low port-caval pressure gradient (V_{DVps} <10th centile) is associated with vasodilation in the SA

and CA.. A vasodilation response is also present at low UV distribution to the right liver lobe (as expressed by flow velocity in the LPV; shown for the SA in Figure 16).

The PI in the MCA and UA were positively associated with the PI in the SA and CA, indicating concurrent vascular regulation of these vessels with cerebral and placental vascular beds under unprovoked physiological conditions.

4.8 Superior mesenteric artery

Knowledge of flow velocity in the SMA and its hemodynamic relationships in human fetuses is lacking. We show that peak systolic and time-averaged maximum flow velocities and PI in the SMA increase throughout the second half of pregnancy (Figure 17). The increasing velocity is related to increased volume flow (Martinussen et al. 1996; Acharya et al. 2004) and confirms increasing perfusion of the intestine towards term, corroborating a study of the portal flow (Kessler et al. 2007b). Our mean PI_{SMA} increases until week 32, when it plateaus; this is in accordance with another small study (Korszun et al. 2002) but shows some variation compared with the values reported by cross-sectional studies (Abuhamad et al. 1997; Achiron et al. 1998). The variation may be caused by differences in study design, population sample or insonation technique.

When we assessed SMA flow velocity and PI for gender effects in the regression analysis, we found no difference in the peak systolic flow velocity and only 1% lower $V_{SMAtamx}$ and 2% higher PI_{SMA} in female fetuses when corrected for estimated fetal weight ($P < 0.0001$).

We examnied for covariation between the hemodynamics in the SMA (PI) and the SA and HA and found weak correlations ($r = 0.39$, 95% CI 0.27 to 0.51 and $r = 0.30$, 95% CI 0.22 to 0.37 respectively), indicating largely independent local regulation of these vessels. PI_{SMA} was positively associated with PI_{MCA} and PI_{UA}, suggesting

concurrent vascular regulation of the SMA with the cerebral and placental vessels in non-compromised fetuses.

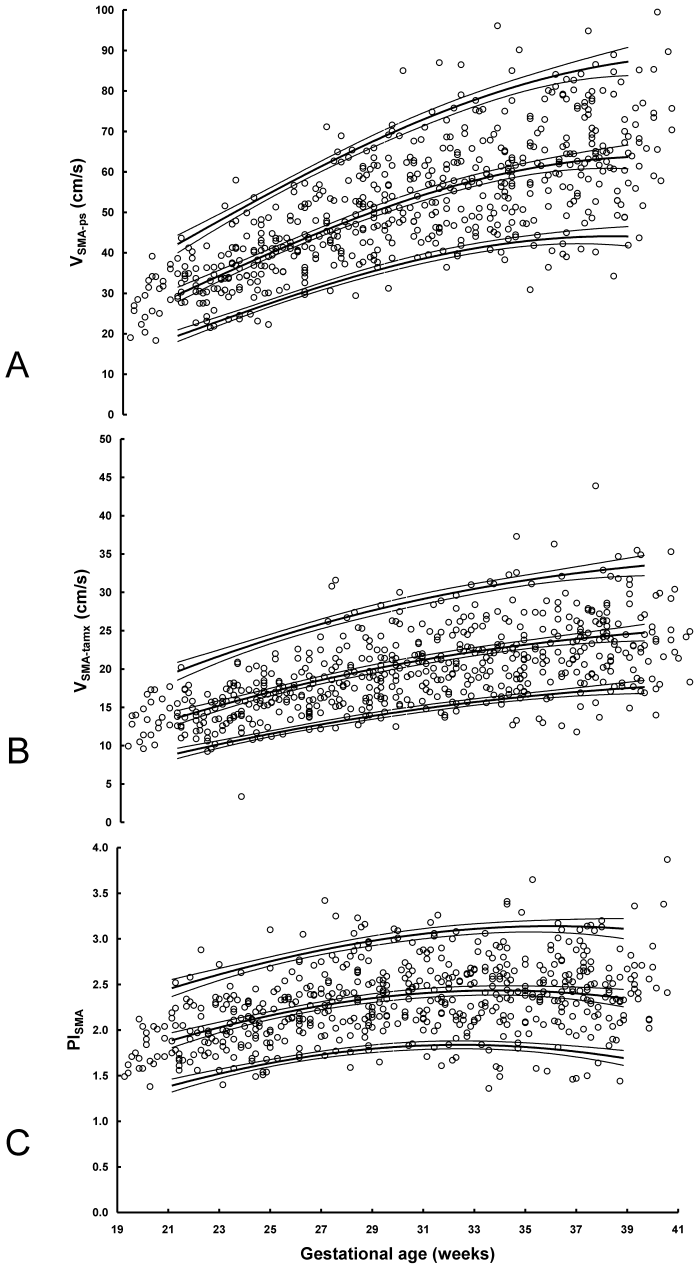

*Figure 17. Longitudinal reference ranges for the superior mesenteric artery systolic peak velocity (v_{SMAps}) (**A**), time-averaged maximum velocity ($v_{SMAtamx}$) (**B**) and pulsatility index (PI_{SMA}) (**C**) with fitted 5th, 50th and 95th centiles and 95% confidence limits for the centiles (thin lines), based on 589 observations*

We tested the hypothesis that port-caval pressure gradient affects PI_{SMA} using regression analyses. A low V_{DVps} was hypothesised to be associated with vasodilation of the SMA as indicated by a low PI_{SMA}. The analysis confirmed that fetuses with

V_{DVps} <10th centile had a lower PI_{SMA} ($P < 0.0001$), but the effects were small (PI_{SMA} variation 0.02–0.03).

5. Conclusions

In the present study, we constructed longitudinal reference ranges for the upper splanchnic arteries and the MCA and the cerebroplacental pulsatility ratio. The present ranges provide the terms for calculating conditional centiles based on a previous measurement in each individual fetus and are thus appropriate for both single and serial measurements in the monitoring of high-risk pregnancies.

Doppler assessment of the CA, SA and SMA can be achieved with a high success rate and with acceptable reproducibility during the second half of pregnancy.

The development of flow velocity in the fetal splanchnic arteries indicates increased perfusion of the splanchnic tissues towards the end of pregnancy.

We suggest the left branch of the HA close to the DV as a standard technique for Doppler assessment of fetal HA.

We found that low port-caval pressure gradient and UV liver perfusion is associated with low impedance (PI) in the HA, supporting the hypothesis that the HABR operates in the fetal liver.

Our study suggests that the SA and SMA also act to support fetal venous liver perfusion by feeding the PV through a vasodilated vasculature when UV perfusion is low (Figure 18).

We have shown that the regulation of the PI in the CA, SA and SMA (in contrast to the HA) is associated with the PI in the MCA and UA.

The UV return is the major contributor to liver perfusion in the fetus (85%), the main portal stem providing the rest (15%). This study suggests that hepatic perfusion is additionally modified by the interaction of the splanchnic arteries (Figure 18). Our reference ranges provide new methods for the differential assessment of the

developing circulation under physiological conditions and in clinical settings using serial measurements.

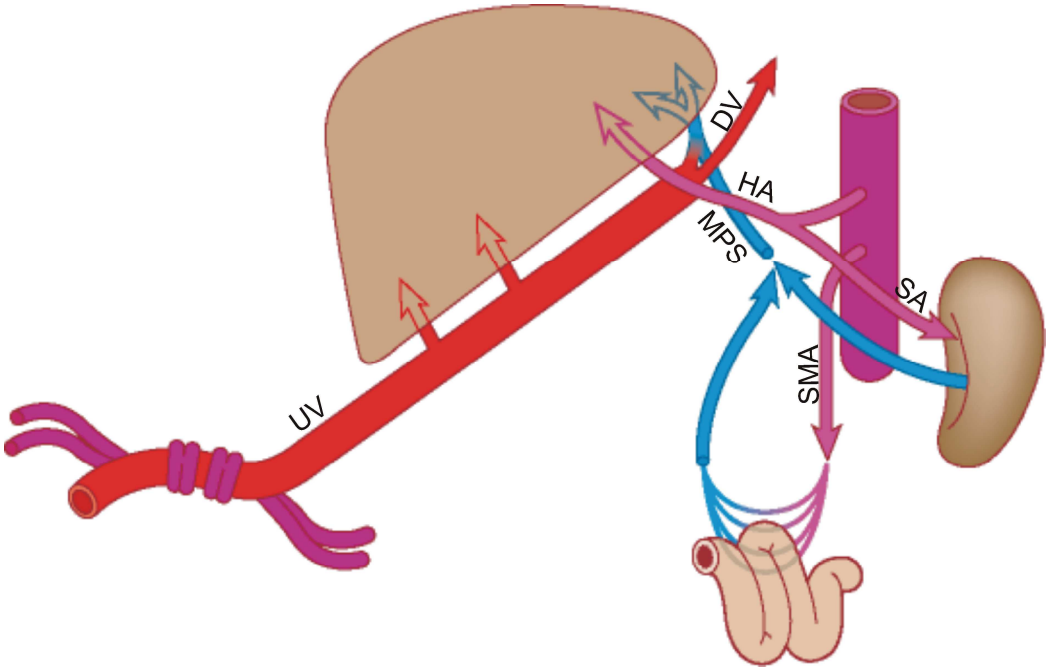

Figure 18: The umbilical vein (UV) is the main supplier of blood for perfusion of the fetal liver. The ductus venosus (DV) partly regulates this, and its blood velocity reflects the port-caval pressure gradient. The hepatic artery (HA) is directly connected to the liver tissue. The superior mesenteric artery (SMA) and splenic artery (SA) contribute to the portal flow through their capillary beds and main portal stem (MPS).

6. Future aspects

We assume that the hemodynamics of the splanchnic arteries will be affected in cases of placental compromise and in conditions that involve the function of the fetal liver and intestinal tract (infections, myeloproliferative infiltration, mitochondrial diseases, tumors, arteriovenous malformations and hemorrhage). Based on the present results, we expect differential responses and adaptation of the CA, HA, SA and SMA in such conditions. Observations suggest that the HA contribution increases in fetal growth restriction, at low UV perfusion and in conditions with increased hematopoietic demand. Likewise, we hypothesise that a regional splanchnic redistribution may occur in fetal growth restriction, possibly favouring splenic perfusion at the expense of the intestines.

We are accordingly conducting a study of 30 fetuses with growth restriction and 30 fetuses with accelerated growth to appreciate the dynamics of the extremes.

Recent studies have shown that maternal factors such as diet, body composition and weight gain affect venous liver flow and intrauterine growth and adaptation (Haugen et al 2005). Whether maternal factors and more immediate influences such as maternal meals are also reflected in alterations in the balance of the UV and splanchnic supply remains to be explored.

We hypothesise that the longitudinal reference ranges and conditional terms for Doppler parameters will improve the ability to identify the fetuses at greatest risk of developing clinically relevant adverse outcome, and we believe that more detailed knowledge of splanchnic adaptation before birth may explain some health differences concerning nutrition and metabolism in adult life.

7. References

Abuhamad, A. Z., G. Mari, D. Bogdan, and A. T. Evans. 1995. Doppler flow velocimetry of the splenic artery in the human fetus – is it a marker of chronic hypoxia? American Journal of Obstetrics and Gynecology 172:820-825.

Abuhamad, A. Z., G. Mari, R. M. Cortina, D. P. Croitoru, and A. T. Evans. 1997. Superior mesenteric artery Doppler velocimetry and ultrasonographic assessment of fetal bowel in gastroschisis: a prospective longitudinal study. American Journal of Obstetrics and Gynecology 176:985-990.

Acharya, G., T. Erkinaro, K. Makikallio, T. Lappalainen, and J. Rasanen. 2004. Relationships among Doppler-derived umbilical artery absolute velocities, cardiac function, and placental volume blood flow and resistance in fetal sheep. American Journal of Physiology – Heart and Circulatory Physiology 286:H1266-H1272.

Acharya, G., T. Wilsgaard, G. K. R. Berntsen, J. M. Maltau, and T. Kiserud. 2005a. Reference ranges for serial measurements of umbilical artery Doppler indices in the second half of pregnancy. American Journal of Obstetrics and Gynecology 192:937-944.

Acharya, G., T. Wilsgaard, G. K. R. Berntsen, J. M. Maltau, and T. Kiserud. 2005b. Doppler-derived umbilical artery absolute velocities and their relationship to fetoplacental volume blood flow: a longitudinal study. Ultrasound in Obstetrics & Gynecology 25:444-453.

Acharya, G., T. Wilsgaard, G. K. R. Berntsen, J. M. Maltau, and T. Kiserud. 2005c. Reference ranges for umbilical vein blood flow in the second half of pregnancy based on longitudinal data. Prenatal Diagnosis 25:99-111.

Achiron, R., R. Orvieto, S. Lipitz, S. Yagel, and Z. Rotstein. 1998. Superior mesenteric artery blood flow velocimetry: cross-sectional Doppler sonographic study in normal fetuses. Journal of Ultrasound in Medicine 17:769-773.

Alfirevic, Z. and J. P. Neilson. 1995. Doppler ultrasonography in high-risk pregnancies - systematic review with metaanalysis. American Journal of Obstetrics and Gynecology 172:1379-1387.

Anagnostou, V.K., I. Doussis-Anagnostopoulou, D.G. Tiniakos, D. Karandrea, E. Agapitos, P. Karakitsos, and C. Kittas. 2007. Ontogeny of intrinsic innervation in the human thymus and spleen. Journal of Histochemistry & Cytochemistry 55:813-820.

Angelsen, B.A.J., 2000. The Ultrasound Book. Pages 3-13. Ultrasound imaging, waves, signals and signal processing. Emantec, Trondheim, Norway.

Aoki, S., T. Hata, and M. Kitao. 1992. Ultrasonographic assessment of fetal and neonatal spleen. American Journal of Perinatology 9:361-367.

Arstrom, K., A. Eliasson, J. H. Hareide, and K. Marsal. 1989. Fetal blood velocity waveforms in normal pregnancies – a longitudinal-study. Acta Obstetricia et Gynecologica Scandinavica 68:171-178.

Bahado-Singh, R., U. Oz, O. Deren, E. Kovanchi, C. D. Hsu, M. J. Copel, and G. Mari. 2000. Splenic artery Doppler peak systolic velocity predicts severe fetal anemia in rhesus disease. American Journal of Obstetrics and Gynecology 182:1222-1226.

Bahlmann, F. 2002. Blood flow velocity waveforms of the fetal middle cerebral artery in a normal population: reference values from 18 weeks to 42 weeks of gestation. Journal of Perinatal Medicine 30:490-501.

Barclay, A.E., K.J. Franklin, and M.M.L. Prichard. 1945. The foetal circulation and cardiovascular system, and the changes that they undergo at birth. Charles C Thomas, Springfield, Illinois.

Barker, D. J. P. and M. A. Hanson. 2004. Altered regional blood flow in the fetus: the origins of cardiovascular disease? Acta Paediatrica 93:1559-1560.

Barnett, S. B. 2001. Intracranial temperature elevation from diagnostic ultrasound. Ultrasound in Medicine and Biology 27:883-888.

Baschat, A. A. 2003. The cerebroplacental Doppler ratio revisited. Ultrasound in Obstetrics & Gynecology 21:124-127.

Baschat, A. A., E. Cosmi, C. M. Bilardo, H. Wolf, C. Berg, S. Rigano, U. Germer, D. Moyano, S. Turan, J. Hartung, A. Bhide, T. Muller, S. Bower, K. H. Nicolaides, B. Thilaganathan, U. Gembruch, E. Ferrazzi, K. Hecher, H. L. Galan, and C. R. Harman. 2007. Predictors of neonatal outcome in early-onset placental dysfunction. Obstetrics and Gynecology 109:253-261.

Behrman, R. E., M. H. Lees, E. N. Peterson, C. W. Delannoy, and A. E. Seeds. 1970. Distribution of circulation in normal and asphyxiated fetal primate. American Journal of Obstetrics and Gynecology 108:956-969.

Bellotti, M., G. Pennati, C. De Gasperi, F. C. Battaglia, and E. Ferrazzi. 2000. Role of ductus venosus in distribution of umbilical blood flow in human fetuses during second half of pregnancy. American Journal of Physiology – Heart and Circulatory Physiology 279:H1256-H1263.

Bellotti, M., G. Pennati, C. De Gasperi, M. Bozzo, F. C. Battaglia, and E. Ferrazzi. 2004. Simultaneous measurements of umbilical venous fetal hepatic, and ductus venosus, blood flow in growth-restricted human fetuses. American Journal of Obstetrics and Gynecology 190:1347-1358.

Bennet, L., J. S. L. T. Quaedackers, A. J. Gunn, S. Rossenrode, and E. Heineman. 2000. The effect of asphyxia on superior mesenteric artery blood flow in the premature sheep fetus. Journal of Pediatric Surgery 35:34-40.

Bennet, L., L. Booth, S. C. Malpas, J. S. Quaedackers, E. Jensen, J. Dean, and A. J. Gunn. 2006. Acute systemic complications in the preterm fetus after asphyxia: role of cardiovascular and blood flow responses. Clinical and Experimental Pharmacology and Physiology 33:291-299.

Bilardo, C. M., H. Wolf, R. H. Stigter, Y. Ville, E. Baez, G. H. A. Visser, and K. Hecher. 2004. Relationship between monitoring parameters and perinatal outcome in severe, early intrauterine growth restriction. Ultrasound in Obstetrics & Gynecology 23:119-125.

Bland, J. M. and D. G. Altman. 1986. Statistical-methods for assessing agreement between 2 methods of clinical measurement. Lancet 1:307-310.

Bland, J. M. and D. G. Altman. 2003. Applying the right statistics: analyses of measurement studies. Ultrasound in Obstetrics & Gynecology 22:85-93.

Brander, L., S. M. Jakob, R. Knuesel, H. Savolainen, M. K. Widmer, J. Schmidli, and J. Takala. 2006. Effects of low abdominal blood flow and dobutamine on blood flow distribution and on the hepatic arterial buffer response in anaesthetized pigs. Shock 25:402-413.

Bristow, M. R., N. E. Kantrowitz, R. Ginsburg, and M. B. Fowler. 1985. Beta-adrenergic function in heart-muscle disease and heart-failure. Journal of Molecular and Cellular Cardiology 17:41-52.

Burrin, D.G. 2004. Physiology of the gastrointestinal tract in the fetus and neonate, trophic factors and regulation of gastointestinal tract and liver development. In Polin R.A., Fox W.W., and Abman S.H., eds. Fetal and Neonatal Physiology. Saunders, Philadelphia, Pennsylvania.

Capponi, A., G. Rizzo, D. Arduini, and C. Romanini. 1997. Splenic artery velocity waveforms in small-for-gestational-age fetuses: relationship with pH and blood gases measured in umbilical blood at cordocentesis. American Journal of Obstetrics and Gynecology 176:300-307.

Ceppa, EP, K. C. Fuh, G. B. Bulkley, and B. Gregory. 2003. Mesenteric hemodynamic response to circulatory shock. Current Opinion in Critical Care 9:127-132.

Chadburn, A. 2000. The spleen: anatomy and anatomical function. Seminars in Hematology 37:13-21.

Christensen, J. L., D. E. Wright, A. J. Wagers, and I. L. Weissman. 2004. Circulation and chemotaxis of fetal hematopoietic stem cells. Plos Biology 2:368-377.

Clark, D.A. and U.K. Munshi. 2004. Development of the gastrointestinal circulation in the fetus and newborn. Pages 701-704 In Polin R.A., Fox W.W., and Abman S.H., eds. Fetal and Neonatal Physiology. Saunders, Philadelphia, Pennsylvania.

Coceani, F. and P. M. Olley. 1988. The control of cardiovascular shunts in the fetal and perinatal-period. Canadian Journal of Physiology and Pharmacology 66:1129-1134.

Combs, C. A., R. K. Jaekle, B. Rosenn, M. Pope, M. Miodovnik, and T. A. Siddiqi. 1993. Sonographic estimation of fetal weight based on a model of fetal volume. Obstetrics and Gynecology 82:365-370.

Cozzi, F. and A.W. Wilkinson. 1969. Intrauterine growth rate in relation to anorectal and oesophageal anomalies. Archives of Disease in Childhood 44:59-62.

Cumano, A. and I. Godin. 2007. Ontogeny of the hematopoietic system. Annual Review of Immunology 25:745-785.

Dawes, G.S. 1994. Fetal physiology: Historical Perspectives. In Thorburn G.D. and Harding R, eds. Textbook of Fetal Physiology. Oxford University Press, Oxford.

Despopoulos, A. and S. Silbernagl. 1986. Heart and Circulation. In Colour Atlas of Physiology. Thieme Inc, Stuttgart-New York.

Dubiel, M., P. Korszun, G. Breborowicz, and S. Gudmundsson. 2001. Fetal hepatic artery blood flow velocimetry in normal and high-risk pregnancies. Prenatal and Neonatal Medicine 6:151-156.

Edelstone, D. I., A. M. Rudolph, and M. A. Heymann. 1978. Liver and ductus venosus blood flows in fetal lambs in utero. Circulation Research 42:426-433.

Edelstone, D. I., A. M. Rudolph, and M. A. Heymann. 1980. Effects of hypoxemia and decreasing umbilical flow on liver and ductus venosus blood flows in fetal lambs. American Journal of Physiology 238:H656-H663.

Ezzat, W. R. and W. W. Lautt. 1987. Hepatic arterial pressure-flow autoregulation is adenosine mediated. American Journal of Physiology 252:H836-H845.

Ferrari, R., C. N. De Cecco, F. Iafrate, P. Paolantonio, M. Rengo, and A. Laghi. 2007. Anatomical variations of the coeliac trunk and the mesenteric arteries evaluated with 64-row CT angiography. Radiologia Medica 112:988-998.

Fouron, J. C. 2003. The unrecognized physiological and clinical significance of the fetal aortic isthmus. Ultrasound in Obstetrics & Gynecology 22:441-447.

Froelich, J. W., H. W. Strauss, R. H. Moore, and K. A. Mckusick. 1988. Redistribution of visceral blood-volume in upright exercise in healthy-volunteers. Journal of Nuclear Medicine 29:1714-1718.

Geboes, K., K. P. Geboes, and G. Maleux. 2001. Vascular anatomy of the gastrointestinal tract. Best Practice & Research in Clinical Gastroenterology 15:1-14.

Giles, W. B., B. J. Trudinger, and P. J. Baird. 1985. Fetal umbilical artery flow velocity waveforms and placental resistance – pathological correlation. British Journal of Obstetrics and Gynaecology 92:31-38.

Gosling, R. and D. King. 1975. Ultrasound angiology. In A. Macus and J. Adamson, eds. Arteries and Veins. Churchill-Livingstone, Edinburgh.

Gouysse, G., A. Couvelard, S. Frachon, R. Bouvier, M. Nejjari, M. C. Dauge, G. Feldmann, D. Henin, and J. Y. Scoazec. 2002. Relationship between vascular development and vascular differentiation during liver organogenesis in humans. Journal of Hepatology 37:730-740.

Gramellini, D., M. C. Folli, S. Raboni, E. Vadora, and A. Merialdi. 1992. Cerebral-umbilical doppler ratio as a predictor of adverse perinatal outcome. Obstetrics and Gynecology 79:416-420.

Greenway, C. V. and R. D. Stark. 1971. Hepatic vascular bed. Physiological Reviews 51:23-65.

Greisen, G. 2005. Autoregulation of cerebral blood flow in newborn babies. Early Human Development 81:423-428.

Gudmundsson, S. and K. Marsal. 1988. Umbilical artery and uteroplacental blood-flow velocity waveforms in normal-pregnancy – a cross-sectional study. Acta Obstetricia et Gynecologica Scandinavica 67:347-354.

Gulberg, V., K. Haag, M. Rossle, and A. L. Gerbes. 2002. Hepatic arterial buffer response in patients with advanced cirrhosis. Hepatology 35:630-634.

Gunther, S., M. A. Gimbrone, and R. W. Alexander. 1980. Identification and characterization of the high-affinity vascular angiotensin-II receptor in rat mesenteric-artery. Circulation Research 47:278-286.

Habek, D., D. Jugovic, B. Hodek, R. Herman, A. Maticevic, J. C. Habek, Z. Pisl, and A. Salihagic. 2004. Fetal biophysical profile and cerebro-umbilical ratio in assessment of brain damage in growth restricted fetuses. European Journal of Obstetrics Gynecology and Reproductive Biology 114:29-34.

Hanif, F., K. Drennan, and G. Mari. 2007. Variables that affect the middle cerebral artery peak systolic velocity in fetuses with anemia and intrauterine growth restriction. American Journal of Perinatology 24:501-505.

Harrington, K., R. G. Carpenter, M. Nguyen, and S. Campbell. 1995. Changes observed in Doppler studies of the fetal circulation in pregnancies complicated by preeclampsia or the delivery of a small-for-gestational-age baby. 1. Cross-sectional analysis. Ultrasound in Obstetrics & Gynecology 6:19-28.

Haugen, G.,M. Hanson, T. Kiserud, S. Crozier, H. Inskip, K. M. Godfrey. 2005. Fetal liver-sparing cardiovascular adaptations linked to mother's slimness and diet. Circulation Research 96:12-14.

Hecher, K., C. M. Bilardo, R. H. Stigter, Y. Ville, B. J. Hackeloer, H. J. Kok, M. V. Senat, and G. H. A. Visser. 2001. Monitoring of fetuses with intrauterine growth restriction: a longitudinal study. Ultrasound in Obstetrics & Gynecology 18:564-570.

Horst, D.A. and S.J. Karpen. 2004. Bile formation and cholestatis. In Polin R.A., Fox W.W., and Abman S.H., eds. Fetal and Neonatal Physiology. Saunders, Philadelphia, Pennsylvania.

Itskovitz-Eldor, J. and T. Israel. 2005. Fetal and maternal cardiovascular physiology. In Maulik D., ed. Doppler Ultrasound in Obstetrics and Gynecology. Springer-Verlag, New York.

Iwao, T., A. Toyonaga, H. Shigemori, K. Oho, T. Sakai, C. Tayama, H. Masumoto, M. Sato, and K. Tanikawa. 1996. Hepatic artery hemodynamic responsiveness to altered portal blood flow in normal and cirrhotic livers. Radiology 200:793-798.

Jensen, A. and M. A. Hanson. 1995. Circulatory responses to acute asphyxia in intact and chemodenervated fetal sheep near term. Reproduction, Fertility and Development 7:1351-1359.

Jensen, A., C. Roman, and A. M. Rudolph. 1991. Effects of reducing uterine blood-flow on fetal blood-flow distribution and oxygen delivery. Journal of Developmental Physiology 15:309-323.

Johnsen, S. L., S. Rasmussen, R. Sollien, T. Kiserud. 2004. Fetal age assessment based on ultrasound head biometry and the effect of maternal and fetal factors. Acta Obstetricia et Gynecologica Scandinavica 83:716-723.

Johnsen, S. L., S. Rasmussen, T. Wilsgaard, R. Sollien, and T. Kiserud. 2006. Longitudinal reference ranges for estimated fetal weight. Acta Obstetricia et Gynecologica Scandinavica 85:286-297.

Johnson, P., D. J. Maxwell, M. J. Tynan, and L. D. Allan. 2000. Intracardiac pressures in the human fetus. Heart 84:59-63.

Kessler, J., S. Rasmussen, and T. Kiserud 2007a. The left portal vein as an indicator of watershed in the fetal circulation: development during the second half of pregnancy and a suggested method of evaluation. Ultrasound in Obstetrics & Gynecology 30:757-764.

Kessler, J., S. Rasmussen, and T. Kiserud. 2007b. The fetal portal vein: normal blood flow development during the second half of human pregnancy. Ultrasound in Obstetrics & Gynecology 30:52-60.

Kessler, J., S. Rasmussen, K. Godfrey, M. Hanson, and T. Kiserud. 2008. Longitudinal study of umbilical and portal venous blood flow to the fetal liver: low pregnancy weight gain is associated with preferential supply to the left fetal liver lobe. Pediatric Research;63:315-20.

Kilavuz, O. and K. Vetter. 1999. Is the liver of the fetus the 4th preferential organ for arterial blood supply besides brain, heart, and adrenal glands? Journal of Perinatal Medicine 27:103-106.

Kiserud, T. and S. Rasmussen. 1998. How repeat measurements affect the mean diameter of the umbilical vein and the ductus venosus. Ultrasound in Obstetrics & Gynecology 11:419-425.

Kiserud, T., S. H. Eiknes, H. G. K. Blaas, and L. R. Hellevik. 1991. Ultrasonographic velocimetry of the fetal ductus venosus. Lancet 338:1412-1414.

Kiserud, T., L. R. Hellevik, S. H. Eiknes, B. A. J. Angelsen, and H. G. Blaas. 1994a. Estimation of the pressure-gradient across the fetal ductus venosus based on Doppler velocimetry. Ultrasound in Medicine and Biology 20:225-232.

Kiserud, T., S. H. Eiknes, H. G. Blaas, L. R. Hellevik, and B. Simensen. 1994b. Ductus venosus blood velocity and the umbilical circulation in the seriously growth-retarded fetus. Ultrasound in Obstetrics & Gynecology 4:109-114.

Kiserud, T., S. Rasmussen, and S. Skulstad. 2000. Blood flow and the degree of shunting through the ductus venosus in the human fetus. American Journal of Obstetrics and Gynecology 182:147-153.

Kiserud, T., C. Ebbing, J. Kessler, and S. Rasmussen. 2006a. Fetal cardiac output, distribution to the placenta and impact of placental compromise. Ultrasound in Obstetrics & Gynecology 28:126-136.

Kiserud, T., J. Kessler, C. Ebbing, and S. Rasmussen. 2006b. Ductus venosus shunting in growth-restricted fetuses and the effect of umbilical circulatory compromise. Ultrasound in Obstetrics & Gynecology 28:143-149.

Konje, J. C., S. C. Bell, and D. J. Taylor. 2001. Abnormal Doppler velocimetry and blood flow volume in the middle cerebral artery in very severe intrauterine growth restriction: is the occurrence of reversal of compensatory flow too late? British Journal of Obstetrics and Gynaecology 108:973-979.

Korszun, P., M. Dubiel, G. Breborowicz, A. Danska, and S. Gudmundsson. 2002. Fetal superior mesenteric artery blood flow velocimetry in normal and high-risk pregnancy. Journal of Perinatal Medicine 30:235-241.

Kunisaki SM, Azpurua H, Fuchs JR, Graves SC, Zurakowski D, and Fauza DO. 2006. Fetal hepatic haematopoiesis is modulated by arterial blood flow to the liver. British Journal of Haematology 134:330-332.

Kurmanavicius, J., A. Streicher, E. M. Wright, J. Wisser, R. Muller, P. Royston, R. Huch, A. Huch, and R. Zimmermann. 2001. Reference values of fetal peak systolic blood flow velocity in the middle cerebral artery at 19-40 weeks of gestation. Ultrasound in Obstetrics & Gynecology 17:50-53.

Kurth, C. D. and L. C. Wagerle. 1992. Cerebrovascular reactivity to adenosine-analogs in 0.6-0.7 gestation and near-term fetal sheep. American Journal of Physiology 262:H1338-H1342.

Lammert, E., O. Cleaver, and D. Melton. 2003. Role of endothelial cells in early pancreas and liver development. Mechanisms of Development 120:59-64.

Lautt, W. W. 1996. The 1995 Ciba-Geigy Award Lecture. Intrinsic regulation of hepatic blood flow. Canadian Journal of Physiology and Pharmacology 74:223-233.

Lautt, W. W. 2007. Regulatory processes interacting to maintain hepatic blood flow constancy: vascular compliance, hepatic arterial buffer response, hepatorenal reflex, liver regeneration, escape from vasoconstriction. Hepatology Research 37:891-903.

Lobritto, S., 2004. Organogenesis and histologic development of the liver. In Polin RA, Fox WW, and Abman SH, eds. Fetal and Neonatal Physiology. Saunders, Philadelphia, Pennsylvania.

Makh, D. S., C. R. Harman, and A. A. Baschat. 2003. Is Doppler prediction of anemia effective in the growth-restricted fetus? Ultrasound in Obstetrics & Gynecology 22:489-492.

Mari, G. 2000. Noninvasive diagnosis by Doppler ultrasonography of fetal anemia due to maternal red-cell alloimmunization. New England Journal of Medicine 342:9-14.

Mari, G. and R. L. Deter. 1992. Middle cerebral-artery flow velocity wave-forms in normal and small-for-gestational-age fetuses. American Journal of Obstetrics and Gynecology 166:1262-1270.

Mari, G., A. Z. Abuhamad, E. Cosmi, M. Segata, M. Altaye, and M. Akiyama. 2005. Middle cerebral artery peak systolic velocity – technique and variability. Journal of Ultrasound in Medicine 24:425-430.

Mari, G., F. Hanif, M. Kruger, E. Cosmi, J. Santolaya-Forgas, and M. C. Treadwell. 2007. Middle cerebral artery peak systolic velocity: a new Doppler parameter in the assessment of growth-restricted fetuses. Ultrasound in Obstetrics & Gynecology 29:310-316.

Marsal, K. 2005. The output display standard: has it missed its target? Ultrasound in Obstetrics & Gynecology 25:211-214.

Martinussen, M., J.-P. Odden, A. M. Brubakk, T. Vik, D. Bratlid, and A. C. Yao. 1996. Validity of Doppler measurements of superior mesenteric artery blood flow velocity: comparison with blood flow measured by microsphere technique. European Journal of Ultrasound 4:55-62.

Martinussen, M., A. M. Brubakk, D. T. Linker, T. Vik, and A. C. Yao. 1994. Mesenteric blood-flow velocity and its relation to circulatory adaptation during the first-week of life in healthy term infants. Pediatric Research 36:334-339.

Martinussen, M., A. M. Brubakk, T. Vik, and A. C. Yao. 1997. Relationship between intrauterine growth retardation and early postnatal superior mesenteric artery blood flow velocity. Biology of the Neonate 71:22-30.

Maulik, D., 2005. Physical principles of Doppler ultrasonography. In Maulik D., ed. Doppler Ultrasound in Obstetrics and Gynecology. Springer-Verlag, New York.

McLellan, K. C., A. D. Bocking, S. E. White, and V. K. M. Han. 1995. Placental and fetal hepatic growth are selectively inhibited by prolonged reductions of uterine blood-flow in pregnant sheep. Reproduction, Fertility and Development 7:405-410.

Meerman, R. J., F. Vanbel, P. H. T. Vanzwieten, D. Oepkes, and L. Denouden. 1990. Fetal and neonatal cerebral blood velocity in the normal fetus and neonate – a longitudinal Doppler ultrasound study. Early Human Development 24:209-217.

Michels, N. A. 1966. Newer anatomy of liver and its variant blood supply and collateral circulation. American Journal of Surgery 112:337-347.

Mielke, G. and N. Benda. 2001. Cardiac output and central distribution of blood flow in the human fetus. Circulation 103:1662-1668.

Mikkola, H. K. A., C. Gekas, S. H. Orkin, and F. Dieterlen-Lievre. 2005. Placenta as a site for hematopoietic stem cell development. Experimental Hematology 33:1048-1054.

Murdoch, E. M., G. C. S. Smith, A. K. Sinha, S. T. Shanmugalingam, and S. T. Kempley. 2006. Neonatal necrotizing enterocolitis is associated with high resistance flow in the superior mesenteric artery on day 1 of life in preterm infants. Early Human Development 82:618-619.

Nava, S., M. Westgren, M. Jaksch, A. Tibell, U. Broome, B. G. Ericzon, and S. Sumitran-Holgersson. 2005. Characterization of cells in the developing human liver. Differentiation 73:249-260.

Oepkes, D., R. H. Meerman, F. P. H. A. Vandenbussche, I. L. Vankamp, F. G. Kok, and H. H. H. Kanhai. 1993. Ultrasonographic fetal spleen measurements in red-blood-cell alloimmunized pregnancies. American Journal of Obstetrics and Gynecology 169:121-128.

Pearce, W. 2006. Hypoxic regulation of the fetal cerebral circulation. Journal of Applied Physiology 100:731-738.

Perko, M. J. 2001. Duplex ultrasound for assessment of superior mesenteric artery blood flow. European Journal of Vascular and Endovascular Surgery 21:106-117.

Perko, M. J., G. Perko, S. Just, N. H. Secher, and T. V. Schroeder. 1996. Changes in superior mesenteric artery Doppler waveform during reduction of cardiac stroke volume and hypotension. Ultrasound in Medicine and Biology 22:11-18.

Pickelsheimer, A.H., D. Oepkes, K. Moise, Kush M.L, Weiner C.P., C. R. Harman, and A. A. Baschat. 2007. Determinants of the middle cerebral artery peak systolic velocity in the human fetus. American Journal of Obstetrics and Gynecology 197:526.e1-526.e4.

Quaedackers, J. S., V. Roelfsema, E. Heineman, A. J. Gunn, and L. Bennet. 2004. The role of the sympathetic nervous system in postasphyxial intestinal hypoperfusion in the pre-term sheep fetus. Journal of Physiology-London 557:1033-1044.

Raio, L., F. Ghezzi, E. Di Naro, M. Franchi, D. Balestreri, P. Durig, and H. Schneider. 2001. In-utero characterization of the blood flow in the Hyrtl anastomosis. Placenta 22:597-601.

Richardson, B. S., D. Rurak, J. E. Patrick, J. Homan, and L. Carmichael. 1989. Cerebral oxidative-metabolism during sustained hypoxemia in fetal sheep. Journal of Developmental Physiology 11:37-43.

Robel-Tillig, E., C. Vogtmann, and J. Bennek. 2002. Prenatal hemodynamic disturbances – pathophysiological background of intestinal motility disturbances in small for gestational age infants. European Journal of Pediatric Surgery 12:175-179.

Rocheleau, B., C. Ethier, R. Houle, P. M. Huet, and M. Bilodeau. 1999. Hepatic artery buffer response following left portal vein ligation: its role in liver tissue homeostasis. American Journal of Physiology – Gastrointestinal and Liver Physiology 277:G1000-G1007.

Rouwet, E. V., J. G. R. De Mey, D. W. Slaaf, E. Heineman, G. Ramsay, and F. A. C. Le Noble. 2000. Development of vasomotor responses in fetal mesenteric arteries. American Journal of Physiology – Heart and Circulatory Physiology 279:H1097-H1105.

Royston, P. 1995. Calculation of unconditional and conditional reference intervals for fetal size and growth from longitudinal measurements. Statistics in Medicine 14:1417-1436.

Royston, P. and D. G. Altman. 1995. Design and analysis of longitudinal-studies of fetal size. Ultrasound in Obstetrics & Gynecology 6:307-312.

Royston, P. and E. M. Wright. 1998. How to construct "normal ranges" for fetal variables. Ultrasound in Obstetrics & Gynecology 11:30-38.

Rudolph, A. M. and M. A. Heymann. 1967. Circulation of fetus in utero – methods for studying distribution of blood flow cardiac output and organ blood flow. Circulation Research 21:163-184.

Rudolph, A. M., M. A. Heymann, K. A. W. Teramo, C. T. Barrett, and N. C. R. Raiha. 1971. Studies on the circulation of previable human fetus. Pediatric Research 5:452-465.

Rudolph, A. M., 1985. Distribution and regulation of blood flow in the fetal and neonatal lamb. Circulation Research 57:811-821.

Sadler TW. 1985a. Embryonic period. In Langman's Medical Embryology. Williams & Wilkins, Baltimore, Maryland.

Sadler, TW. 1985b. Cardiovascular system. In Langman's Medical Embryology. Williams & Wilkins, Baltimore, Maryland.

Salvesen, K. A. 2007. Epidemiological prenatal ultrasound studies. Progress in Biophysics & Molecular Biology 93:295-300.

Scherjon, S., J. Briet, H. Oosting, and J. Kok. 2000. The discrepancy between maturation of visual-evoked potentials and cognitive outcome at five years in very preterm infants with and without hemodynamic signs of fetal brain-sparing. Pediatrics 105:385-391.

Skjaerven, R., H. K. Gjessing, and L. S. Bakketeig. 2000. Birthweight by gestational age in Norway. Acta Obstetricia et Gynecologica Scandinavica 79:440-449.

Stuart, B., J. Drumm, D. E. Fitzgerald, and N. M. Duignan. 1980. Fetal blood velocity waveforms in normal-pregnancy. British Journal of Obstetrics and Gynaecology 87:780-785.

Sutton, M.S.J., T. Plappert, and P. Doubilet. 1991. Relationship between placental blood flow and combined ventricular output with gestational age in normal fetuses. Cardiovascular Research 25:603-608.

Tarantal, A. F., F. Chu, W. D. O'Brien, and A. G. Hendrickx. 1993. Sonographic heat-generation in vivo in the gravid long-tailed macaque (*Macaca fascicularis*). Journal of Ultrasound in Medicine 12:285-295.

Tchirikov, M., C. Rybakowski, B. Huneke, and H. J. Schroder. 1998. Blood flow through the ductus venosus in singleton and multifetal pregnancies and in fetuses with intrauterine growth retardation. American Journal of Obstetrics and Gynecology 178:943-949.

Tchirikov, M., S. Kertschanska, and H. J. Schroder. 2001. Obstruction of ductus venosus stimulates cell proliferation in organs of fetal sheep. Placenta 22:24-31.

Tchirikov, M., S. Kertschanska, H. J. Sturenberg, and H. J. Schroder. 2002. Liver blood perfusion as a possible instrument for fetal growth regulation. Placenta 23:S153-S158.

Tchirikov, M., S. Kertschanska, and H. J. Schroder. 2003. Differential effects of catecholamines on vascular rings from ductus venosus and intrahepatic veins of fetal sheep. Journal of Physiology – London 548:519-526.

Tchirikov, M., N. E. Schlabritz-Loutsevitch, G. B. Hubbard, H. J. Schroder, and P. W. Nathanielsz. 2005. Structural evidence for mechanisms to redistribute hepatic and ductus venosus blood flows in nonhuman primate fetuses. American Journal of Obstetrics and Gynecology 192:1146-1152.

Trahair, J. 2001. Digestive system. In Harding R and Bocking A.D, eds. Fetal Growth and Development. Press Syndicate of the University of Cambridge, Cambridge.

Trahair, J. and P. T. Sangild. 2000. Fetal organ growth in response to oesophagal infusion of amniotic fluid, colostrum, milk or gastrin-releasing peptide:a study in fetal sheep. Reproduction, Fertility and Development 12:87-95.

Vellguth, S., B. Vongaudecker, and H. K. Mullerhermelink. 1985. The development of the human spleen – ultrastructural studies in fetuses from the 14th to 24th week of gestation. Cell and Tissue Research 242:579-592.

Verburg, B. O., V. W. Jaddoe, J. W. Wladimiroff, A. Hofman, J. C. Witteman, and E. A. Steegers. 2008. Fetal hemodynamic adaptive changes related to intrauterine growth. Circulation (in press) DOI:10.1161/CIRCULATTIONAHA.107.709717.

Ville, Y., I. Sideris, K. Hecher, R. J. M. Snijders, and K. H. Nicolaides. 1994. Umbilical venous-pressure in normal, growth-retarded, and anemic fetuses. American Journal of Obstetrics and Gynecology 170:487-494.

Vyas, S., K. H. Nicolaides, S. Bower, and S. Campbell. 1990. Middle cerebral-artery flow velocity wave-forms in fetal hypoxemia. British Journal of Obstetrics and Gynaecology 97:797-803.

Weiner, C. P. 1990. The relationship between the umbilical artery systolic diastolic ratio and umbilical blood-gas measurements in specimens obtained by cordocentesis. American Journal of Obstetrics and Gynecology 162:1198-1202.

Weinstein, B. 2002. Building the house around the plumbing. Bioessays 24:397-400.

Wladimiroff, J. W., H. M. Tonge, and P. A. Stewart. 1986. Doppler ultrasound assessment of cerebral blood-flow in the human-fetus. British Journal of Obstetrics and Gynaecology 93:471-475.

Wolf, B. C., E. Luevano, and R. S. Neiman. 1983. Evidence to suggest that the human-fetal spleen is not a hematopoietic organ. American Journal of Clinical Pathology 80:140-144.

Zimmermann, R., P. Durig, R. J. Carpenter, and G. Mari. 2002. Longitudinal measurement of peak systolic velocity in the fetal middle cerebral artery for monitoring pregnancies complicated by red cell alloimmunisation: a prospective multicentre trial with intention-to-treat. BJOG: An International Journal of Obstetrics and Gynaecology 109:746-752.

Ziskin, M. C. and S. B. Barnett. 2001. Ultrasound and the developing central nervous system. Ultrasound in Medicine and Biology 27:875-876.

Errata

Article III:

Third paragraph page 10: reference no 24 should be 25

Reference list:

Reference 14 should be:

Murdoch EM, Sinah AK, Shanmugalingam ST, Smith GCS, Kempley ST. Doppler flow velocimetry in the superior mesenteric artery on the first day of life of preterm infants and the risk of neonatal necrotizing enterocolitis. Pediatrics 2006;118:1999-2003.

Reference 22 should be:

Mari G, Abuhamad AZ, Cosmi E, Segata M, Altaye M, Akiyama M. Middle cerebral artery peak systolic velocity- Technique and variability. *J Ultrasound Med* 2005;24:425-430.

Reference 26 and 14 should be identical and only be listed once (14).

Reference 27 should exchange number with reference 29.

Article IV:

Table 4, first row, fifth column (*Intraobserver variation, PSV upper*):–0.31 should be 0.31.

Original articles

Article I

Hepatic Artery Hemodynamics Suggest Operation of a Buffer Response in the Human Fetus

Cathrine Ebbing, MD, Svein Rasmussen, MD, PhD, Keith M. Godfrey, BM, PhD, FRCP, Mark A. Hanson, DPhil, and Torvid Kiserud, MD, PhD

After birth, the hepatic artery buffer response helps to maintain liver perfusion. Here, the authors establish a Doppler technique to measure fetal hepatic artery flow velocity and test the hypothesis that the buffer response also operates prenatally. Women with low-risk pregnancies were recruited to a longitudinal study (N = 161). Measurement techniques and reference ranges for hepatic artery velocities and pulsatility index (PI) were established. Ductus venosus peak velocity (V_{DVps}) represented the portocaval pressure gradient, and umbilical venous flow (Q_{UV}) represented portal flow. Reference ranges were established for the more accessible left hepatic artery branch. Hepatic artery PI was lower in fetuses with V_{DVps} <10th centile (P < .05) and in those with Q_{UV} <10th centile (P < .0001). Conversely, hepatic artery PI was higher in those with Q_{UV} >90th centile (P < .0001). The authors establish a method for measuring fetal hepatic arterial blood velocity, provide reference ranges, and show that the hepatic artery buffer response operates prenatally.

Key words: Fetus, circulation, blood flow, Doppler, hepatic artery, reference ranges, hepatic artery buffer response.

The placenta, crucial for fetal development, receives one-third to one-fifth of the combined cardiac output through the umbilical arteries.[1] However, when nutrient-rich blood returns to the fetal body, it is the liver that has the highest priority, taking 75% to 80% of it.[2] The fetal liver has 2 additional important blood supplies: one is the portal vein, connected to the umbilical vein (UV) through the left portal branch and contributing 20% of the venous supply,[3,4] and the other is the hepatic artery, which is the focus of this study (Figure 1). The arterial contribution to the liver circulation in the human fetus is not known, but fetal sheep data suggest that it is <10%.[5]

The prominent role of the liver in fetal growth has been demonstrated in experimental studies that increase umbilical venous liver perfusion; this results in increased proliferation of fetal hepatocytes,[6] greater expression of insulin-like growth factor 1 and 2 mRNA, and increased fetal growth.[7] A study of human fetuses in late pregnancy has suggested that maternal body composition and diet may modify this distribution of umbilical venous blood to the liver.[8]

Venous perfusion of the fetal liver is strongly influenced by variations in pressure and blood viscosity[9,10] but is also actively controlled by changes in the portal vasculature[11,12] and ductus venosus (DV).[13,14] Umbilical pressure in the human fetus is 2 to 11 mm Hg,[15] and the portal perfusion pressure has been calculated to vary between 0.5 mm Hg and 3.5 mm Hg during the cardiac cycle,[16] which is in line with direct measurements in fetal sheep.[17]

Although the hepatic artery has a modest contribution to the liver blood supply, it plays an important role in maintaining total liver perfusion postnatally.[18,19] The mechanism is termed *hepatic arterial buffer response* and is an adenosine-mediated vasodilatation in the hepatic artery. A reduced portal liver perfusion leads to a reduced washout and a corresponding local increase in adenosine concentrations,

From the Department of Clinical Medicine, University of Bergen, Norway (CE, SR, TK); Department of Obstetrics and Gynecology, Haukeland University Hospital, Bergen, Norway (CE, SR, TK); Medical Birth Registry of Norway, Locus of Registry Based Epidemiology, University of Bergen and the Norwegian Institute of Public Health, Bergen, Norway (SR); and Division of Developmental Origins of Health and Disease, University of Southampton, Southampton, UK (KMG, MAH).

The study was supported by the Western Norway Regional Health Authority (grant 911160). M.A.H. is supported by the British Heart Foundation.

Address correspondence to: Cathrine Ebbing, Department of Obstetrics and Gynecology, Haukeland University Hospital, N-5021 Bergen, Norway. E-mail: cathrine.ebbing@molmed.uib.no

Reproductive Sciences Vol. 15 No. 2 February 2008 166-178
DOI. 10.1177/1933719107310307

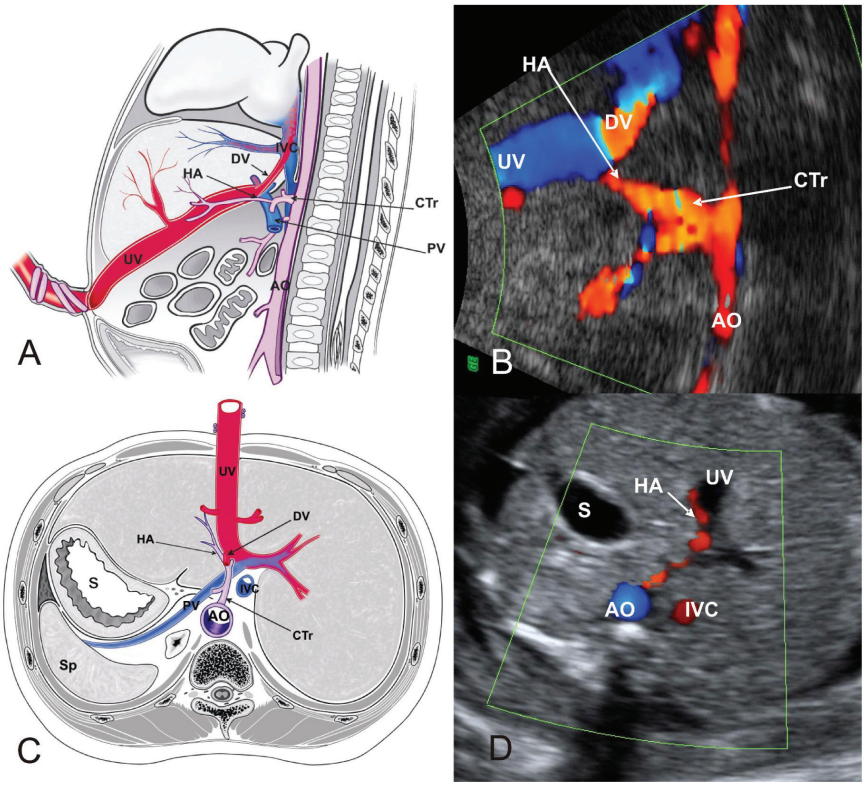

Figure 1. Fetal vasculature of the upper abdomen and the corresponding ultrasound images in sagittal (A and B) and horizontal views (C and D). The common hepatic artery (HA) arises from the celiac trunk (CTr); its left branch can be visualized as it approaches the ductus venosus (DV) to continue distally to the left of the intrahepatic umbilical vein (UV) and has a direction of flow opposite to that in the neighboring DV and UV. AO indicates aorta, PV, main portal stem; IVC, inferior vena cava; Sp, spleen; and S, stomach.

which in turn cause an instantaneous reduction in arterial impedance, even during generalized splanchnic vasoconstriction due to hemorrhage and hypovolemia.[20] Whether this mechanism operates during prenatal life is not known, but Doppler measurements in growth-restricted fetuses suggest that a similar response may exist.[21,22] However, there is little information about the fetal hepatic artery in normal pregnancies, and standardized measurement techniques have not been described.

The aim of this study is to establish a standardized technique for measuring blood velocity in the hepatic artery, to establish reference ranges, and to test the hypothesis that the hepatic artery buffer response can operate prenatally.

METHODS

Participants

Twenty-seven women were recruited for a pilot study, after which 161 women with low-risk pregnancies were recruited to a larger prospective longitudinal observational study of the cerebral, splanchnic, and umbilical circulations. The Regional Committee for Medical Research Ethics approved the study protocol (REK Vest no. 203.03), and all participants gave prior written consent. We have previously presented the results of the middle cerebral and umbilical artery measurements.[23] Here, we present arterial and venous data from the study of liver perfusion.

Gestational age had been assessed by head biometry[24] at the routine ultrasound scan at 17 to 20 weeks of gestation. Those who agreed to participate entered the study at a median of 23 weeks of gestation (range, 19-28 weeks). Reasons for not being enrolled were multiple pregnancy, fetal abnormality, any maternal chronic disease, and a previous history of pregnancy-induced hypertension, fetal growth restriction, placental abruption, or delivery before 37 weeks. Each woman was examined 3 to 5 times, at 3-week to 5-week intervals.

Birth weight, gender, placental weight, Apgar score, mode of delivery, duration of gestation at delivery, and congenital abnormalities were noted.

Measurements

In the pilot study, we sought to visualize the branches from the celiac trunk directed to the fetal liver using color Doppler. The celiac trunk branches off from the aorta and divides into the left gastric, splenic, and common hepatic artery. The splenic artery was regularly identified traversing behind the stomach, while the common hepatic artery was less obvious, running along the portal vein before dividing into the left and right hepatic artery (Figure 1). Flow in the common hepatic artery and the right branch has the same direction as the neighboring main portal stem and right portal vein, causing interference in the corresponding pulsed Doppler recording, making these sites less suitable for the assessment (Figure 2). However, the left branch of the hepatic artery could be visualized as it approached the DV to continue distally to the left of the intrahepatic UV (Figure 1). Since blood in the left branch of the hepatic artery flows in the opposite direction than that in the neighboring DV and UV (Figure 1), the Doppler recording at this point can be analyzed without interference and was chosen as the standard technique for the present study.

We used a 2-5, 2-7, or 4-8 MHz abdominal transducer (Voluson 730 Expert; GE Medical Systems, Kretz Ultrasound, Zipf, Austria). The high-pass filter was 70 Hz. The mechanical and thermal indices were below 1.1 and 0.9, respectively, in most of the sessions and were always kept below 1.9 and 1.5.

Based on the experience of the pilot study, the left branch of the hepatic artery was visualized using color Doppler in a sagittal or oblique horizontal view of the fetal abdomen (Figure 1). Using either approach of insonation, the Doppler beam was directed along the intrahepatic part of the UV and the inlet to the DV. The pulse repetition frequency was kept low to visualize low-flow velocities. Insonation was adjusted according to the direction of the vessel, kept as low as possible and always ≤30°. The Doppler gate was placed at the left branch of the hepatic artery close to the DV and when needed the Doppler shift was corrected for angle of insonation. The recordings were acquired in the absence of fetal breathing or body movements over at least 3 uniform heart cycles. The observation with the best quality (ie, lowest insonation angle and most uniform pulse waves) was included in the statistics. Doppler waveforms were automatically traced, the systolic peak and time averaged maximum velocity (V_{HAps} and $V_{HAta-max}$) were determined, and pulsatility index (PI) was calculated.[25]

The inner diameter of the UV (D_{UV}) was measured by an insonation perpendicular to the vessel wall in the intra-abdominal portion distal to the portal branches. The mean of at least 3 measurements was included in the statistics. The maximum UV blood flow velocity (V_{UVmax}) was recorded in an axial direction of the vessel. The umbilical blood flow, Q_{UV} (mL/min), was calculated as $\pi \times (D_{UV}/2)^2 \times V_{UVmax} \times 0.5 \times 60$.[26]

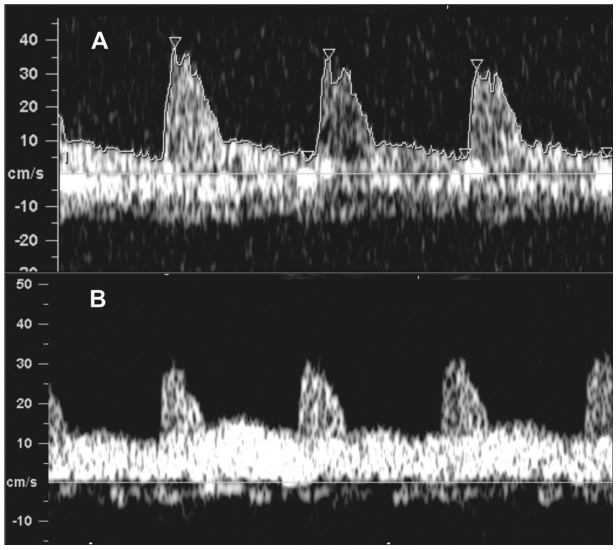

Figure 2. Doppler recordings of the hepatic artery waveform. (A) Recording from the left hepatic artery. (B) Recording from the common hepatic artery with interference from the neighboring portal vein.

The DV connects the UV to the inferior vena cava, and its blood velocity reflects the portocaval pressure gradient.[16,27] It was therefore used as a surrogate measure for portal perfusion pressure in the present study. The DV was assessed in a sagittal or oblique section of the fetal abdomen using a standardized technique.[28] The maximum velocity (V_{DVps}) was determined based on waveforms that were either automatically or manually traced.

To determine the relationship between hepatic artery haemodynamics and the general circulation, we assessed the middle cerebral artery (MCA) and umbilical artery (UA). For the MCA and UA recordings, an insonation angle close to 0° was used.[29] For the MCA measurements, the Doppler gate was placed at the proximal part of the vessel,[30] and measurements of the UA were done in a free-floating loop of the umbilical cord. Measurements of head and abdominal circumference and femur length were performed at each session, and estimated fetal weight was calculated by the formula of Combs et al.[31]

Clinical Cases

Three clinical cases were studied to examine the potential clinical use of fetal hepatic artery Doppler assessment.

Table 1. Reference Ranges for the Hepatic Artery Peak Systolic Velocity Based on 176 Observations in 104 Low-Risk Pregnancies

	Percentile								
Gestation, wk	**2.5**	**5**	**10**	**25**	**50**	**75**	**90**	**95**	**97.5**
21	11.65	12.43	13.41	15.30	17.82	20.91	24.33	26.72	29.06
22	12.24	13.07	14.13	16.15	18.86	22.20	25.90	28.50	31.05
23	12.81	13.69	14.81	16.96	19.86	23.43	27.42	30.23	32.98
24	13.35	14.28	15.46	17.74	20.82	24.63	28.89	31.90	34.85
25	13.86	14.84	16.09	18.49	21.74	25.78	30.31	33.52	36.68
26	14.36	15.39	16.69	19.22	22.64	26.91	31.71	35.11	38.47
27	14.84	15.91	17.28	19.93	23.52	28.01	33.07	36.68	40.23
28	15.31	16.43	17.85	20.62	24.38	29.09	34.42	38.22	41.98
29	15.77	16.93	18.41	21.30	25.23	30.16	35.76	39.76	43.71
30	16.23	17.43	18.97	21.97	26.07	31.23	37.09	41.29	45.45
31	16.68	17.93	19.53	22.65	26.92	32.30	38.43	42.84	47.20
32	17.13	18.43	20.08	23.32	27.76	33.38	39.79	44.40	48.98
33	17.59	18.93	20.64	24.01	28.62	34.47	41.17	45.99	50.79
34	18.05	19.43	21.21	24.70	29.50	35.59	42.58	47.62	52.65
35	18.52	19.95	21.79	25.41	30.39	36.73	44.03	49.30	54.57
36	19.00	20.48	22.39	26.13	31.31	37.91	45.53	51.04	56.56
37	19.49	21.03	23.00	26.89	32.26	39.14	47.09	52.85	58.63
38	20.00	21.59	23.64	27.67	33.26	40.42	48.72	54.75	60.81

Case 1 had experienced fetomaternal bleeding following abdominal trauma at gestational week 30. Case 2 had fetal anemia due to human parvovirus B19 infection diagnosed at 24 weeks' gestation. Case 3 had severe intrauterine growth restriction (IUGR) in late gestation.

Statistics

Multilevel modeling was used to calculate the mean and centiles for the hepatic artery systolic peak and time-averaged maximum velocity (V_{HAps} and $V_{HAta\text{-}max}$) and PI_{HA} at different gestational ages. To achieve normal distributions for the outcome variables, we used power transformation. The outcome variables were regressed against gestational age using fractional polynomials. The 2.5th, 5th, 10th, and 25th centiles were calculated by subtracting 1.96 standard deviation (SD), 1.645 SD, 1.282 SD, and 0.674 SD from the mean, respectively. The 97.5th, 95th, 90th, and 75th centiles were calculated by adding the respective multiples of the SD to the mean. The 95% confidence interval (CI) of the mean, 5th, and 95th centiles were derived.

To assess the effect of V_{DVps}, $Q_{UV\ norm}$, V_{UVmax}, and Q_{UV} on V_{HAps} and PI_{HA}, we included these measurements (in 3 categories: <10th centile, 10th-90th centile, and >90th centile, since responses were assumed to occur more commonly in extreme conditions) as indicator variables in the multilevel regressions models, which describe the mean of V_{HAps} and PI_{HA}. The gestational age–dependent centiles of these independent variables were also calculated by multilevel regression. Indicator variables with significant improvement in the goodness of fit to the models, as assessed by the deviance statistics (χ^2 with $P < .05$), were considered to significantly influence the outcome variables.

Intraobserver and interobserver reproducibilities were expressed as intraclass and interclass correlation coefficients based on repeat blinded observations in 15 and 12 participants, respectively. Limits of agreement were based on the same samples.[32]

The statistical analysis was performed using the Statistical Package for the Social Sciences (SPSS Inc, Chicago, IL) and the MlWin program (Centre for Multilevel Modelling, University of Bristol, UK).

RESULTS

Median maternal height and weight at booking was 167 cm (range, 150-183 cm) and 65 kg (range, 49-122 kg), respectively; maternal age was 29 years (range, 20-40 years) at recruitment; 48% were primiparous. Median gestational age at delivery was 40^{+3} weeks (range, 35^{+3}-42^{+4} weeks). The cesarean delivery rate (10.6%) and birth weights (median, 3700 g; range, 2260-4980 g) were similar to values in the local population (cesarean rate of 11.8%).[33] Five women developed preeclampsia (3.1%). Participants who developed complications after enrollment in the study were not excluded. Population characteristics have been described in detail previously.[23]

We obtained 176 measurements of the hepatic artery in 104 participants. No angle correction was required in 84

Table 2. Reference Ranges for the Hepatic Artery Time-Averaged Maximum Velocity Based on 176 Observations in 104 Low-Risk Pregnancies

	Percentile								
Gestation, wk	**2.5**	**5**	**10**	**25**	**50**	**75**	**90**	**95**	**97.5**
21	6.88	7.23	7.67	8.47	9.50	10.69	11.93	12.76	13.54
22	6.87	7.25	7.71	8.57	9.68	10.97	12.34	13.26	14.13
23	6.87	7.26	7.75	8.67	9.86	11.27	12.77	13.78	14.75
24	6.86	7.28	7.79	8.77	10.05	11.57	13.21	14.33	15.40
25	6.87	7.30	7.84	8.88	10.24	11.88	13.66	14.89	16.07
26	6.88	7.33	7.90	9.00	10.44	12.20	14.13	15.47	16.77
27	6.91	7.38	7.98	9.12	10.66	12.54	14.62	16.07	17.48
28	6.94	7.44	8.06	9.27	10.89	12.89	15.12	16.69	18.23
29	6.99	7.51	8.16	9.42	11.13	13.26	15.65	17.34	19.01
30	7.06	7.59	8.27	9.59	11.39	13.65	16.20	18.02	19.82
31	7.13	7.69	8.39	9.78	11.67	14.06	16.79	18.74	20.68
32	7.23	7.80	8.54	9.98	11.97	14.51	17.41	19.50	21.59
33	7.33	7.93	8.69	10.21	12.30	14.98	18.07	20.32	22.56
34	7.45	8.07	8.87	10.45	12.66	15.49	18.79	21.19	23.61
35	7.59	8.24	9.07	10.73	13.04	16.05	19.56	22.13	24.73
36	7.75	8.42	9.29	11.02	13.47	16.65	20.39	23.16	25.95
37	7.92	8.62	9.53	11.35	13.93	17.30	21.30	24.27	27.28
38	8.11	8.85	9.80	11.71	14.43	18.02	22.30	25.48	28.73

Table 3. Reference Ranges for the Hepatic Artery Pulsatility Index Based on 176 Observations in 104 Low-Risk Pregnancies

	Percentile								
Gestation, wk	**2.5**	**5**	**10**	**25**	**50**	**75**	**90**	**95**	**97.5**
21	1.07	1.12	1.19	1.32	1.49	1.69	1.89	2.03	2.16
22	1.10	1.15	1.23	1.36	1.53	1.74	1.95	2.09	2.23
23	1.12	1.18	1.26	1.40	1.58	1.79	2.01	2.16	2.30
24	1.15	1.21	1.29	1.43	1.62	1.84	2.07	2.22	2.37
25	1.18	1.24	1.32	1.47	1.66	1.89	2.12	2.29	2.44
26	1.20	1.27	1.35	1.50	1.70	1.93	2.18	2.35	2.51
27	1.23	1.29	1.38	1.53	1.74	1.98	2.23	2.40	2.57
28	1.25	1.32	1.40	1.56	1.77	2.02	2.28	2.46	2.63
29	1.27	1.34	1.43	1.59	1.80	2.06	2.32	2.51	2.68
30	1.28	1.36	1.45	1.61	1.83	2.09	2.36	2.55	2.72
31	1.30	1.37	1.46	1.63	1.85	2.11	2.39	2.58	2.76
32	1.31	1.38	1.47	1.65	1.87	2.13	2.42	2.61	2.79
33	1.32	1.39	1.48	1.66	1.88	2.15	2.43	2.62	2.81
34	1.32	1.39	1.49	1.66	1.88	2.15	2.44	2.63	2.82
35	1.32	1.39	1.48	1.66	1.88	2.15	2.43	2.63	2.81
36	1.31	1.38	1.48	1.65	1.87	2.14	2.42	2.61	2.79
37	1.30	1.37	1.46	1.63	1.85	2.11	2.39	2.58	2.76
38	1.28	1.35	1.44	1.61	1.83	2.08	2.36	2.54	2.72

recordings; in 13 recordings, the angle of insonation was ≤10°, and in 79 recordings, the angle of insonation was 10° to 30°. The median sample volume was 4 mm (range, 2-9 mm). Measurements were performed with the vessel visualized in the oblique transverse view of the fetal abdomen in 89 observations and in the sagittal view in 87 observations (Figure 1). Unfavorable fetal position and movement, insufficient visualization of the artery, or uncertain anatomical identification were the reasons for not achieving a measurement.

The individual results of the V_{HAps}, $V_{HAta\text{-}max}$, and PI_{HA} with fitted mean and reference intervals are presented in Figures 3 to 5. The corresponding gestational age–specific values for the 2.5th, 5th, 10th, 50th, 75th, 90th, 95th, and 97.5th centiles are presented in Tables 1 to 3. Hepatic artery velocities increased through the second half of

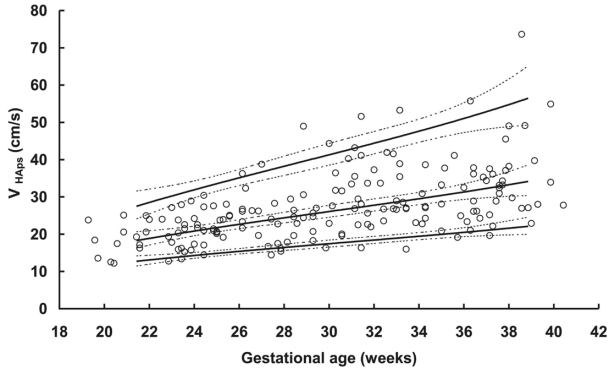

Figure 3. Left hepatic artery systolic peak velocity (V_{HAps}) with fitted 5th, 50th, and 95th centiles and 95% confidence limits for the centiles based on 176 observations.

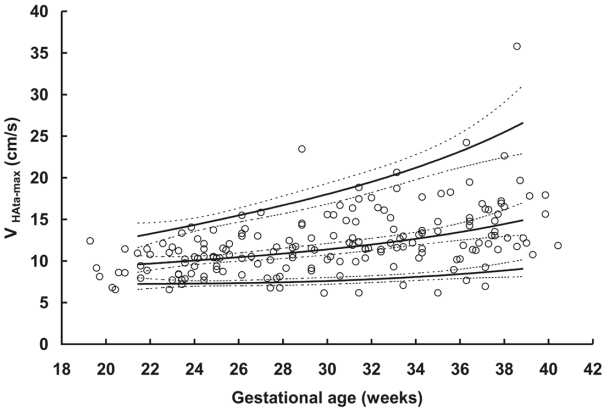

Figure 4. Left hepatic artery time-averaged maximum velocity ($V_{HATa-max}$) with fitted 5th, 50th, and 95th centiles and 95% confidence limits for the centiles based on 176 observations.

pregnancy. The mean V_{HAps} increased from 18 cm/s to 33 cm/s during 21 to 38 weeks of gestation. Similarly, the mean $V_{HATa-max}$ increased from 9 cm/s to 14 cm/s, while the mean PI_{HA} increased from 1.49 to 1.83.

For the $V_{UV\ max}$, Q_{UV}, and Q_{Uvnorm}, the centiles calculated for the regression analyses are based on 598, 568, and 553 observations, respectively (not presented). For the UV velocity measurements, the median angle of insonation was 9° (range, 0°-30°). The mean inner diameter of the UV (D_{uv}) was calculated when at least 3 measurements were obtained during a session (which was the case in 606 sessions, not presented). The $V_{DV\ ps}$ centiles were calculated on the basis of 596 observations, and the median angle of insonation was 10° (range, 0°-30°, not presented).

Regression analysis showed that fetuses at >90th centiles for Q_{UV} and Q_{UVnorm} tended to have a higher hepatic artery PI ($P < .0001$). (Detailed information for this and the following analyses is presented in the appendix.) Similarly,

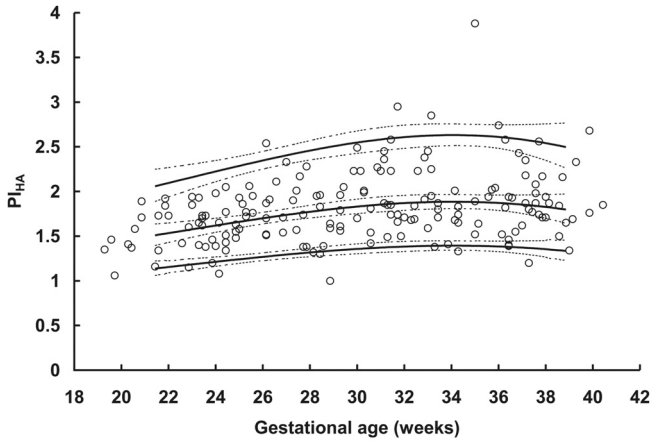

Figure 5. Left hepatic artery pulsatility index (PI_{HA}) with fitted 5th, 50th, and 95th centiles and 95% confidence limits for the centiles based on 176 observations.

V_{DVps} <10th centile was associated with a lower hepatic artery PI ($P < .05$; Figure 6A; Table 4). These findings indicate a vasodilatation response in the hepatic artery to low portocaval pressures and less vasodilatation (higher PI) when the umbilical venous contribution to the liver perfusion is high. Both findings support the hypothesis that there is intrinsic regulation of the hepatic artery in the fetal liver, reflecting a functioning hepatic artery buffer response.

Fetuses with V_{DVps} <10th centile also tended to have lower V_{HAps} ($P < .003$); for the other parameters, the effect was U shaped (10th-90th centile lowest; Figure 6B; Table 4).

When the centiles for PI_{MCA}, $V_{UA\ ps}$, and PI_{UA} were examined for possible associations with hepatic arterial waveform parameters, we found no significant relations in this group of normally growing fetuses (not presented).

The intraobserver and interobserver variation is presented in Table 5.

Clinical Cases

Case 1 (fetomaternal bleeding) showed low PI and high systolic peak velocity, indicating priority of hepatic artery flow (Figure 7). The high velocities and low PI in the hepatic artery changed to reference ranges simultaneously with the reduction in fetal blood measured in the maternal circulation. A healthy girl (3400 g) was born at 40^{+2} weeks of gestation.

Case 2, a fetus with nonimmune hydrops caused by human parvovirus B19 infection, was treated with 1 intrauterine blood transfusion at 24^{+4} weeks' gestation because of fetal anemia (hemoglobin concentration = 7.3 g/dL). The

Table 4. Effects of the Portocaval Pressure Gradient (V_{DVps}) and Parameters of Umbilical Venous Liver Perfusion (Q_{UVnorm}, V_{UVmax}, Q_{UV}) on the Hepatic Artery Pulsatiliy Index (PI_{HA}) (Upper Panel) and Systolic Peak Velocity (V_{HAps}; Lower Panel) Assessed by Deviance Statistics[a]

	Percentile	PIHA	*P* Value
DV PSV	<10	1.68	<.05
	10-90	1.88	
	>90	1.93	
UV flow/kg	<10	1.83	<.0001
	10-90	1.87	
	>90	1.93	
UV max	<10	1.90	<.0004
	10-90	1.85	
	>90	1.98	
UV flow	<10	1.81	<.0001
	10-90	1.86	
	>90	1.95	
	Percentile	**VHAPS, cm/s**	***P* Value**
DV PSV	<10	24.16	<.003
	10-90	28.07	
	>90	28.68	
UV flow/kg	<10	27.57	<.0001
	10-90	27.04	
	>90	29.49	
UV max	<10	29.46	<.0001
	10-90	27.14	
	>90	28.87	
UV flow	<10	28.76	<.0001
	10-90	26.90	
	>90	29.87	

Abbreviations: PI_{HA}, hepatic artery pulsatility index; Q_{UV}, umbilical vein flow; Q_{uvnorm}, umbilical vein flow per estimated fetal weight; V_{DVps}, ductus venosus systolic peak velocity; V_{HAps}, hepatic artery systolic peak velocity (cm/s); V_{UVmax}, umbilical vein maximal velocity.
[a]The values are given for 32 weeks of gestation to illustrate the magnitude of the effects.

initial high V_{HAps} declined to reference values after the transfusion, while the PI_{HA} remained low throughout the observation period (Figure 7). The baby boy was born at 37^{+2} weeks of gestation, with a birth weight <10th centile (2680 g).

Case 3, a fetus with severe IUGR at term (estimated fetal weight <2.5th centile), had low PI_{HA} and high V_{HAps} (Figure 7). Hemodynamic evaluation by Doppler revealed signs of placental compromise and fetal compensation (PI_{UA} >95th centile, PI_{MCA} <5th centile, and PI_{DV} and V_{DVps} >97.5th centile[34]). A girl (2550 g) was delivered by cesarean section at 40^{+2} weeks of gestation.

DISCUSSION

In the present study, we have established a method of assessing the hepatic artery flow velocities and PI in the human fetus using Doppler examination of the left hepatic artery close to the isthmus of the DV in the human fetus. We have constructed reference ranges and shown that during prenatal life, the artery is involved in a hemodynamic buffer mechanism maintaining perfusion of the liver when portal (umbilical) flow and pressure are reduced. Our clinical cases underscore the potential clinical use of this examination, showing substantial changes in the hepatic artery PI and velocities in fetomaternal hemorrhage, fetal anemia, and severe IUGR.

While the prenatal contribution of the hepatic artery to the total liver blood flow is <10% in lambs,[5,35] postnatally, the contribution is 20% to 30%.[35] With the UV occluded at birth, the main source for the venous liver perfusion is switched from the umbilical to the portal vein. The prenatally developed hepatic artery buffer response shown in the present study is apparently a necessary preparation for the dramatic transition of the liver circulation at birth. The existence of a prenatal buffer effect was supported by the significant effects of the intra-abdominal umbilical venous flow and portocaval pressure gradient (represented by the DV flow velocity) on the hepatic artery activity in our study (Figure 6). As expected, the magnitude of the effect is modest under unprovoked physiological conditions (Table 4). The 3 clinical examples suggest that substantial effects result during extreme conditions (Figure 7).

The fetal liver differentiates throughout gestation. From being essentially a hematopoietic organ in the first trimester, it shifts to an increasing hepatopoietic activity during the second trimester.[36] Between 25 weeks and birth, however, there is little change in the vascular architecture of the liver.[37] Systolic peak velocity and time-averaged velocity are known to have a close relationship to the volume of blood flowing in other sections of the fetal arterial system.[38] We believe that the increase in hepatic artery blood velocity from 22 weeks to 39 weeks of gestation may reflect a similar relationship. The impedance increases according to the hepatic artery PI but only until 32 weeks, when a plateau is reached. A corresponding plateau of development was previously described for the DV shunting and foramen ovale size and shunting, possibly signifying a transition to a different level of developmental physiology.[2,39,40]

One previous small study examining hepatic artery velocities, without specifying gestational age or site of

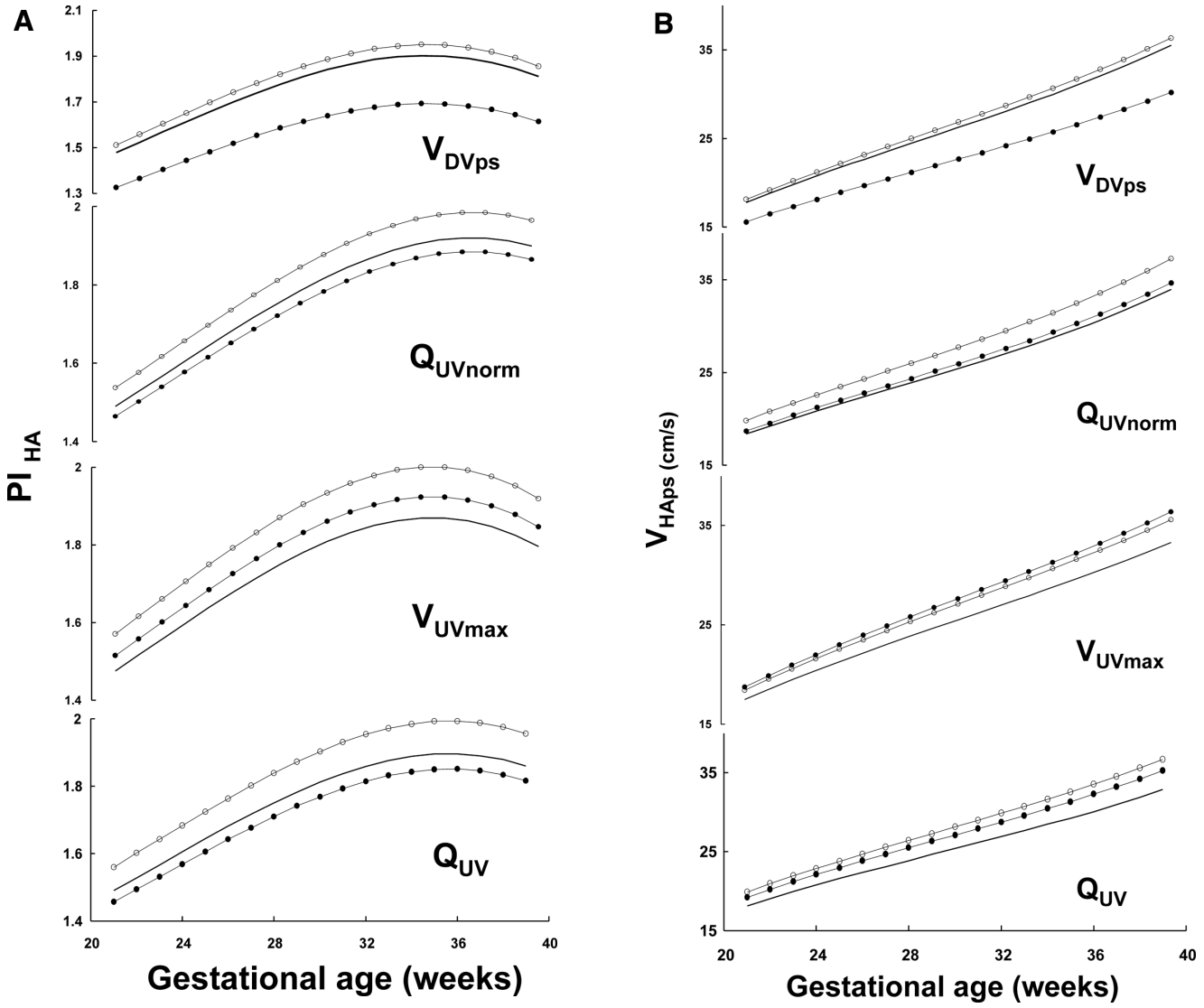

Figure 6. Influence of portocaval pressure gradient expressed by the ductus venosus peak velocity (V_{DVps}) and parameters of umbilical venous liver perfusion (Q_{UVnorm},V_{uvmax}, Q_{UV}) on the (A) hepatic artery pulsatility index (PI_{HA}) and (B) systolic peak velocity (V_{HAps}) according to deviance statistics using centiles of the parameters. The difference between the lines represents the effects, all being significant. The effect sizes are shown in Table 4. Lines with closed circles = <10th centile, thick lines =10th to 90th centile, and lines with open circles = >90th centile for the variables. Q_{UVnorm} indicates umbilical vein flow/kg;V_{UVmax}, umbilical vein maximal velocity; and Q_{UV}, umbilical vein flow.

measurement,[22] found velocities in line with our results. We believe the presently established reference ranges are suitable for clinical use; the reliability of the ranges is reflected in the 95% CI of the 5th, 50th, and 95th centiles (Figures 3-5).

Although measurements were increasingly successful as the study developed, our overall success rate was low, with 176 observations compared with more than 500 for other sections of the study. Based on our increasing experience in clinical cases (Figure 7), we expect that the increased hepatic artery blood velocities will enhance visualization and improve the success rate in clinical conditions. The variation of the arterial anatomy of the fetal liver may also cause problems[41-43] since the left hepatic artery arises from the left gastric artery in about 15% of fetuses and from the splenic or gastroduodenal artery or aorta in 4%.[44] One or two aberrant hepatic arteries from the left gastric or superior mesenteric artery are found in 30% of human fetal livers.[43] We believe that the landmarks we suggest for recording the arterial hepatic circulation

Table 5. Intraobserver and Interobserver Variation of Hepatic Artery Flow Velocities and Pulsatility Index

	Paired Differences									
				95% CI				Limits of Agreement		
	Mean	SD	SE	Lower	Upper	*df*	*P*	Lower	Upper	ICCC, %
Intraobserver variation										
V_{HAps}	–0.47	4.03	1.04	–2.70	1.76	14	0.657	–8.37	7.43	84
$V_{HAta-mx}$	–0.28	1.92	0.50	–1.35	0.78	14	0.575	–4.04	3.48	80
PI_{HA}	0.07	0.22	0.06	–0.05	0.19	14	0.248	–0.37	0.51	68
Interobserver variation										
V_{HAps}	–1.70	5.38	1.55	–5.11	1.72	11	0.299	–12.24	8.85	88
$V_{HAta-mx}$	–0.88	3.25	0.94	–2.94	1.19	11	0.371	–7.25	5.50	64
PI_{HA}	0.00	0.39	0.11	–0.25	0.24	11	0.971	–0.77	0.76	61

Abbreviations: *df*, degrees of freedom; ICCC, intraclass and interclass correlation coefficients, respectively; PI_{HA}, hepatic artery pulsatility index; V_{HAps}, hepatic artery systolic peak velocity; $V_{HAta-mx}$, hepatic artery time-averaged maximum velocity.

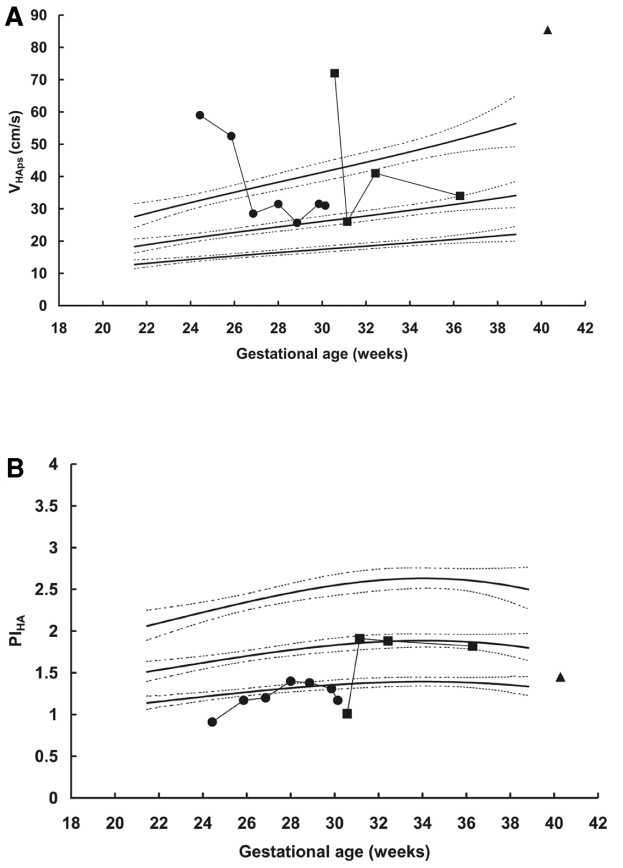

Figure 7. Results from cases 1 to 3 plotted against the reference centiles illustrate how hepatic artery monitoring could provide new hemodynamic information in clinical cases. (A) Hepatic artery systolic peak velocity (V_{HAps}). (B) Hepatic artery pulsatility index (PI_{HA}). Fetomaternal bleeding (case 1): line with squares. Human parvovirus B19–infected fetus (case 2): line with circles. IUGR fetus <2.5th centile, at term (case 3): triangle.

should provide reliable and comparable measurements as the left hepatic artery enters the liver close to the DV.

When selecting the left branch for the hepatic artery standardization, it is important to be aware that there is increasing evidence that the left and right liver lobe represent different functional units in the fetus.[4,45,46] Venous splanchnic blood is almost exclusively distributed to the right liver lobe (with an addition of umbilical blood), while the left liver lobe receives exclusively umbilical venous blood under physiologic conditions.[3-5] Gene expression patterns are also different in the 2 lobes; 6 genes related to oxygen transport and iron availability are downregulated in the right compared with the left lobe in fetal baboons.[46] In our study, we have focused on the left hepatic artery supplying the left lobe, and the flow velocity pattern in this branch might not be representative of the entire hepatic arterial supply; thus, interpretation must be cautious. Postnatally, the hepatic artery buffer response seems to operate differently in the liver lobes after left portal vein ligation or right portal vein embolization, respectively, indicating independent responses to ipsilateral portal flow changes.[47,48] Although desirable, it seems unlikely that we will be able to measure blood velocity with any regularity using the present techniques in the main stem of the common hepatic artery or its right branch. The reason is the close vicinity to the portal vein and its right branch. The blood flow direction is the same in the vein and artery for these sections, and interference in the Doppler recording is a common problem (Figure 2B).

Under experimental conditions, hypovolemia and hypoxemia increase the fraction of UV flow shunted through the DV, thus reducing the UV supply to the liver.[10]

The observed reduction in PI_{HA} and increase in systolic peak velocity PSV_{HA} in case 1 may reflect a compensatory mechanism to buffer the effects of acute reduction of UV perfusion of the liver and to mobilize the hepatic blood reservoir, thus protecting the liver against passive changes in the central venous pressure.[49] In animal experiments, the fetal vascular response to hemorrhage comprises generalized arterial vasoconstriction with the exception of the cerebral, coronary, and hepatic beds[50]; our study, however, found no relationship between hemodynamics in the middle cerebral or umbilical and hepatic arteries, suggesting that these circulatory beds have a high degree of independent regulation and less common determinants.

In cases of fetal growth restriction (case 3), venous liver perfusion is reduced.[51,52] Our observations of the hepatic artery in cases 1 and 3 (Figure 7) could be seen as a similar response to the postnatal hepatic artery buffer response (ie, a compensatory increase in hepatic artery flow to buffer the reduction in venous liver perfusion).

Case 2 had nonimmune hydrops arising from suppression of hepatic erytropoiesis by human parvovirus B19 infection.[53] A recent lamb study[54] showed that increased hepatic artery flow was associated with increased density of hematopoietic cells, while hepatic artery ligation decreased hematopoietic activity. Case 2 illustrates initial high velocities and persisting low PI in the hepatic artery. After intrauterine transfusion at 24^{+6} weeks of gestation the velocities in the hepatic artery decreased while the PI stayed low, indicating a persisting priority of hepatic artery flow, possibly in response to an increased hematopoietic demand.

Our findings in this low-risk population support the hypothesis that the hepatic arterial buffer response operates in the fetal liver. The buffer response is prominent during extreme conditions, and our observations underline the high priority of maintaining liver perfusion and homeostasis also during prenatal life. We have established a standardized technique and reference ranges for the fetal hepatic arterial Doppler waveforms, applicable for use in clinical situations.

APPENDIX

Associations of hepatic artery systolic peak velocity (V_{Haps}) and pulsatility index (PI_{HA}) with ductus venosus systolic peak velocity (V_{DVps}), umbilical vein flow (Q_{UV}), umbilical vein flow/estimated fetal weight (Q_{Uvnorm}), and Uv maximal velocity (UV_{max}).

Hepatic Artery Systolic Peak Velocity (V_{HAps})

V_{DVps}

Regression model for estimated V_{HAps} by gestational age (GA) in weeks and $V_{DVps.}$ V_{HAps} is transformed to the –0.309 power and may be back-transformed as $V_{HAps}^{(1/-0.309)}$. *i* and *j* denote the measurement and fetus, respectively.

$$\text{Mean} = \mu_{ij} = 0.3610725 + 31.75537\ GA_{ij}^{-2} - 0.000000558\ GA_{ij}^{3} - 0.0169254V_{DVps2j} - 0.0193233V_{DVps3j}$$

Significance level of decrease in the log likelihood including V_{DVps} in the model: $P < .003$.

$$\text{Variance} = \sigma_{ij}^2 = 0.000842116$$

$V_{DVps\,2}$: 10th-90th centile = 1, other values = 0
$V_{DVps\,3}$: >90th centile = 1, other values = 0

Q_{UVnorm}

Regression model for estimated V_{HAps} by GA in weeks and umbilical vein flow/kg. V_{HAps} is transformed to the –0.309 power and may be back-transformed as $V_{HAps}^{(1/-0.309)}$. *i* and *j* denote measurement and fetus, respectively.

$$\text{Mean} = \mu_{ij} = 0.3560188 + 24.07714\ GA_{ij}^{-2} - 0.000000631\ GA_{ij}^{3} + 0.002156323Q_{UVnorm2j} - 0.007385144Q_{UVnorm3j}$$

Significance level of decrease in the log likelihood including Q_{UVnorm} in the model: $P < .0001$.

$$\text{Variance} = \sigma_{ij}^2 = 0.000803505$$

$Q_{UVnorm2}$: 10^{th}-90th centile = 1, other values = 0
$Q_{UVnorm3}$: >90th centile = 1, other values = 0

V_{UVmax}

Regression model for estimated V_{HAps} by GA in weeks and V_{UVmax}. V_{HAps} is transformed to the –0.309 power and may be back-transformed as $V_{HAps}^{(1/-0.309)}$. *i* and *j* denote the measurement and fetus, respectively.

$$\text{Mean} = \mu_{ij} = 0.3341441 + 32.6641\ GA_{ij}^{-2} - 0.000004418\ GA_{ij}^{3} + 0.009017382V_{UVmax2j} + 0.002215618V_{UVmax3j}$$

(continued)

APPENDIX (continued)

Significance level of decrease in the log likelihood including Q_{UVnorm} in the model: $P < .0001$.

$$\text{Variance} = \sigma^2_{ij} = 0.000854265$$

V_{UVmax2}: 10th-90th centile = 1, other values = 0
V_{UVmax3}: >90th centile = 1, other values = 0

Q_{UV}

Regression model for estimated V_{HAps} by GA in weeks and Q_{UV} flow. V_{HAps} is transformed to the –0.309 power and may be back-transformed as $V_{HAps}^{(1/-0.309)}$. *i* and *j* denote the measurement and fetus, respectively.

$$\text{Mean} = \mu_{ij} = 0.3433651 + 27.40524\ GA_{ij}^{-2} - 0.000000486\ GA_{ij}^{3} + 0.007393046Q_{UV2j} - 0.00412429Q_{UV3j}.$$

Significance level of decrease in the log likelihood including Q_{UVnorm} in the model: $P < .0001$.

$$\text{Variance} = \sigma^2_{ij} = 0.000790182$$

Q_{UV2}: 10th-90th centile = 1, other values = 0
Q_{UV3}: >90th centile = 1, other values = 0

Hepatic Artery Pulsatility Index (PI_{HA})

V_{DVps}

Regression model for estimated PI_{HA} by GA in weeks and $V_{DVps.}$ PI_{HA} is transformed to the –0.31 power and may be back-transformed as $PI_{HA}^{(1/-0.31)}$. *i* and *j* denote the measurement and fetus, respectively.

$$\text{Mean} = \mu_{ij} = 1\ 04977 - 0.000512676\ GA_{ij}^{-2} + 0.000009982\ GA_{ij}^{3} - 0.0302817V_{DVps2j} - 0.0365477V_{DVps3j}.$$

Significance level of decrease in the log-likelihood including V_{DVps} in the model: $P < .05$.

$$\text{Variance} = \sigma^2_{ij} = 0.00233934$$

V_{DVps2}: 10th-90th centile = 1, other values = 0
V_{DVps3}: >90th centile = 1, other values = 0

Q_{UVnorm}

Regression model for estimated PI_{HA} by GA in weeks and Q_{UVnorm}. PI_{HA} is transformed to the –0.31 power and may be back-transformed as $PI_{HA}^{(1/-0.31)}$. *i* and *j* denote the measurement and fetus, respectively.

$$\text{Mean} = \mu_{ij} = 0.9946803 - 000391262\ GA_{ij}^{2} + 0.000007161\ GA_{ij}^{3} - 0.004735979Q_{UVnorm2j} - 0.01317954QU_{Vnorm3j}$$

Significance level of decrease in the log likelihood including Q_{UVnorm} in the model: $P < .0001$.

$$\text{Variance} = \sigma^2_{ij} = 0.00249416$$

$Q_{UVnorm2}$: 10th-90th centile = 1, other values = 0
$Q_{UVnorm3}$: >90th centile = 1, other values = 0

V_{UVmax}

Regression model for estimated PI_{HA} by GA in weeks and V_{UVmax}. PI_{HA} is transformed to the –0.31 power and may be back-transformed as $PI_{HA}^{(1/-0.31)}$. *i* and *j* denote the measurement and fetus, respectively.

$$\text{Mean} = \mu_{ij} = 1.001664 - .0\ 000467799\ GA_{ij}^{2} + 0.000009047\ GA_{ij}^{3} + 0.007268004V_{UVmax2j} - 0.009860503V_{UVmax3j}.$$

Significance level of decrease in the log-likelihood including V_{UVmax} in the model: $P < .0004$.

$$\text{Variance} = \sigma^2_{ij} = 0.002425939$$

$V_{UVmax\ 2}$: 10th-90th centile = 1, other values = 0
V_{UVmax3}: >90th centile = 1, other values = 0

Q_{UV}

Regression model for estimated PI_{HA} by GA in weeks and Q_{UV}. PI_{HA} is transformed to the –0.31 power and may be back-transformed as $PI_{HA}^{(1/-0.31)}$. *i* and *j* denote the measurement and fetus, respectively.

$$\text{Mean} = \mu_{ij} = 0.9994314 - 0.0004084734\ GA_{ij}^{-2} + 000007634968\ GA_{ij}^{3} - 0.006185075Q_{UV2j} - 0.01876463Q_{UV3j}$$

Significance level of decrease in the log likelihood including Q_{UV} in the model: $P < .0001$.

$$\text{Variance} = \sigma^2_{ij} = 0.00246936$$

Q_{UV2}: 10th-90th centile = 1, other values = 0
Q_{UV3}: >90th centile = 1, other values = 0

REFERENCES

1. Kiserud T, Ebbing C, Kessler J, Rasmussen S. Fetal cardiac output, distribution to the placenta and impact of placental compromise. *Ultrasound Obstet Gynecol*. 2006;28(2):126-136.
2. Kiserud T, Rasmussen S, Skulstad S. Blood flow and the degree of shunting through the ductus venosus in the human fetus. *Am J Obstet Gynecol*. 2000;182(1):147-153.
3. Kessler J, Rasmussen S, Godfrey K, Hanson M, Kiserud T. Longitudinal study of umbilical and portal venous blood flow to the fetal liver: low pregnancy weight gain is associated with preferential supply to the fetal left lobe. *Pediatr Res*. In press.
4. Haugen G, Kiserud T, Godfrey K, Crozier S, Hanson M. Portal and umbilical venous blood supply to the liver in the human fetus near term. *Ultrasound Obstet Gynecol*. 2004;24(6): 599-605.
5. Edelstone DI, Rudolph AM, Heymann MA. Liver and ductus venosus blood flows in fetal lambs in utero. *Circ Res*. 1978;42(3):426-433.
6. Tchirikov M, Kertschanska S, Sturenberg HJ, Schroder HJ. Liver blood perfusion as a possible instrument for fetal growth regulation. *Placenta*. 2002;23:S153-S158.
7. Tchirikov M, Kertschanska S, Schroder HJ. Obstruction of ductus venosus stimulates cell proliferation in organs of fetal sheep. *Placenta*. 2001;22(1):24-31.
8. Haugen G, Hanson M, Kiserud T, Crozier S, Inskip H, Godfrey KM. Fetal liver-sparing cardiovascular adaptations linked to mother's slimness and diet. *Circ Res*. 2005;96(1):12-14.
9. Kiserud T, Stratford L, Hanson MA. Umbilical flow distribution to the liver and the ductus venosus: an in vitro investigation of the fluid dynamic mechanisms in the fetal sheep. *Am J Obstet Gynecol*. 1997;177(1):86-90.
10. Edelstone DI, Rudolph AM, Heymann MA. Effects of hypoxemia and decreasing umbilical flow on liver and ductus venosus blood flows in fetal lambs. *Am J Physiol*. 1980;238(5): H656-H663.
11. Paulick RP, Meyers RL, Rudolph CD, Rudolph AM. Umbilical and hepatic venous responses to circulating vasoconstructive hormones in the fetal lamb. *Am J Physiol*. 1991; 260:H1205-H1213.
12. Tchirikov M, Kertschanska S, Schroder HJ. Differential effects of catecholamines on vascular rings from ductus venosus and intrahepatic veins of fetal sheep. *J Physiol*. 2003;548(2):519-526.
13. Coceani F, Olley PM. The control of cardiovascular shunts in the fetal and perinatal-period. *Can J Physiol Pharmacol*. 1988; 66(8):1129-1134.
14. Kiserud T, Ozaki T, Nishina H, Rodeck C, Hanson MA. Effect of NO, phenylephrine, and hypoxemia on ductus venosus diameter in fetal sheep. *Am J Physiol Heart Circ Physiol*. 2000;279(3): H1166-H1171.
15. Ville Y, Sideris I, Hecher K, Snijders RJM, Nicolaides KH. Umbilical venous-pressure in normal, growth-retarded, and anemic fetuses. *Am J Obstet Gynecol*. 1994;170(2): 487-494.
16. Kiserud T, Hellevik LR, Eiknes SH, Angelsen BAJ, Blaas HG. Estimation of the pressure-gradient across the fetal ductus venosus based on doppler velocimetry. *Ultrasound Med Biol*. 1994;20(3):225-232.
17. Schroder HJ, Tchirikov M, Rybakowski C. Pressure pulses and flow velocities in central veins of the anesthetized sheep fetus. *Am J Physiol Heart Circ Physiol*. 2003;284(4):H1205-H1211.
18. Lautt WW. The 1995 Ciba-Geigy Award Lecture. Intrinsic regulation of hepatic blood flow. *Can J Physiol Pharmacol*. 1996;74(3):223-233.
19. Yokoyama Y, Wawrzniak A, Sarmadi AH, et al. Hepatic arterial flow becomes the primary supply of sinusoids following partial portal vein ligation in rats. *Hepatology*. 2006;21:1567-1574.
20. Lautt WW, Mcquaker JE. Maintenance of hepatic arterial blood-flow during hemorrhage is mediated by adenosine. *Can J Physiol Pharmacol*. 1989;67(9):1023-1028.
21. Dubiel M, Korszun P, Breborowicz G, Gudmundsson S. Fetal hepatic artery blood flow velocimetry in normal and high-risk pregnancies. *Prenat Neonat Med*. 2001;6(3):151-156.
22. Kilavuz O, Vetter K. Is the liver of the fetus the 4th preferential organ for arterial blood supply besides brain, heart, and adrenal glands? *J Perinat Med*. 1999;27(2):103-106.
23. Ebbing C, Rasmussen S, Kiserud T. Middle cerebral artery blood flow velocities and pulsatility index and the cerebroplacental ratio: longitudinal reference ranges and terms for serial measurements. *Ultrasound Obstet Gynecol*. 2007;30(3):287-296.
24. Johnsen SL, Rasmussen S, Sollien R, Kiserud T. Fetal age assessment based on ultrasound head biometry and the effect of maternal and fetal factors. *Acta Obstet Gynecol Scand*. 2004;83(8):716-723.
25. Gosling R, King D. Ultrasound angiology. In: Macus A, Adamson J, eds. *Arteries and veins*. Edinburgh, UK: Churchill-Livingstone; 1975:61-98.
26. Kiserud T, Eiknes SH, Blaas HG, Hellevik LR, Simensen B. Ductus venosus blood velocity and the umbilical circulation in the seriously growth-retarded fetus. *Ultrasound Obstet Gynecol*. 1994;4(2):109-114.
27. Kiserud T. Ductus venosus. In: Dev Maulik, Ivica Zalud, eds. *Doppler ultrasound in obstetrics and gynecology*. New York, NY: Springer-Verlag; 2005:413-423.
28. Kiserud T, Eiknes SH, Blaas HGK, Hellevik LR. Ultrasonographic velocimetry of the fetal ductus venosus. *Lancet*. 1991;338(8780):1412-1414.
29. Acharya G, Wilsgaard T, Berntsen GKR, Maltau JM, Kiserud T. Reference ranges for serial measurements of umbilical artery Doppler indices in the second half of pregnancy. *Am J Obstet Gynecol*. 2005;192(3):937-944.
30. Mari G, Abuhamad AZ, Cosmi E, Segata M, Altaye M, Akiyama M. Middle cerebral artery peak systolic velocity: technique and variability. *J Ultrasound Med*. 2005;24(4):425-430.
31. Combs CA, Jaekle RK, Rosenn B, Pope M, Miodovnik M, Siddiqi TA. Sonographic estimation of fetal weight based on a model of fetal volume. *Obstet Gynecol*. 1993;82(3):365-370.

32. Bland JM, Altman DG. Applying the right statistics: analysis of measurement studies. *Ultrasound Obstet Gynecol*. 2003;22:85-93.
33. Skjaerven R, Gjessing HK, Bakketeig LS. Birthweight by gestational age in Norway. *Acta Obstet Gynecol Scand*. 2000;79: 440-449.
34. Kessler J, Rasmussen S, Hanson M, Kiserud T. Longitudinal reference ranges for ductus venosus flow velocities and waveform indices. *Ultrasound Obstet Gynecol*. 2007;28(7):890-898.
35. Rudolph AM. Hepatic and ductus venosus blood flows during fetal life. *Hepatology*. 1983;3(2):254-258.
36. Nava S, Westgren M, Jaksch M, et al. Characterization of cells in the developing human liver. *Differentiation*. 2005;73(5): 249-260.
37. Gouysse G, Couvelard A, Frachon S, et al. Relationship between vascular development and vascular differentiation during liver organogenesis in humans. *J Hepatol*. 2002;37(6): 730-740.
38. Acharya G, Wilsgaard T, Berntsen GKR, Maltau JM, Kiserud T. Doppler-derived umbilical artery absolute velocities and their relationship to fetoplacental volume blood flow: a longitudinal study. *Ultrasound Obstet Gynecol*. 2005;25(5):444-453.
39. Kiserud T, Rasmussen S. Ultrasound assessment of the fetal foramen ovale. *Ultrasound Obstet Gynecol*. 2001;17(2):119-124.
40. Rasanen J, Wood DC, Weiner S, Ludomirski A, Huhta JC. Role of the pulmonary circulation in the distribution of human fetal cardiac output during the second half of pregnancy. *Circulation*. 1996;94(5):1068-1073.
41. Aoki T, Imamura H, Kaneko J, et al. Intraoperative direct measurement of hepatic arterial buffer response in patients with or without cirrhosis. *Liver Transpl*. 2005;11(6):684-691.
42. Michels NA. Newer anatomy of liver and its variant blood supply and collateral circulation. *Am J Surg*. 1966;112(3): 337-347.
43. Miyaki T. Patterns of arterial supply of the human-fetal liver: the significance of the accessory hepatic-artery. *Acta Anat*. 1989;136(2):107-111.
44. Jones RM, Hardy KJ. The hepatic artery: a reminder of surgical anatomy. *J R Coll Surg Edinb*. 2001;46(3):168-170.
45. Bristow J, Rudolph AM, Itskovitz J, Barnes R. Hepatic oxygen and glucose-metabolism in the fetal lamb: response to hypoxia. *J Clin Invest*. 1983;71(5):1047-1061.
46. Cox LA, Schlabritz-Loutsevitch N, Hubbard GB, Nijland MJ, McDonald TJ, Nathanielsz PW. Gene expression profile differences in left and right liver lobes from mid-gestation fetal baboons: a cautionary tale. *J Physiol*. 2006;572(1):59-66.
47. Kito Y, Nagino M, Nimura Y. Doppler sonography of hepatic arterial blood flow velocity after percutaneous transhepatic portal vein embolization. *AJR Am J Roentgenol*. 2001;176(4): 909-912.
48. Rocheleau B, Ethier C, Houle R, Huet PM, Bilodeau M. Hepatic artery buffer response following left portal vein ligation: its role in liver tissue homeostasis. *Am J Physiol*. 1999;277(5):1000-1007.
49. Lautt WW, Greenway CV. Conceptual review of the hepatic vascular bed. *Hepatology*. 1987;7(5):952-963.
50. Meyers RL, Paulick RP, Rudolph CD, Rudolph AM. Cardiovascular-responses to acute, severe hemorrhage in fetal sheep. *J Dev Physiol*. 1991;15(4):189-197.
51. Bellotti M, Pennati G, De Gasperi C, Bozzo M, Battaglia FC, Ferrazzi E. Simultaneous measurements of umbilical venous fetal hepatic, and ductus venosus, blood flow in growth-restricted human fetuses. *Am J Obstet Gynecol*. 2004;190(5): 1347-1358.
52. Kiserud T, Kessler J, Ebbing C, Rasmussen S. Ductus venosus shunting in growth-restricted fetuses and the effect of umbilical circulatory compromise. *Ultrasound Obstet Gynecol*. 2006; 28(2):143-149.
53. Berry PJ, Gray ES, Porter HJ, Burton PA. Parvovirus infection of the human fetus and newborn. *Semin Diagn Pathol*. 1992; 9(1):4-12.
54. Kunisaki SM, Azpurua H, Fuchs JR, Graves SC, Zurakowski D, Fauza DO. Fetal hepatic haematopoiesis is modulated by arterial blood flow to the liver. *Br J Haematol*. 2006;134:330-332.

Article II

Fetal celiac and splenic artery flow velocities and pulsatility index: longitudinal reference ranges and evidence for vasodilatation at a low porto-caval pressure gradient

Short title: Fetal celiac and splenic artery

Cathrine Ebbing[1,2], Svein Rasmussen[1,2,3], Keith M. Godfrey[4], Mark A. Hanson[4], Torvid Kiserud[1,2]

[1]Department of Obstetrics and Gynecology, Haukeland University Hospital, Bergen, Norway

[2]Department of Clinical Medicine, University of Bergen, Norway

[3]Medical Birth Registry of Norway, Locus of Registry Based Epidemiology, University of Bergen and the Norwegian Institute of Public Health, Bergen, Norway

[4]Division of Developmental Origins of Health and Disease, University of Southampton, Southampton, UK

Correspondence: Cathrine Ebbing MD

Department of Obstetrics and Gynecology,

Haukeland University Hospital, N-5021 Bergen, Norway

Fax: +47 55974968

Tel: +47 55974200 and private +47 99730026

E-mail:cathrine.ebbing@molmed.uib.no

Key words: Fetus, Doppler, circulation, celiac artery, splenic artery, reference ranges, hemodynamics, porto-caval pressure

ABSTRACT

Objective: To establish longitudinal reference ranges for the fetal celiac and splenic artery flow velocities and pulsatility index (PI) and to determine if vasodilatation occurs at a low porto-caval pressure gradient.

Methods: Prospective longitudinal study of 161 low-risk pregnancies using repeat Doppler recordings of the celiac and splenic arteries. To establish reference ranges for blood velocities and PI measurements were made on 3-5 occasions at 3-5 weekly intervals. Ductus venosus peak velocity was used to represent porto-caval pressure gradient and the left portal vein blood velocity to represent the umbilical distribution to the right liver lobe. Celiac and splenic artery Doppler measurements were also related to the middle cerebral (MCA) and umbilical artery (UA) PI and to umbilical flow.

Results: Longitudinal reference ranges were established based on 510 and 521 observations during gestational weeks 21-39. Terms for calculating conditional reference ranges to be used for repeat observations were also provided. Celiac and splenic artery peak velocity and PI showed covariation, r=0.7 (95% CI 0.6-0.8), and r=0.5 (95% CI 0.3-0.6), respectively. Their PI was low when porto-caval pressure and umbilical supply to the right lobe were low ($p<0.0001$). Additionally, there was concordant variation with the MCA PI, UA PI and the umbilical flow (all $p<0.0001$).

Conclusion: We provide longitudinal reference ranges for the fetal celiac and splenic artery flow velocities and PI and show that although the PIs of these arteries covary with those in other circulatory beds, they also show evidence of vasodilatation when the porto-caval pressure gradient is low.

Word count:250

INTRODUCTION

In the mid gestation human fetus, one third of the combined ventricular output is directed to the placenta[1,2] declining to one fifth near term[1]. Nutrient-rich blood returning from the placenta primarily perfuses the fetal liver, 70% and 80% at 20 and 30-40 weeks of gestation, respectively[3-6], and a correspondingly small fraction (30-20%) is shunted through the ductus venosus[7] to supply the left heart with oxygenated blood through the foramen ovale[8]. Blood velocity in the ductus venosus directly reflects the porto-caval pressure gradient that drives liver perfusion[9-11].

The large proportion of umbilical venous blood perfusing the liver is linked to liver tissue proliferation, production of IGF 1 and 2 and overall fetal growth[12,13] and can be modified by external factors such as maternal body composition and diet[14]. While the umbilical vein is the most important supplier of venous blood to the fetal liver, with advancing gestation an increasing contribution of oxygen depleted splanchnic blood comes from the portal stem[15], 14-20% at 21-39 weeks of gestation[4,6], this mixes with the umbilical blood in the right liver lobe, maintaining portal perfusion. Differences in perfusion between the left and right of the fetal liver could be important as they may underlie the differences in cellular architecture[16], haematopoiesis[17], distribution of enzymes[18] and gene expression[19] between the two liver lobes.

A recent study has shown that the equilibrium between the portal and umbilical perfusion of the fetal liver is closely reflected in the blood velocity of the left portal branch[20], and can be used as a measure of left-right distribution. This was utilised in the present study.

The arterial supply to the upper abdomen, the celiac and superior mesenteric arteries, is also involved in maintaining liver perfusion. One of the three celiac branches (Figure 1), the hepatic artery (HA), is directly connected to the liver while the other two branches, the splenic and left gastric artery, feed the splanchnic circuit that drains into the portal vein.

During postnatal life increases in HA blood flow buffer liver tissue perfusion by an adenosine-mediated vasodilatation in the face of a fall in portal flow[21]. We have recently reported that this mechanism also operates in the human fetus even though at this time the portal system is connected to the umbilical circuit[22]. The fetal HA has not been easy to investigate using Doppler ultrasound[22] although the celiac artery (CA) arising directly from the aorta is more accessible. To date a standardised insonation technique and reference ranges have not been available for the CA, and there is no information as to whether a fall in umbilical venous liver perfusion leads to a compensatory vasodilatation in the CA as in the HA.

The splenic artery (SA), another of the celiac branches (Figure 1), is a major contributor to portal flow through the splenic vein in postnatal life; during fasting it makes the major contribution to portal flow[23]. During prenatal life, the spleen has a higher density of adrenergic neurons than in adults[24], operates as a blood reservoir and is involved in immunologic and haematopoietic activities[25,26]. However, little is known of its hemodynamic regulation in human fetuses e.g. whether local variation in portal liver perfusion or changes in the systemic circulation reflected in the umbilical and cerebral artery parameters influence SA blood flow velocities. Changes in peak velocity and pulsatility index (PI) of the SA in anemic and growth-restricted fetuses[27-31] indicate a potential clinical use, and cross-sectional reference ranges have been introduced[27,28,30]. Serial measurements and longitudinal reference ranges provide a more secure basis for clinical and research purposes[32] but have yet to be published.

The aim of the present study was to establish longitudinal reference ranges for CA and SA flow velocities and PI and the necessary conditional terms needed for serial measurements. We addressed the hemodynamic relationship between HA, CA and SA, to test whether these vessels show covariation or have different regulatory mechanisms. We

specifically tested the hypotheses 1) that the PI`s in the CA and SA will covary with those of the umbilical and middle cerebral arteries (UA and MCA), reflecting regulation by similar influences and 2) that the portal perfusion pressure and distribution are local regulatory determinants for the CA and SA.

METHODS

Subjects

The present study is part of a larger prospective longitudinal study of the fetal cerebral, umbilical and splanchnic circulation approved by the Regional Committee for Medical Research Ethics (REK Vest no 203.03). Here we present the results for CA and SA hemodynamics. The participants were 161 women with low-risk pregnancies recruited after written consent, and ultrasound confirmation of gestational age at 17-20 weeks[33]. Exclusion criteria were twin pregnancy, fetal anomaly, history of pregnancy complications (e.g. pregnancy-induced hypertension, fetal growth restriction and abruptio placentae), or any general chronic disease. Participants who developed complications after enrolment, were not excluded. Each woman was scheduled for examination 3-5 times, at 3-5 weeks intervals. Pregnancy complications, birthweight, Apgar score, gestational age at delivery, gender and congenital abnormalities were noted.

Measurements

Doppler ultrasound measurements were recorded using a 2-5, 2-7 or 4-8 MHz abdominal transducer (Voluson730 Expert, GE Medical systems, Kretz Ultrasoud, Zipf, Austria) with the high-pass filter set to 70 Hz. Mechanical and thermal indices in the majority of sessions were<1.1 and <0.9 respectively, and always <1.9 and <1.5, respectively.

The CA was identified as the most proximal of the unpaired branches of the abdominal aorta (Figure 1). The fetal abdomen was insonated in a sagittal (or horizontal) direction using

colour Doppler and flow velocity waveforms were recorded close to the abdominal aorta using pulsed Doppler with median sample volume 3 mm (range 1-8).

The SA was visualised in a horizontal insonation that identified its origin at the CA in front of the aorta and its course behind the stomach to the spleen (Figure 1). The sample volume (median 4 mm, range 2-8) was placed over the proximal part of the vessel and velocity parameters calculated as mentioned above.

The portocaval (i.e. umbilicocaval) pressure gradient drives the venous perfusion of the liver. The blood velocity in the portocaval shunt of the ductus venosus is a direct representation of this pressure gradient [9,10,34]. The ductus venosus peak blood velocity was recorded[7] and included in the analysis to determine the effect of portocaval pressure on PI_{CA} and PI_{SA}.

Prenatally, the left portal vein (LPV) connects the umbilical vein to the portal circulation and represents a watershed between the two circuits[35,36] (Figure 1). The flow velocity in the LPV is a direct reflection of the umbilical venous supply to the right liver lobe[20]. Thus a reduced LPV blood velocity indicates a shift towards less oxygenated umbilical supply and relatively more oxygen depleted portal blood to the liver. We used the time-averaged maximum velocity of the LPV ($V_{LPVtamx}$) to assess whether such a shift of venous liver perfusion was associated with PI_{CA} and PI_{SA} changes. The velocity was recorded in an oblique insonation of the fetal abdomen using a standardised technique[20] that included a sample volume of median 2 mm (range 0.7-4.0).

We used the PI_{UA} and PI_{MCA} as well as the umbilical venous flow (Q_{UV}) to determine a possible covariance with the PI_{CA} and PI_{SA} in order to test the assumption that these vessels have a common dependency on central fetal hemodynamics. Umbilical venous flow (Q_{UV}), PI_{UA} and PI_{MCA} were recorded using standardised techniques[22,37-39].

All insonations for Doppler measurements were aligned in the direction of the vessel, and the angle of interrogation was always kept $\leq$30 degrees. When this angle was not zero, the Doppler shift was corrected accordingly. The recordings were acquired during fetal quiescence over at least 3 uniform heart cycles to determine systolic peak and time averaged maximum velocities and PI[40].

Statistics

Multilevel modelling was used in order to calculate mean and centiles for the CA and SA systolic peak and time averaged maximum velocity and PI by gestational age. To achieve normal distribution of the outcome variables, we used power transformation. The outcome variables were regressed against gestational age using fractional polynomials. The 2.5, 5, 10 and 25th centiles were calculated by subtracting 1.96 standard deviation (SD), 1.645 SD, 1.282 SD, and 0.674 SD from the mean, respectively. The 97.5, 95, 90 and 75th centiles were calculated by adding the respective multiples of the SD to the mean. The 95% CI of the mean, 5 and 95th centiles were derived.

To assess the effect of $V_{DV\text{-}ps}$, $V_{LPV\text{-}tamx}$, Q_{UV}, PI_{MCA}, and PI_{UA} on PI and systolic peak velocity in the CA and SA, we included these measurements (in three categories, <10th centile, 10–90th centile, and >90th centile, since responses were assumed to occur more commonly in extreme conditions) as indicator variables in the multilevel regressions models, which describe the mean of PI_{CA} and PI_{SA} and $V_{CA\text{-}ps}$ and $V_{SA\text{-}ps}$. The gestational age-dependent centiles of these independent variables were also calculated by multilevel regression. Indicator variables with significant improvement in the goodness of fit to the models, as assessed by the deviance statistics (χ^2 with p <0.05), were considered to significantly influence the outcome variables.

Associations of peak systolic velocity and PI in the CA and SA on HA and SA peak systolic velocity and PI were assessed by simple linear regression of transformed data.

The intra- and inter-observer reproducibility for the CA and SA measurements was expressed as intra-and interclass correlation.

The statistical analysis was performed using SPSS (Statistical Package for the Social Sciences, SPSS Inc, Chicago, IL) and the MlWin program (MlWin, Centre for Multilevel Modelling, University of Bristol, UK).

RESULTS

Median maternal age at inclusion was 29 years (range 20-40) and median gestational age at delivery was 40 weeks+3 days (range35+3 to 42+4 weeks). The caesarean section rate (10.6 %) and birth weights (median 3700 g, range 2260-4980) were similar to values in the local population (caesarean rate being 11.8%)[41]. Five women developed pre-eclampsia (3.1%). Population characteristics have been further detailed previously [37]. The intra- and inter-observer study showed reproducibility with intra- and inter-class correlation coefficient >85% for all parameters tested (table 1).

We obtained 510 measurements of the CA in a total of 633 sessions (80.6% success rate). Unfavourable fetal position and fetal movements were reasons for not obtaining measurements. The diaphragm, abdominal aorta and the neighbouring superior mesenteric artery proved to be valuable anatomical landmarks when identifying the CA (Figure 1). No angle correction was required in 179 recordings; median angle correction of the Doppler shift was 12° (range 0-30°). The systolic peak velocity ($V_{CA\text{-}ps}$) and time averaged maximum velocity ($V_{CA\text{-}tamx}$) and pulsatility index (PI_{CA}) with fitted mean and reference intervals are presented in Figure 2. The corresponding gestational age-specific centiles are presented in tables 2-4. The mean $V_{CA\text{-}ps}$ increased from 26 to 50 cm/s and mean $V_{CA\text{-}tamx}$ from 12 to 22

cm/s during 21-39 weeks of gestation. The mean PI_{CA} increased from 1.73 to a plateau at 2.10 at 29-30 weeks and decreased to 1.81 at 39 weeks.

We obtained 521 measurements of the SA (82.3% success rate). The median angle of insonation was 0° (306 observations with no correction, range 0-30°). Anatomical landmarks for identifying the SA were the stomach and spleen, and the point of branching off at the CA (Figure 1). Similar to the CA, the SA velocities increased throughout the second half of pregnancy, mean $V_{SA\text{-}ps}$ from 19 to 49 cm/s during week 21-39, and correspondingly the $V_{SA\text{-}tamx}$ from 11 to 24 cm/s (Figure 3 and Tables 5-6). The PI_{SA} increased from 1.39 to reach a plateau of 1.85 at 29-30 weeks followed by a decline to 1.58 at 39 weeks of gestation (Figure 3 and Table 7). Terms for calculating conditional ranges for repeat measurements of the CA and SA are presented in the appendix.

For the LPV measurements the median angle of insonation was 1° (range 0-30°) degrees. The mean $V_{LPV\text{-}tamx}$ increased from 8.9 cm/s at 21weeks to 12.1 at 32 weeks, and then decreased to 10.9 cm/s at 38 weeks (Figure 4).

In the following we assumed that absolute velocities predominantly reflected volume flow and the kinetic condition of the central circulation (i.e. cardiac output)[42,43], while PI to a larger extent reflected degree of vasodilatation and local regulation.

Concerning local regulation, when examining for covariation between hemodynamics in the CA and HA, we found a weak correlation between PI_{HA} and PI_{CA} (r=0.3, 95% CI 0.1-0.5). When analysing the CA vs. SA we found a stronger correlation between the PI_{SA} and PI_{CA} (r=0.5, 95% CI 0.3-0.6) (Figure 5). Finally, there was a weak correlation between the PI`s in the splenic and hepatic arteries (PI_{SA} vs. PI_{HA}), (r=0.1, 95%CI –0.05-0.3) (Figure 5), indicating that the SA and HA have independent local regulatory mechanisms, and that the PI_{CA} is more closely related to the PI_{SA} than to PI_{HA}.

A ratio of the CA and SA (PI_{CA} /PI_{SA}) showed a stable relationship throughout the second half of pregnancy, mean 1.0 (95%CI 1.016-1.023) (Figure 6).

The hypothesis that the portocaval perfusion pressure is a local determinant for CA and SA was tested using regression analyses. A low $V_{DV\text{-}ps}$, representing portocaval pressure[10], should then be associated with a vasodilatation, i.e. low PI_{CA} and PI_{SA}. The analysis confirmed that fetuses with $V_{DV\text{-}ps}$ <10th centile had a lower PI_{CA} and PI_{SA} ($p<0.0001$) (Figure 7).

Another possible local determinant for vasodilatation in the CA and SA is the umbilical and portal distribution between the left and right liver lobe reflected in the velocity ($V_{LPV\text{-}tamx}$) of the LPV. We hypothesised that low velocity (indicating less oxygenated umbilical blood to the right lobe) was associated with vasodilatation in the arteries (low PI_{CA} and PI_{SA}). The regression analysis confirmed that $V_{LPV\text{-}max}$ <10th centile was associated with lower PI_{CA} and PI_{SA} ($p<0.0001$) (Figure 7).

Q_{UV} <10th centile was associated with low PI_{CA} and PI_{SA} ($P< 0.0001$) which is in line with the hypothesis. However, we also found a reduced PI_{CA} and PI_{SA} when the umbilical blood flow was high (Q_{UV} >90th centile) (Figure 7) which is difficult to interpret.

Assuming that MCA and UA are indicators of the general fetal circulation (e.g. cardiac output) we tested whether a low PI_{MCA} and PI_{UA} covaried with a low PI_{CA} and PI_{SA}. Again, using regression analysis, PI_{MCA} and PI_{UA} <10th centile were indeed associated with low PI_{CA} and PI_{SA} ($p<0.0001$) (Figure 8).

Absolute blood velocities are positively related to volume flow[42,43]. We used this relationship to test the hypothesis that high blood velocities in CA and SA covary with high volume flow in the umbilical circuit (Q_{UV}) and high velocities in the DV and LPV. Regression analysis showed that $V_{DV\text{-}ps}$,$V_{LPV\text{-}tamx}$ and Q_{UV}>90th centile were associated with high velocities in the CA and SA ($p<0.005$ for $V_{DV\text{-}ps}$ $V_{CA\text{-}ps}$ relationship, for all others

p<0.0001) (result not shown). The hypothesis was further supported by the close relationship in absolute velocities found between the arteries: $V_{HA\text{-}ps}$ vs. $V_{CA\text{-}ps}$ (r=0.6, 95% CI 0.5-0.8), and $V_{SA\text{-}ps}$ vs. $V_{CA\text{-}ps}$ (r=0.7 95% CI 0.6-0.8).

DISCUSSION

The spleen has important hematopoietic and immunologic functions in the developing fetus[24,26,44]. Here we show that the fetal spleen, rich in adrenergic neurons[24], is also involved in maintaining portal perfusion (Figure 7), but independently from the hepatic artery (Figure 5), which buffers liver perfusion[22] via an adenosine mediated mechanism[21]. A vasodilatation in the SA (as indicated by the low PI_{SA}) is also present when the right liver lobe has a reduced umbilical supply (as indicated by low $V_{LPV\text{-}tam}$) (Figure 7). We suggest that active regulation of SA under physiological conditions is augmented in extreme cases, explaining the previously reported changes in PI_{SA} and $V_{SA\text{-}ps}$ in fetal growth-restriction and anemia[27-31].

The celiac artery feeds both the hepatic and splenic arteries, and our results suggest CA to be closer related to splenic than hepatic hemodynamics (Figure 5). Thus, the PI_{CA} cannot be used as a substitute for a less accessible PI_{HA} (as had been hoped for), nor can their absolute velocities be used interchangeably. Rather, we found the ratio of the PI_{CA} and PI_{SA} (PI_{CA}/PI_{SA}) to be constant through second half of gestation (Figure 6). This finding might be surprising since most growth velocities and hemodynamic relationships are gestational age dependent. Whether the priority of flow from the celiac artery to the spleen is altered in growth restricted or anemic fetuses remains to be explored.

The longitudinal reference ranges established for the SA and CA in this study, together with those recently established for the HA[22], provide the methods for a differential hemodynamic assessment of the fetus, particularly in cases such as fetal growth-restriction or anemia. In addition to being suitable for single measurements, these longitudinal ranges are

appropriate for serial observations[32] when used in combination with the terms for calculating conditional reference ranges (Appendix). The narrow 95% CI for the centiles indicates that the reference ranges are reliable also for extreme values (Figure 2 and 3).

The variation seen between the present results and previous cross-sectional studies of the SA[27,29,30] may be due to differences in design, population sample, insonation technique and analysis. Bahado-Singh *et al* showed that their reference values for $V_{SA\text{-}ps}$ were less suitable for predicting anemia at <28 weeks of gestation[29]. Comparing our new reference ranges with their results of anemic fetuses, it seems justified to reassess the method particularly for pregnancies <28 weeks.

The inverted u-shaped curve of our reference ranges for the PI_{CA} and PI_{SA} (Figure 2 and 3) is in line with a previous cross-sectional study of the SA[27] and similar to those of the middle cerebral artery PI[37,45] probably reflecting organ growth and vascularisation. The spleen exhibits linear growth during the second half of pregnancy[46,47], while there is a curvilinear increase in normalised portal flow (where SA is an important contributor) towards term, supporting the assumption of increased vascularisation of the spleen[15].

Arterial blood velocities are not only related to volume of blood flowing through an organ but also to central hemodynamics and cardiac output[43]. Our findings of increasing flow velocities in the superior splanchnic arteries during late pregnancy are in line with this concept and underscore the increasing perfusion of the splanchnic organs towards the end of pregnancy. We also showed that low PI_{CA} and PI_{SA} were linked with low PI in the umbilical and cerebral arteries indicating a common dependence on general hemodynamics(Figure 8), further supported by the fact that $V_{SA\text{-}ps}$ and $V_{CA\text{-}ps}$ were high when Q_{UV} was high.

When comparing our results for the mean V_{LPV}-tamx with those of another longitudinal study[20] we find similar results.

In short, we have shown that the CA feeds two independently regulated arteries, the HA and SA, of which both are involved in maintaining fetal venous liver perfusion. Our reference ranges for the arteries and their interrelationship (CA vs. SA) provide new methods for a differential assessment of the developing circulation under physiological conditions and in clinical settings using serial measurements.

Acknowledgement

The Western Norway Regional Health Authority (Grant no 911160) supported the study. M.A.H is supported by the British Heart Foundation.

Reference List

1. Kiserud T, Ebbing C, Kessler J, Rasmussen S. Fetal cardiac output, distribution to the placenta and impact of placental compromise. *Ultrasound Obstet Gynecol* 2006;**28**:126-136.

2. Sutton M.S.J, Plappert T., Doubilet P. Relationship between placental blood flow and combined ventricular output with gestational age in normal fetuses. *Cardiovasc Res* 1991;603-608.

3. Bellotti M, Pennati G, De Gasperi C, Battaglia FC, Ferrazzi E. Role of ductus venosus in distribution of umbilical blood flow in human fetuses during second half of pregnancy. *Am J Physio Heart Circ Physiol* 2000;**279**:H1256-H1263.

4. Haugen G, Kiserud T, Godfrey K, Crozier S, Hanson M. Portal and umbilical venous blood supply to the liver in the human fetus near term. *Ultrasound Obstet Gynecol* 2004;**24**:599-605.

5. Kiserud T, Rasmussen S, Skulstad S. Blood flow and the degree of shunting through the ductus venosus in the human fetus. *Am J Obstet Gynecol* 2000;**182**:147-153.

6. Kessler J, Rasmussen S, Godfrey K, Hanson M, Kiserud T. Longitudinal study of umbilical and portal venous blood flow to the fetal liver: low pregnancy weight gain is associated with preferential supply to the left fetal liver lobe. *Ped Res* 2007;*in press*.

7. Kiserud T, Eiknes SH, Blaas HGK, Hellevik LR. Ultrasonographic Velocimetry of the Fetal Ductus Venosus. *Lancet* 1991;**338**:1412-1414.

8. Kiserud T, Eiknes SH, Blaas HG, Hellevik LR. Foramen ovale - an ultrasonographic study of its relation to the inferior vena-cava, ductus venosus and hepatic veins. *Ultrasound Obstet Gynecol* 1992;**2**:389-396.

9. Hellevik LR, Kiserud T, Irgens F, Ytrehus T, Eik-Nes SH. Simulation of pressure drop and energy dissipation for blood flow in a human fetal bifurcation. *J Biomech Eng* 1998;**120**:455-462.

10. Kiserud T, Hellevik LR, Eiknes SH, Angelsen BAJ, Blaas HG. Estimation of the pressure-gradient across the fetal ductus venosus based on doppler velocimetry. *Ultrasound Med Biol* 1994;**20**:225-232.

11. Schroder HJ, Tchirikov M, Rybakowski C. Pressure pulses and flow velocities in central veins of the anesthetized sheep fetus. *Am J Physiol Heart Circ Physiol* 2003;**284**:H1205-H1211.

12. Tchirikov M, Kertschanska S, Schroder HJ. Obstruction of ductus venosus stimulates cell proliferation in organs of fetal sheep. *Placenta* 2001;**22**:24-31.

13. Tchirikov M, Kertschanska S, Sturenberg HJ, Schroder HJ. Liver blood perfusion as a possible instrument for fetal growth regulation. *Placenta* 2002;**23**:S153-S158.

14. Haugen G, Hanson M, Kiserud T, Crozier S, Inskip H, Godfrey KM. Fetal liver-sparing cardiovascular adaptations linked to mother's slimness and diet. *Circ Res* 2005;**96**:12-14.

15. Kessler J, Rasmussen S, Kiserud T. The fetal portal vein: normal blood flow development during the second half of human pregnancy. *Ultrasound Obstet Gynecol* 2007;**30**:52-60.

16. Emery JL. Functional Asymmetry of Liver. *Annals of the New York Academy of Sciences* 1963;**111**:37-44.

17. Emery JL. The Distribution of Haemopoietic Foci in the Infantile Human Liver. *J Anat* 1956;**90**:293-297.

18. Ring JA, Ghabrial H, Ching MS, Shulkes A, Smallwood RA, Morgan DJ. Propranolol elimination by right and left fetal liver: Studies in the intact isolated perfused fetal sheep liver. *J Pharmacol Exp Ther* 1998;**284**:535-541.

19. Cox LA, Schlabritz-Loutsevitch N, Hubbard GB, Nijland MJ, McDonald TJ, Nathanielsz PW. Gene expression profile differences in left and right liver lobes from mid-gestation fetal baboons: a cautionary tale. *J Physiol* 2006;**572**:59-66.

20. Kessler J, Rasmussen S., Kiserud T. The left portal vein as an indicator of watershed in the fetal circulation: development during the second half of pregnancy and a suggested method of evaluation. *Ultrasound Obstet Gynecol* 2007;**30**:757-764.

21. Lautt WW. The 1995 Ciba-Geigy Award Lecture. Intrinsic regulation of hepatic blood flow. *Can J Physiol Pharmacol* 1996;**74**:223-233.

22. Ebbing C, Rasmussen S, Godfrey K.M, Hanson M.A., Kiserud T. Hepatic artery hemodynamics suggest operation of a buffer response in the human fetus. *Reproductive Sciences* 2007;*in press*.

23. Tsukuda T, Ito K, Koike S, Sasaki K, Shimizu A, Fujita T et al. Pre- and postprandial alterations of portal venous flow: Evaluation with single breath-hold three dimensional half-Fourier fast spin-echo MR imaging and a selective inversion recovery tagging pulse. *J Magn Res Imaging* 2005;**22**:527-533.

24. Anagnostou V.K, Doussis-Anagnostopoulou I, Tiniakos D.G, Karandrea D, Agapitos E, Karakitsos P et al. Ontogeny of intrinsic innervation in the human thymus and spleen. *J Histochem Cytochem* 2007;**55**:813-820.

25. Vatner SF. Effects of Hemorrhage on Regional Blood-Flow Distribution in Dogs and Primates. *J Clin Invest* 1974;**54**:225-235.

26. Cumano A, Godin I. Ontogeny of the Hematopoietic System. *Ann Rev Immunol* 2007;**25**:745-785.

27. Abuhamad AZ, Mari G, Bogdan D, Evans AT. Doppler Flow Velocimetry of the Splenic Artery in the Human Fetus - Is It A Marker of Chronic Hypoxia. *Am J Obstet Gynecol* 1995;**172**:820-825.

28. Bahado-Singh R, Oz U, Deren O, Pirhonen J, Kovanci E, Copel J et al. A new splenic artery Doppler velocimetric index for prediction of severe fetal anemia associated with Rh alloimmunization. *Am J Obstet Gynecol* 1999;180:49-54.

29. Bahado-Singh R, Oz U, Deren O, Kovanchi E, Hsu CD, Copel MJ et al. Splenic artery Doppler peak systolic velocity predicts severe fetal anemia in rhesus disease. *Am J Obstet Gynecol* 2000;**182**:1222-1226.

30. Capponi A, Rizzo G, Arduini D, Romanini C. Splenic artery velocity waveforms in small-for-gestational-age fetuses: Relationship with pH and blood gases measured in umbilical blood at cordocentesis. *Am J Obstet Gynecol* 1997;**176**:300-307.

31. Oz U, Kovanci E, Jeffress A, Mendilicioglu I, Mari G, Bahado-Singh RO. Splenic artery Doppler in the prediction of the small-for-gestational age infant. *Ultrasound Obstet Gynecol* 2002;**20**:346-350.

32. Royston P. Calculation of Unconditional and Conditional Reference Intervals for Fetal Size and Growth from Longitudinal Measurements. *Stat Med* 1995;**14**:1417-1436.

33. Johnsen SL, Rasmussen S, Sollien R, Kiserud T. Fetal age assessment based on ultrasound head biometry and the effect of maternal and fetal factors. *Acta Obstet Gynecol Scand* 2004;**83**:716-723.

34. Schroder HJ, Tchirikov M, Rybakowski C. Pressure pulses and flow velocities in central veins of the anesthetized sheep fetus. *Am J Physiol Heart Circ Physiol* 2003;**284**:H1205-H1211.

35. Kiserud T, Kilavuz O, Hellevik LR. Venous pulsation in the fetal left portal branch: the effect of pulse and flow direction. *Ultrasound Obstet Gynecol* 2003;**21**:359-364.

36. Kilavuz O, Vetter K, Kiserud T, Vetter P. The left portal vein is the watershed of the fetal venous system. *J Perinat Med* 2003;**31**:184-187.

37. Ebbing C., Rasmussen S., Kiserud T. Middle cerebral artery blood flow velocities and pulsatility index and the cerebroplacental ratio: longitudinal reference ranges and terms for serial measurements. *Ultrasound Obstet Gynecol* 2007;**30**:287-296.

38. Acharya G, Wilsgaard T, Berntsen GKR, Maltau JM, Kiserud T. Reference ranges for serial measurements of umbilical artery Doppler indices in the second half of pregnancy. *Am J Obstet Gynecol* 2005;**192**:937-944.

39. Mari G, Abuhamad AZ, Cosmi E, Segata M, Altaye M, Akiyama M. Middle cerebral artery peak systolic velocity - Technique and variability. *J Ultrasound Med* 2005;**24:**425-430.

40. Gosling R, King D. Ultrasound angiology. In: *Arteries and veins* Macus A, Adamson J, (eds). Churchill-Livingstone: Edinburgh, 1975. 61-98.

41. Skjaerven R, Gjessing HK, Bakketeig LS. Birthweight by gestational age in Norway. *Acta Obst Gynecol Scand* 2000;**79**:440-449.

42. Acharya G, Erkinaro T, Makikallio K, Lappalainen T, Rasanen J. Relationships among Doppler-derived umbilical artery absolute velocities, cardiac function, and placental volume blood flow and resistance in fetal sheep. *Am J Physiol Heart Circ Physiol* 2004;**286**:H1266-H1272.

43. Acharya G, Wilsgaard T, Berntsen GKR, Maltau JM, Kiserud T. Doppler-derived umbilical artery absolute velocities and their relationship to fetoplacental volume blood flow: a longitudinal study. *Ultrasound Obstet Gynecol* 2005;**25**:444-453.

44. Christensen JL, Wright DE, Wagers AJ, Weissman IL. Circulation and chemotaxis of fetal hematopoietic stem cells. *PLoS Biol* 2004;**2:**368-377.

45. Mari G, Deter RL. Middle Cerebral-Artery Flow Velocity Wave-Forms in Normal and Small-For-Gestational-Age Fetuses. *Am J Obstet Gynecol* 1992;**166**:1262-1270.

46. Aoki S, Hata T, Kitao M. Ultrasonographic Assessment of Fetal and Neonatal Spleen. *Am J Perinat* 1992;**9**:361-367.

47. Oepkes D, Meerman RH, Vandenbussche FPHA, Vankamp IL, Kok FG, Kanhai HHH. Ultrasonographic Fetal Spleen Measurements in Red-Blood-Cell Alloimmunized Pregnancies. *Am J Obstet Gynecol* 1993;**169**:121-128.

APPENDIX

$V_{CA\text{-}ps}$

An actual transformed $V_{CA\text{-}ps}$ observation may be expressed by the regression mean as a function of gestational age (GA) in weeks and residuals as

$y_{ij} = \hat{\beta}_0 + u_{0j} + e_{0ij} + \hat{\beta}_1 GA_{ij} + \hat{\beta}_2 GA_{ij}^2$, where $\hat{\beta}_0 = 0.512302$, $\hat{\beta}_1 = 0.1311896$, and $\hat{\beta}_2 = -0.001712879$, and u_{0j} and e_{0ij} residuals, and $_i$ denotes level 1 (observation) and $_j$ level 2 (fetus)

1) Unconditional mean and variance

$V_{CA\text{-}ps}$ was transformed to the 0.283 power.

Transformed mean= μ

=0.512302+0.1311896 GA–0.001712879 GA^2

which may be "backtransformed" as $\mu^{(1/0.283)}$

Variance

$=\sigma^2$

$= \hat{\sigma}_{u0}^2 + \hat{\sigma}_{e0}^2$

=0.028399

2) Unconditional reference interval is given by

$= \mu + \hat{z}\sigma$,
where σ is the standard deviation and $\hat{z} = -1.96, -1.645, -1.282, -0.674, 0.674, 1.282, 1.645$, and 1.96 for the $2.5^{th}, 5^{th}, 10^{th}, 25^{th}, 50^{th}, 75^{th}, 90^{th}, 95^{th}$, and 97.5^{th} percentiles, respectively.

3) Conditional mean and variance

The covariance between the first and a later observation (at gestational ages GA1 and GA2) is set as the level-2 covariance as the level-1 covariance is assumed to be zero. The covariance is given by

$$\sigma_{12} = \hat{\sigma}^2_{u0}$$
$$= 0.005154862$$

Conditional mean $\mu_{2|1}$ is given by

$$\mu_2 + (y_1 - \mu_1)\sigma_{12} / \sigma_1^2$$

were μ_2 and μ_1 are means at GA_2 and GA_1, y_1 is the observation at GA_1,

and σ_1^2 the variance at GA_1; in this case the variance is independent of gestational age.

Conditional variance is given by

$$\sigma^2_{2|1}$$
$$= \sigma_2^2 - \sigma_{12}^2 / \sigma_1^2$$

4) Conditional reference interval

$\mu_{2|1} + z\ \sigma_{2|1}$

PI_{CA}

An actual transformed PI_{CA} observation may be expressed by the regression mean as a function of gestational age (GA) in weeks and residuals as

$$y_{ij} = \hat{\beta}_0 + u_{0j} + e_{0ij} + \hat{\beta}_1 GA_{ij} + \hat{\beta}_2 \ln(GA)_{ij}, \text{where} \hat{\beta}_0 = 2.380166,$$

$\hat{\beta}_1 = 0.02139268$, and $\hat{\beta}_2 = -0.6350049$, and u_{0j} and e_{0ij} residuals, and $_i$ denotes level1(observation) and $_j$ level 2 (fetus)

1) Unconditional mean and variance

PI_{CA} was transformed to the –0.2 power.

Transformed mean= μ

=2.3801666+0.02139268 GA–0.6350049 ln(GA)

which may be ”backtransformed” as $\mu^{(1/-0.2)}$

Variance

$= \hat{\sigma}^2$

$= \hat{\sigma}_{u0}^2 + \hat{\sigma}_{e0}^2$

=0.0010406152

2) Unconditional reference interval is given by

$= \mu + \hat{z}\sigma,$
where σ is the standard deviation and $\hat{z} = -1.96, -1.645, -1.282, -0.674, 0.674, 1.282, 1.645,$ and 1.96 for the $2.5^{th}, 5^{th}, 10^{th}, 25^{th}, 50^{th}, 75^{th}, 90^{th}, 95^{th},$ and 97.5^{th} percentiles, respectively.

3) Conditional mean and variance

The covariance between the first and a later observation (at gestational ages GA1 and GA2) is set as the level-2 covariance as the level-1 covariance is assumed to be zero. The covariance is given by

$\sigma_{12} = \hat{\sigma}_{u0}^2$

$= 0.00007916$

Conditional mean $\mu_{2|1}$ is given by

$$\mu_2 + (y_1 - \mu_1)\sigma_{12} / \sigma_1^2$$

were μ_2 and μ_1 are means at GA_2 and GA_1, y_1 is the observation at GA_1,

and σ_1^2 the variance at GA_1; in this case the variance is independent of gestational age.

Conditional variance is given by

$$\sigma_{2|1}^2 = \sigma_2^2 - \sigma_{12}^2 / \sigma_1^2$$

4) Conditional reference interval

$$\mu_{2|1} + z\ \sigma_{2|1}$$

$V_{CA\text{-}tamx}$

An actual transformed $V_{CA\text{-}tamx}$ observation may be expressed by the regression mean as a function of gestational age (GA) in weeks and residuals as

$$y_{ij} = \hat{\beta}_0 + u_{0j} + e_{0ij} + \hat{\beta}_1 GA_{ij}^2 + \hat{\beta}_2 GA_{ij}, \text{where} \hat{\beta}_0 = 1.152027,$$

$\hat{\beta}_1 = -13.3413$, and $\hat{\beta}_2 = 0.001027558$, and u_{0j} and e_{0ij} residuals, and $_i$ denotes level 1 (observation) and $_j$ level 2 (fetus)

1) Unconditional mean and variance

$V_{CA\text{-}tamx}$ was transformed to the 0.054 power.

Transformed mean= μ

$=1.152027–13.35413\ GA^{-2}+0.001027558\ GA$

which may be ”backtransformed” as $\mu^{(1/0.054)}$

Variance

$= \hat{\sigma}^2$

$= \hat{\sigma}_{u0}^2 + \hat{\sigma}_{e0}^2$

=0.0001734746

2) Unconditional reference interval is given by

$= \mu + \hat{z}\sigma,$
where σ is the standard deviation and $\hat{z} = -1.96, -1.645, -1.282, -0.674, 0.674, 1.282, 1.645,$ and 1.96 for the $2.5^{th}, 5^{th}, 10^{th}, 25^{th}, 50^{th}, 75^{th}, 90^{th}, 95^{th},$ and 97.5^{th} percentiles, respectively.

3) Conditional mean and variance

The covariance between the first and a later observation (at gestational ages GA1 and GA2) is set as the level-2 covariance as the level-1 covariance is assumed to be zero. The covariance is given by

$\sigma_{12} = \hat{\sigma}_{u0}^2$
$= 0.00002405$

Conditional mean $\mu_{2|1}$ is given by

$\mu_2 + (y_1 - \mu_1)\sigma_{12} / \sigma_1^2$

were μ_2 and μ_1 are means at GA_2 and GA_1, y_1 is the observation at GA_1,

and σ_1^2 the variance at GA_1; in this case the variance is independent of gestational age.

Conditional variance is given by

$$\sigma^2_{2|1} = \sigma^2_2 - \sigma^2_{12} / \sigma^2_1$$

4) Conditional reference interval

$\mu_{2|1} + z\ \sigma_{2|1}$

$V_{SA\text{-}ps}$

An actual transformed $V_{SA\text{-}ps}$ observation may be expressed by the regression mean as a function of gestational age in weeks and residuals as

$y_{ij} = \hat{\beta}_0 + u_{0j} + e_{0ij} + \hat{\beta}_1 GA_{ij}^{0.5} + \hat{\beta}_2 GA_{ij}^{3}$, where $\hat{\beta}_0 = -27.11945$, $\hat{\beta}_1 = 7.831183$, and $\hat{\beta}_2 = -0.000120349$, and u_{0j} and e_{0ij} residuals, and $_i$ denotes level 1 (observation) and $_j$ level 2 (fetus)

denotes level 1 (measurement) and *j* level 2 (fetus).

1) Unconditional mean and variance

$V_{SA\text{-}ps}$ was transformed to the 0.69 power.

Transformed mean= μ

=–27.11945+7.831183 gestational age$^{0.5}$–0.000120349 gestational age^3

which may be ”backtransformed” as $\mu^{(1/0.69)}$

Variance

$=\sigma^2$

$= \hat{\sigma}^2_{u0} + \hat{\sigma}^2_{e0}$

=3.257004

2) Unconditional reference interval is given by

$=\mu + z\ \sigma,$

where σ is the standard deviation and z= −1.96, −1.645, −1.282, −0.674, 0.674, 1.282, 1.645, 1.96, for the 2.5th, 5th, 10th, 25th, 75th, 90th, 95th, and 97.5th percentiles, respectively.

3) Conditional mean and variance

The covariance between the first and a later observation (at gestational ages GA1 and GA2) is set as the level-2 covariance as the level-1 covariance is assumed to be zero. The covariance is given by

$\sigma_{12} = \hat{\sigma}^2_{u0}$

$= 0.8889915$

Conditional mean $\mu_{2|1}$ is given by

$\mu_2 + (y_1 - \mu_1)\sigma_{12} / \sigma_1^2$

were μ_2 and μ_1 are means at GA_2 and GA_1, y_1 is the observation at GA_1,

and σ_1^2 the variance at GA_1; in this case the variance is independent of gestational age.

Conditional variance is given by

$\sigma^2_{2|1}$
$= \sigma_2^2 - \sigma_{12}^2 / \sigma_1^2$

4) Conditional reference interval

$\mu_{2|1} + z\ \sigma_{2|1}$

PI_{SA}

An actual transformed PI_{SA} observation may be expressed by the regression mean as a function of gestational age in weeks and residuals as

$y_{ij} = \hat{\beta}_0 + u_{0j} + e_{0ij} + \hat{\beta}_1 GA_{ij}^{-1} + \hat{\beta}_2 GA_{ij}^{-0.5}$, where $\hat{\beta}_0 = 2.825513$,

$\hat{\beta}_1 = 57.60801$, and $\hat{\beta}_2 = -21.30113$, and u_{0j} and e_{0ij} residuals, and $_i$ denotes level 1 (observation) and $_j$ level 2 (fetus)

denotes level 1 (measurement) and *j* level 2 (fetus).

1) Unconditional mean and variance

PI_{SA} was transformed to the –0.252 power.

Transformed mean= μ

=2.825513 +57.60801 gestational age^{-1}–21.30113 gestational age$^{-0.5}$

which may be ”backtransformed” as $\mu^{(1/-0.252)}$

Variance

$=\sigma^2$

$= \hat{\sigma}_{u0}^2 + \hat{\sigma}_{e0}^2$

= 0.00302078

2) Unconditional reference interval is given by

=μ + z σ,

where σ is the standard deviation and z= −1.96, −1.645, −1.282, −0.674, 0.674, 1.282, 1.645, 1.96, for the 2.5th, 5th, 10th, 25th, 75th, 90th, 95th, and 97.5th percentiles, respectively.

3) Conditional mean and variance

The covariance between the first and a later observation (at gestational ages GA1 and GA2) is set as the level-2 covariance as the level-1 covariance is assumed to be zero. The covariance is given by

$$\sigma_{12} = \hat{\sigma}^2_{u0}$$
$$= 0.00054649$$

Conditional mean $\mu_{2|1}$ is given by

$$\mu_2 + (y_1 - \mu_1)\sigma_{12} / \sigma_1^2$$

were μ_2 and μ_1 are means at GA_2 and GA_1, y_1 is the observation at GA_1,

and σ_1^2 the variance at GA_1; in this case the variance is independent of gestational age.

Conditional variance is given by

$$\sigma^2_{2|1}$$
$$= \sigma_2^2 - \sigma_{12}^2 / \sigma_1^2$$

4) Conditional reference interval

$$\mu_{2|1} + z\ \sigma_{2|1}$$

$V_{SA\text{-}tamx}$

An actual transformed $V_{SA\text{-}tamx}$ observation may be expressed by the regression mean as a function of gestational age in weeks and residuals as

$y_{ij} = \hat{\beta}_0 + u_{0j} + e_{0ij} + \hat{\beta}_1 GA_{ij}^3 + \hat{\beta}_2 \ln(GA_{ij} GA_{ij}^3$, where $\hat{\beta}_0 = 2.077274$,

$\hat{\beta}_1 = 0.0002964$, and $\hat{\beta}_2 = -0.0000724$, and u_{0j} and e_{0ij} residuals, and $_i$ denotes level 1 (observation) and $_j$ level 2 (fetus)

denotes level 1 (measurement) and *j* level 2 (fetus).

1) Unconditional mean and variance

$V_{SA\text{-}tamx}$ was transformed to the 0.432 power.

Transformed mean= μ

=2.077274+0.0002964497gestational age^3–0.0000724184 ln(gestational age) gestational age^3

which may be ”backtransformed” as $\mu^{(1/0.432)}$

Variance

$=\sigma^2$

$= \hat{\sigma}_{u0}^2 + \hat{\sigma}_{e0}^2$

= 0.105805

2) Unconditional reference interval is given by

$=\mu + z\ \sigma$,

where σ is the standard deviation and z= −1.96, −1.645, −1.282, −0.674, 0.674, 1.282, 1.645, 1.96, for the 2.5th, 5th, 10th, 25th, 75th, 90th, 95th, and 97.5th percentiles, respectively.

3) Conditional mean and variance

The covariance between the first and a later observation (at gestational ages GA1 and GA2) is set as the level-2 covariance as the level-1 covariance is assumed to be zero. The covariance is given by

$$\sigma_{12} = \hat{\sigma}^2_{u0}$$
$$= 0.02022107$$

Conditional mean $\mu_{2|1}$ is given by

$$\mu_2 + (y_1 - \mu_1)\sigma_{12} / \sigma_1^2$$

were μ_2 and μ_1 are means at GA_2 and GA_1, y_1 is the observation at GA_1,

and σ_1^2 the variance at GA_1; in this case the variance is independent of gestational age.

Conditional variance is given by

$$\sigma^2_{2|1}$$
$$= \sigma_2^2 - \sigma_{12}^2 / \sigma_1^2$$

4) Conditional reference interval

$\mu_{2|1} + z\ \sigma_{2|1}$

LEGENDS

Figure 1: The fetal vasculature of the upper abdomen in a sagittal (panel A) and horizontal (panel C) view with corresponding colour Doppler images (panel B and D). The celiac artery (CA) is the first anterior branch from the descending aorta (AO) below the diaphragm, the Doppler gate is placed over the proximal part of the vessel (Panel A and B). The splenic artery (SA) arises from the celiac artery and continues posterior to the stomach (S) to reach the hilum of the spleen (Spl), the Doppler gate is placed over the proximal part of the vessel (panel C and D). Inferior vena cava (IVC), portal vein (PV), superior mesenteric artery (SMA), ductus venosus (DV).

Figure 2: Longitudinal reference ranges for the celiac artery systolic peak velocity ($V_{CA\text{-}ps}$) (Panel A), time averaged maximum velocity ($V_{CA\text{-}tamx}$) (Panel B), and pulsatility index (PI_{CA}) (Panel C) with fitted 5^{th}, 50^{th} and 95^{th} centiles and 95% confidence limits for the centiles based on 510 observations.

Figure 3: Longitudinal reference ranges for the splenic artery systolic peak velocity ($V_{SA\text{-}ps}$) (Panel A), time averaged maximum velocity ($V_{SA\text{-}tamx}$) (Panel B), and pulsatility index (PI_{SA}) (Panel C) with fitted 5^{th}, 50^{th} and 95^{th} centiles and 95% confidence limits for the centiles based on 521 observations.

Figure 4: Longitudinal reference ranges for left portal vein time averaged maximum velocity ($V_{LPV\text{-}tamx}$) with fitted 5^{th}, 50^{th} and 95^{th} centiles and 95% confidence limits for the centiles based on 282 observations.

Figure 5: Panel A: The hemodynamic relationship between the celiac and splenic artery is shown in a simple linear regression analysis of transformed data of their pulsatility indices (PI_{CA} and PI_{SA}) r=0.5 (Panel A). The independency between the hepatic and splenic artery is demonstrated with r=0.1 for their pulsatility indices, PI_{HA} and PI_{SA} (Panel B). Thin lines represent the 95%CI for the regression line.

Figure 6: The ratio of the celiac and-splenic artery pulsatility indices (PI_{CA}/PI_{SA}) with fitted 5^{th}, 50^{th} and 95^{th} centiles and 95% confidence limits for the centiles based on 427 sets of observations.

Figure 7: The influence of porto-caval pressure gradient expressed by the ductus venosus peak blood velocity ($V_{DV\text{-}ps}$)(Panel A), umbilical venous distribution to the right liver lobe expressed by the left portal vein blood velocity ($V_{LPV\text{-}tamx}$) (Panel B) and umbilical venous flow (Q_{UV}) (Panel C), on splenic artery pulsatility index (PI_{SA}). The difference between the lines represents the effect, all being significant. Lines with closed circles =<10^{th} centile, simple lines =10-90^{th} centile, lines with open circles=>90^{th} centile for the variables.

Figure 8: Influence of the general circulatory status expressed by the umbilical and middle cerebral artery pulsatility index (PI_{UA} and PI_{MCA}) on local regulation expressed by splenic artery pulsatility index (PI_{SA}) (Panel A: PI_{UA}, and Panel B: PI_{MCA}). The difference between the lines represents the effect, all being significant. Lines with closed circles= <10^{th} centile, simple lines=10-90^{th} centile, lines with open circles=>90^{th} centile for the variables.

Tables

Table 1: Intra- and interobserver variation of celiac and splenic artery flow velocities and pulsatility index.

Table 2: Longitudinal reference ranges for the celiac artery pulsatility index based on 510 observations in 161 low-risk pregnancies.

Table 3: Longitudinal reference ranges for the celiac artery peak systolic velocity based on 510 observations in 161 low-risk pregnancies.

Table 4: Longitudinal reference ranges for the celiac artery time averaged maximum velocity based on 510 observations in 161 low-risk pregnancies.

Table 5: Longitudinal reference ranges for the splenic artery pulsatility index based on 521 observations in 161 low-risk pregnancies.

Table 6: Longitudinal reference ranges for the splenic artery peak systolic velocity based on 521 observations in 161 low-risk pregnancies.

Table 7: Longitudinal reference ranges for the splenic artery time averaged maximum velocity based on 521 observations in 161 low-risk pregnancies.

Table 1 : Intra-and interobserver variation of celiac and splenic artery flow velocities and pulsatility index

Intraobserver variation

	Paired differences						
				95% CI			
	Mean	SD	SE	Lower	Upper	p	ICCC (%)
$V_{CA\text{-}ps}$	0.37	2.87	0.72	-1.2	1.9	0.612	98
$V_{CA\text{-}tamx}$	-0.28	1.92	0.50	-1.35	0.78	0.126	97
PI_{CA}	0.07	0.22	0.06	-0.05	0.19	0.152	88
$V_{SA\text{-}ps}$	0.13	3.14	0.78	-1.54	1.80	0.866	99
$V_{SA\text{-}tamx}$	0.37	3.13	0.78	-1.30	2.04	0.642	94
PI_{SA}	-0.05	0.28	0.07	-0.20	0.10	0.506	85

Interobserver variation

	Paried differences						
				95% CI			
	Mean	SD	SE	Lower	Upper	p	ICCC (%)
$V_{CA\text{-}ps}$	-1.47	6.37	1.70	-5.15	2.20	0.402	93
$V_{CA\text{-}tamx}$	-0.46	3.10	0.83	-2.26	1.31	0.576	87
PI_{CA}	-0.02	0.25	0.07	-0.16	0.13	0.779	86
$V_{SA\text{-}ps}$	0.54	4.21	1.09	-1.80	2.87	0.630	97
$V_{SA\text{-}tamx}$	-0.16	2.76	0.71	-1.69	1.37	0.828	95
PI_{SA}	0.06	0.20	0.05	-0.05	0.17	0.282	89

$V_{CA\text{-}ps;}$ Celiac artery systolic peak velocity; $V_{CA\text{-}tamx;}$ Celiac artery time averaged maximum velocity; $PI_{CA:}$ Celiac artery pulsatility index; $V_{SA\text{-}ps;}$ Splenic artery systolic peak velocity; $V_{SA\text{-}tamx;}$ Splenic artery time averaged maximum velocity; $PI_{SA:}$ Splenic artery pulsatility index; SD; standard deviation; SE; standard error; p; two tailed significance. ICCC: Intra – and inter class correlation coeffesient. respectively.

Table 2 Reference ranges for the celiac artery pulsatility index based on 510 observations in 161 low-risk pregnancies.

Gestation (weeks)	Centile								
	50	**2.5**	**5**	**10**	**25**	**75**	**90**	**95**	**97.5**
21	**1.73**	1.23	1.30	1.38	1.53	1.96	2.19	2.35	2.49
22	**1.81**	1.28	1.36	1.44	1.60	2.05	2.30	2.46	2.62
23	**1.88**	1.33	1.41	1.50	1.67	2.13	2.39	2.57	2.73
24	**1.94**	1.37	1.45	1.54	1.72	2.20	2.48	2.66	2.83
25	**2.00**	1.41	1.48	1.58	1.76	2.26	2.54	2.73	2.91
26	**2.04**	1.43	1.51	1.61	1.80	2.31	2.60	2.79	2.97
27	**2.07**	1.45	1.53	1.64	1.83	2.35	2.64	2.84	3.02
28	**2.09**	1.47	1.55	1.65	1.84	2.37	2.67	2.87	3.05
29	**2.10**	1.47	1.56	1.66	1.85	2.38	2.68	2.88	3.07
30	**2.10**	1.47	1.56	1.66	1.85	2.39	2.68	2.88	3.07
31	**2.09**	1.47	1.55	1.66	1.85	2.38	2.67	2.87	3.06
32	**2.08**	1.46	1.54	1.64	1.83	2.36	2.65	2.85	3.04
33	**2.06**	1.44	1.53	1.63	1.82	2.33	2.62	2.82	3.00
34	**2.03**	1.43	1.51	1.61	1.79	2.30	2.59	2.78	2.96
35	**1.99**	1.40	1.48	1.58	1.76	2.26	2.54	2.73	2.90
36	**1.95**	1.38	1.45	1.55	1.73	2.21	2.49	2.67	2.84
37	**1.91**	1.35	1.42	1.52	1.69	2.16	2.43	2.61	2.77
39	**1.81**	1.28	1.35	1.44	1.60	2.05	2.30	2.46	2.62

Table 3 Reference ranges for the celiac artery systolic peak velocity (cm/s) based on 510 observations in 161 low-risk pregnancies.

Gestation (weeks)	Centile								
	50	**2.5**	**5**	**10**	**25**	**75**	**90**	**95**	**97.5**
21	**26**	16	17	19	22	30	35	38	40
22	**28**	17	19	21	24	33	37	40	43
23	**30**	19	20	22	26	35	40	43	46
24	**32**	20	22	24	28	37	43	46	49
25	**34**	22	24	26	30	40	45	48	52
26	**36**	23	25	27	31	42	47	51	54
27	**38**	25	27	29	33	44	50	53	57
28	**40**	26	28	30	35	46	52	56	59
29	**42**	27	29	32	36	48	54	58	61
30	**43**	28	30	33	38	50	56	60	63
31	**45**	29	32	34	39	51	58	62	65
32	**46**	30	33	35	40	53	59	63	67
33	**47**	31	33	36	41	54	60	65	68
34	**48**	32	34	37	42	55	62	66	70
35	**49**	32	35	38	43	56	62	67	71
36	**49**	33	35	38	43	56	63	67	71
37	**50**	33	35	38	43	57	64	68	72
39	**50**	33	36	38	44	57	64	68	72

Table 4 Reference ranges for the celiac artery time averaged maximum velocity (cm/s) based on 510 observations in 161 low-risk pregnancies.

Gestation	Centile								
(weeks)	**50**	**2.5**	**5**	**10**	**25**	**75**	**90**	**95**	**97.5**
21	**12**	8	8	9	10	14	16	17	18
22	**13**	8	9	10	11	15	17	18	19
23	**13**	9	9	10	12	15	18	19	20
24	**14**	9	10	11	12	16	18	20	21
25	**15**	10	10	11	13	17	19	21	22
26	**15**	10	11	12	13	18	20	22	23
27	**16**	11	11	12	14	18	21	23	24
28	**17**	11	12	13	14	19	22	23	25
29	**17**	11	12	13	15	20	22	24	26
30	**18**	12	13	14	15	20	23	25	27
31	**18**	12	13	14	16	21	24	26	27
32	**19**	12	13	14	16	22	25	26	28
33	**19**	13	14	15	17	22	25	27	29
34	**20**	13	14	15	17	23	26	28	30
35	**20**	14	15	16	18	24	27	29	31
36	**21**	14	15	16	18	24	27	29	31
37	**22**	14	15	16	19	25	28	30	32
39	**23**	15	16	17	20	26	29	32	34

Table 5 Reference ranges for the splenic artery pulsatility index based on 521 observations in 161 low-risk pregnancies.

Gestation (weeks)	Centile								
	50	**2.5**	**5**	**10**	**25**	**75**	**90**	**95**	**97.5**
21	**1.39**	0.90	0.96	1.04	1.19	1.64	1.91	2.09	2.28
22	**1.50**	0.96	1.03	1.11	1.28	1.77	2.07	2.28	2.49
23	**1.60**	1.01	1.09	1.18	1.36	1.89	2.22	2.45	2.67
24	**1.68**	1.06	1.14	1.23	1.42	1.99	2.34	2.58	2.82
25	**1.74**	1.10	1.18	1.28	1.48	2.07	2.43	2.69	2.94
26	**1.79**	1.12	1.20	1.31	1.51	2.13	2.51	2.77	3.03
27	**1.82**	1.14	1.22	1.33	1.54	2.17	2.56	2.83	3.10
28	**1.84**	1.15	1.24	1.35	1.56	2.19	2.59	2.87	3.14
29	**1.85**	1.16	1.24	1.35	1.56	2.20	2.60	2.88	3.15
30	**1.85**	1.15	1.24	1.35	1.56	2.20	2.60	2.88	3.15
31	**1.84**	1.15	1.23	1.34	1.55	2.19	2.58	2.86	3.13
32	**1.82**	1.14	1.22	1.33	1.54	2.16	2.55	2.82	3.09
33	**1.79**	1.12	1.21	1.31	1.52	2.13	2.51	2.78	3.04
34	**1.76**	1.11	1.19	1.29	1.49	2.10	2.47	2.73	2.99
35	**1.73**	1.09	1.17	1.27	1.47	2.06	2.42	2.67	2.92
36	**1.69**	1.07	1.15	1.25	1.44	2.01	2.36	2.61	2.85
37	**1.66**	1.05	1.12	1.22	1.41	1.96	2.31	2.55	2.78
39	**1.58**	1.00	1.07	1.17	1.34	1.86	2.18	2.41	2.63

Table 6 Reference ranges for the splenic artery systolic peak velocity (cm/s) based on 521 observations in 161 low-risk pregnancies.

Gestation (weeks)	Centile								
	50	**2.5**	**5**	**10**	**25**	**75**	**90**	**95**	**97.5**
21	**19**	8	9	11	15	24	28	31	33
22	**22**	10	11	13	17	26	31	34	36
23	**24**	12	13	16	19	29	34	36	39
24	**26**	14	15	18	22	31	36	39	42
25	**29**	15	17	20	24	34	39	42	44
26	**31**	17	19	22	26	36	41	44	47
27	**33**	19	21	24	28	39	44	47	49
28	**35**	21	23	26	30	41	46	49	52
29	**37**	23	25	27	32	43	48	51	54
30	**39**	24	26	29	34	45	50	53	56
31	**41**	26	28	31	35	46	52	55	58
32	**42**	27	29	32	37	48	53	57	60
33	**44**	28	31	33	38	49	55	58	61
34	**45**	29	32	34	39	51	56	60	63
35	**46**	30	33	35	40	52	57	61	64
36	**47**	31	34	36	41	53	58	62	65
37	**48**	32	34	37	42	54	59	63	66
39	**49**	33	35	38	43	55	61	64	67

Table 7 Reference ranges for the splenic artery time averaged maximum velocity (cm/s) based on 521 observations in 161 low-risk pregnancies.

Gestation (weeks)	Centile								
	50	**2.5**	**5**	**10**	**25**	**75**	**90**	**95**	**97.5**
21	**11**	6	7	7	9	13	15	16	17
22	**11**	6	7	8	9	13	15	17	18
23	**12**	7	7	8	10	14	16	18	19
24	**13**	7	8	9	11	15	17	19	20
25	**13**	8	9	10	11	16	18	19	21
26	**14**	8	9	10	12	17	19	20	22
27	**15**	9	10	11	13	17	20	21	23
28	**16**	10	10	11	13	18	21	22	24
29	**17**	10	11	12	14	19	22	23	25
30	**17**	11	12	13	15	20	23	24	26
31	**18**	11	12	14	16	21	24	25	27
32	**19**	12	13	14	16	22	25	26	28
33	**20**	13	14	15	17	23	25	27	29
34	**21**	13	14	16	18	23	26	28	30
35	**21**	14	15	16	19	24	27	29	31
36	**22**	14	15	17	19	25	28	30	31
37	**23**	15	16	17	20	26	29	31	32
39	**24**	16	17	18	21	27	30	32	34

Figure 1

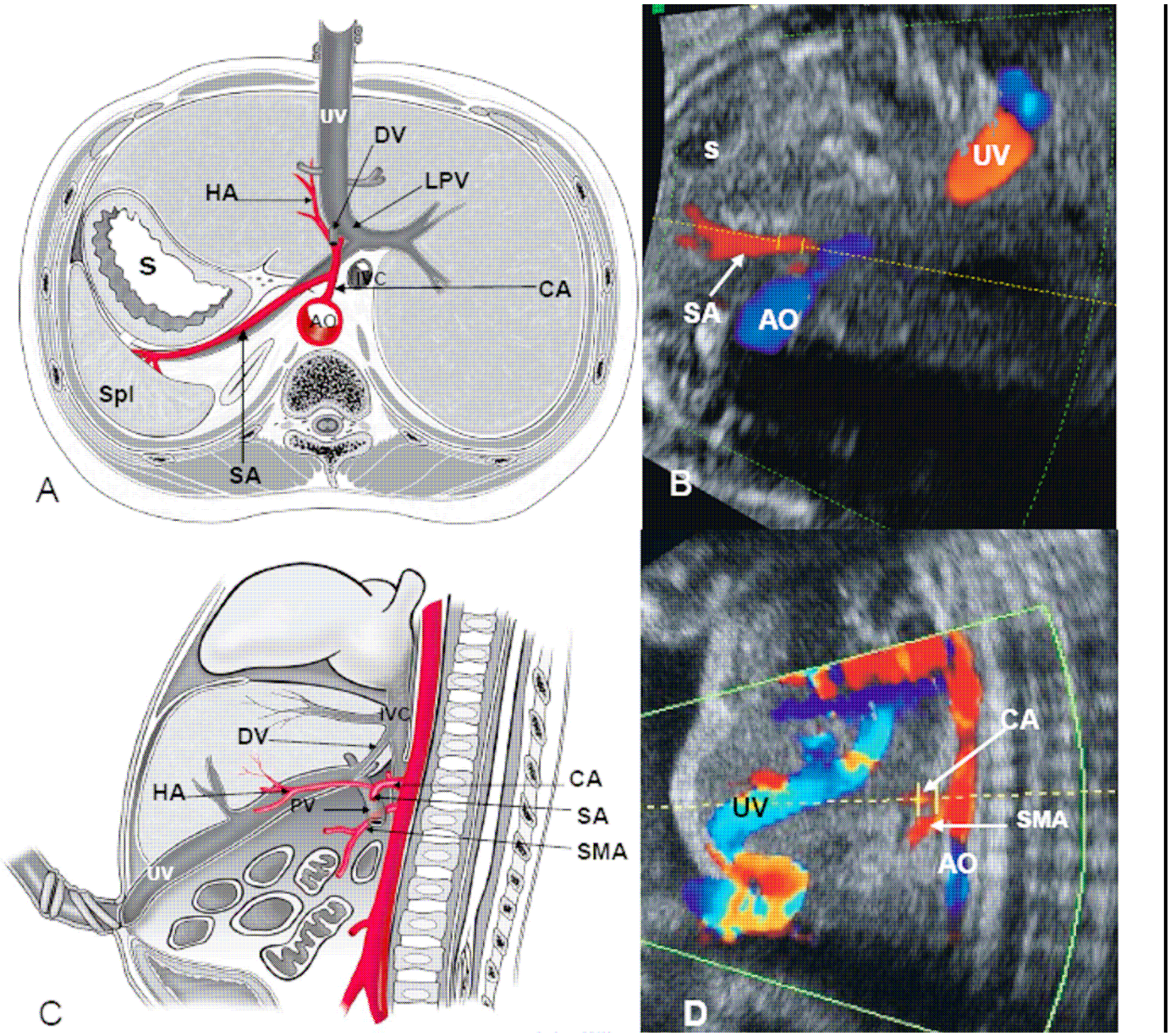
UV
DV
HA
LPV
S
IVC
CA
AO
Spl
SA
A
S
UV
SA
AO
B
IVC
DV
CA
HA
PV
SA
SMA
UV
C
CA
UV
SMA
AO
D

Figure 2

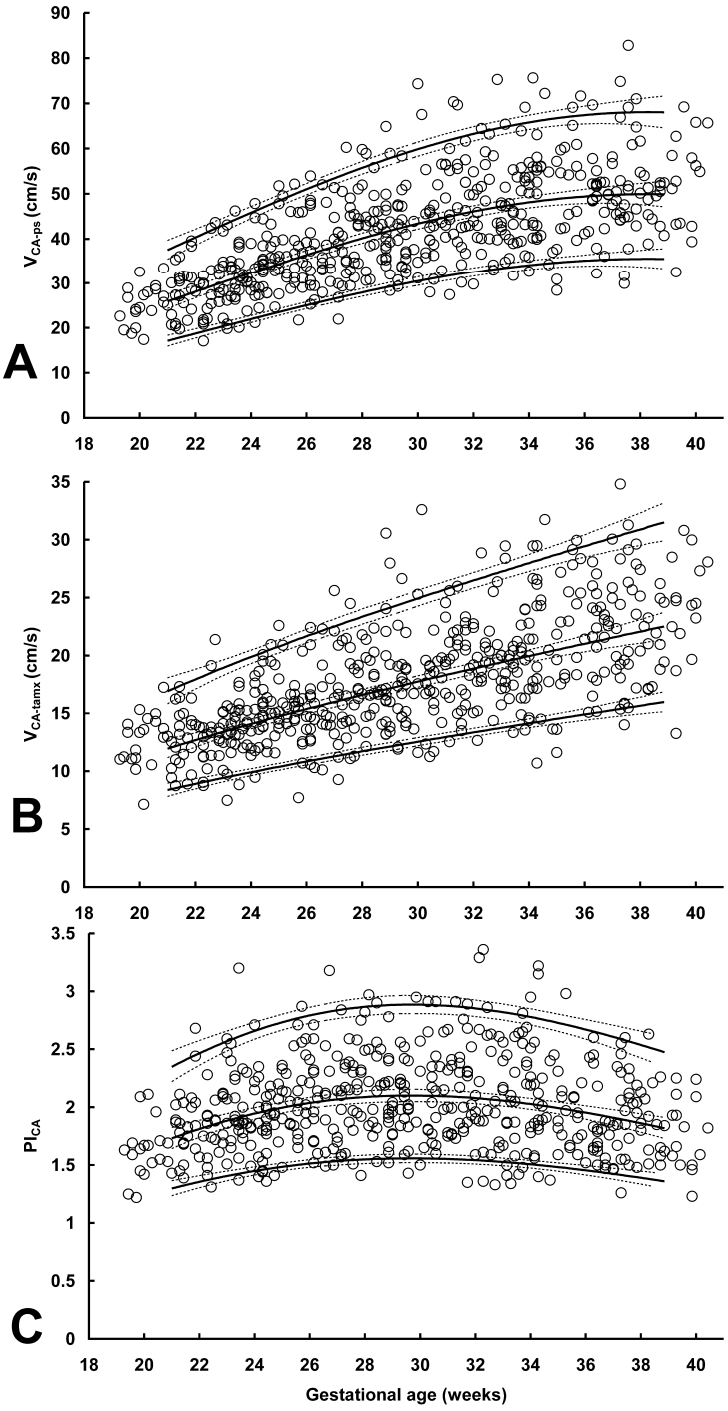
A
B
C
$V_{CA\text{-}ps}$ (cm/s)
$V_{CA\text{-}tamx}$ (cm/s)
PI_{CA}
Gestational age (weeks)

Figure 3

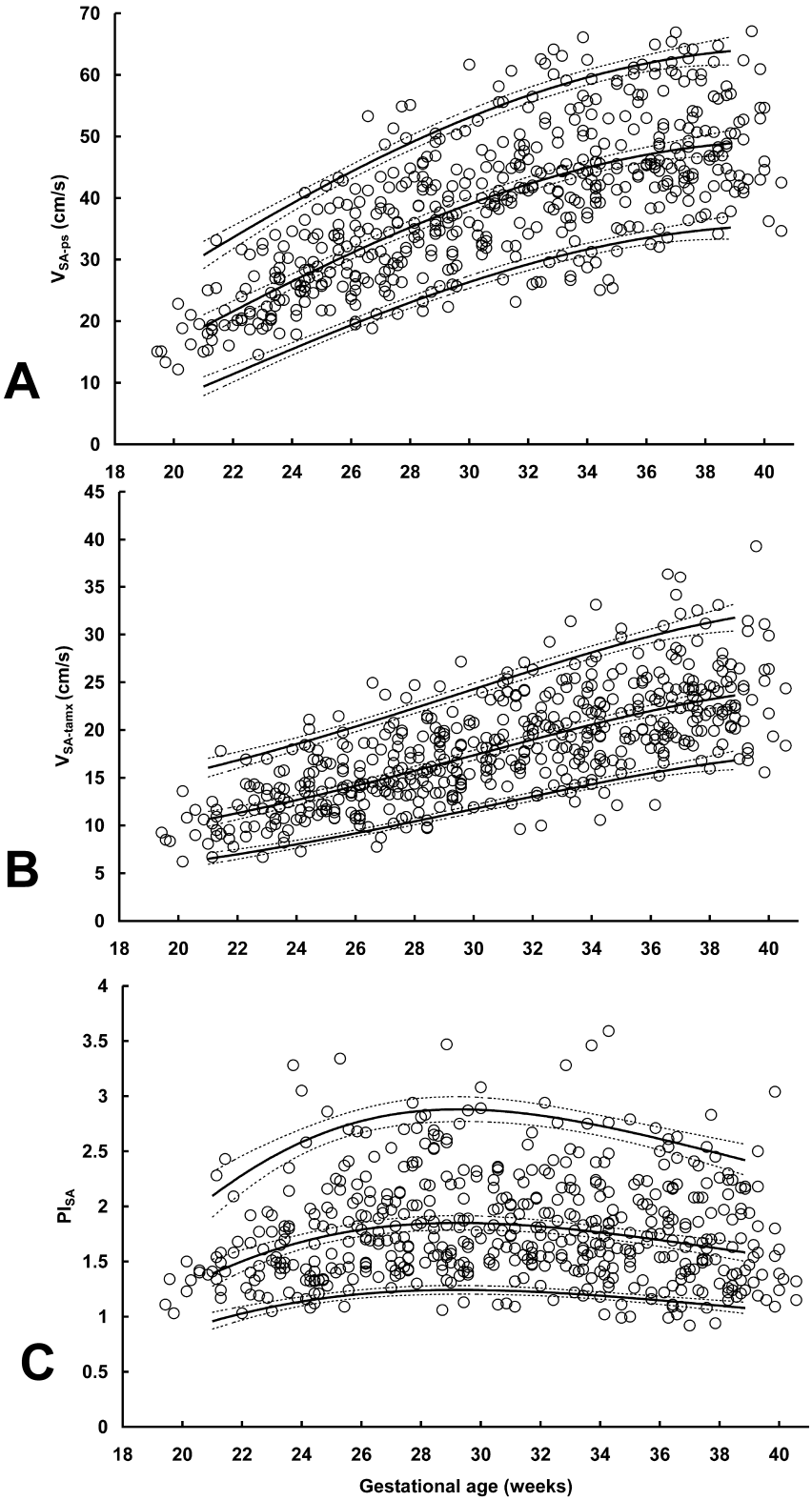

Figure 4

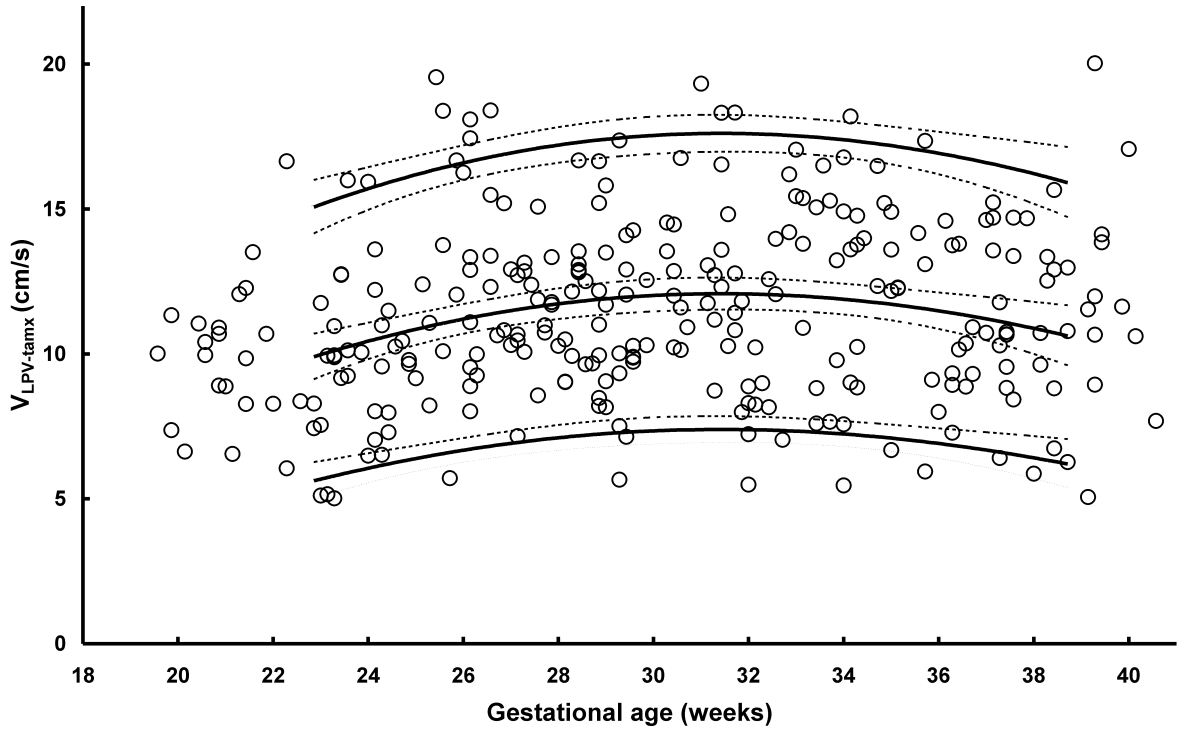
20
15
10
5
0
$V_{LPV\text{-}tamx}$ (cm/s)
18
20
22
24
26
28
30
32
34
36
38
40
Gestational age (weeks)

Figure 5

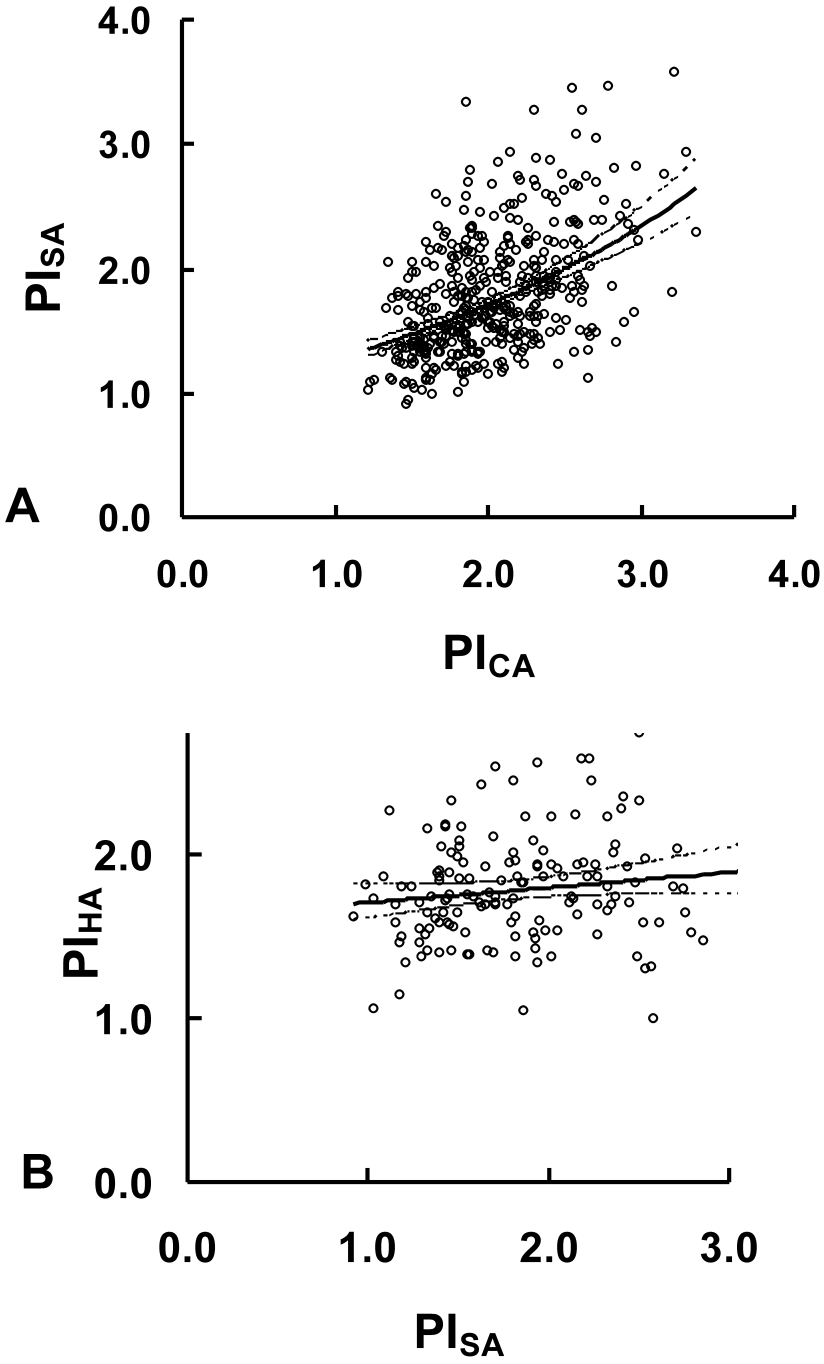
4.0
3.0
2.0
1.0
0.0
PISA
A
0.0
1.0
2.0
3.0
4.0
PICA
2.0
1.0
0.0
PIHA
B
0.0
1.0
2.0
3.0
PISA

Figure 6

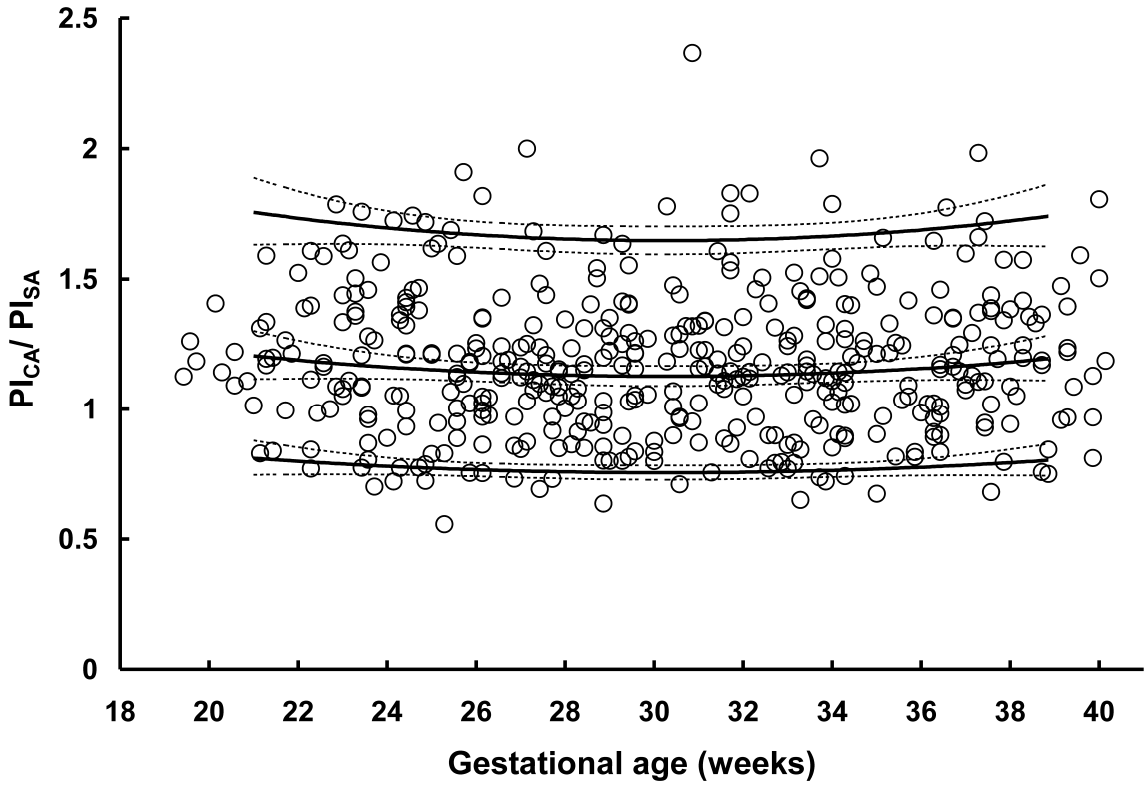
2.5
2
1.5
1
0.5
0
PICA/ PISA
18
20
22
24
26
28
30
32
34
36
38
40
Gestational age (weeks)

Figure 7

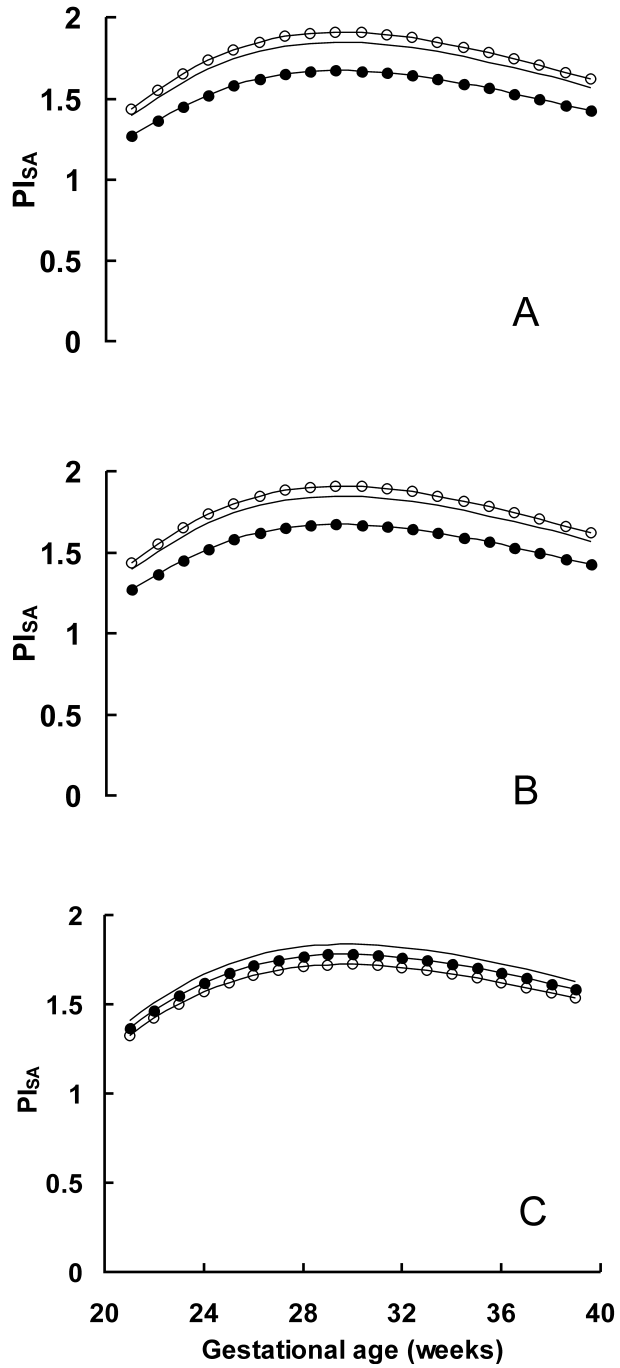

Figure 8

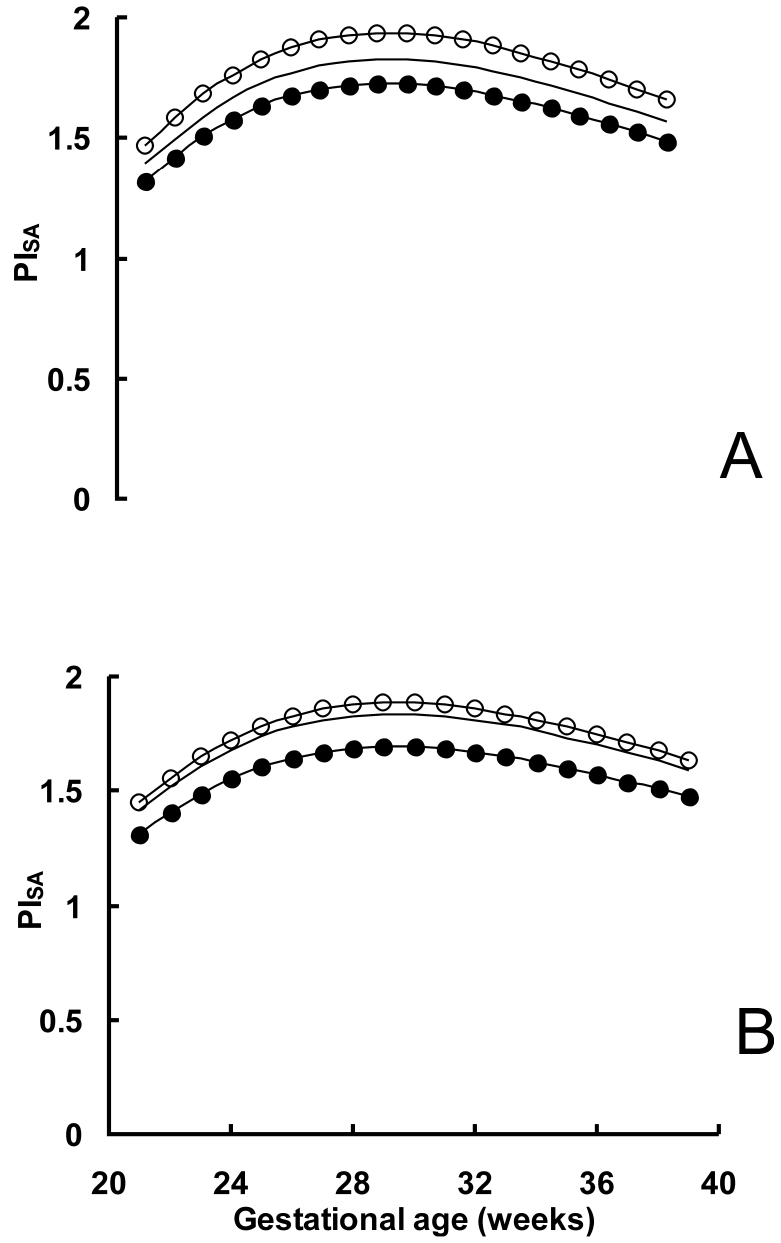
2
1.5
1
0.5
0
PISA
A
2
1.5
1
0.5
0
PISA
B
20
24
28
32
36
40
Gestational age (weeks)

Article III

Fetal superior mesenteric artery: longitudinal reference ranges and evidence of regulatory link to portal liver circulation

(Limit 25 words)

Cathrine Ebbing[1,2], Svein Rasmussen[1,2,3], Keith M. Godfrey[4], Mark A. Hanson[4], Torvid Kiserud[1,2]

[1]Department of Obstetrics and Gynecology, Haukeland University Hospital, Bergen, Norway

[2]Department of Clinical Medicine, University of Bergen, Norway

[3]Medical Birth Registry of Norway, Locus of Registry Based Epidemiology, University of Bergen and the Norwegian Institute of Public Health, Bergen, Norway

[4]Division of Developmental Origins of Health and Disease, University of Southampton, Southampton, UK

Acknowledgement

The study was supported by the Western Norway Regional Health Authority (Grant no 911160). M.A.H is supported by the British Heart Foundation.

Keywords: Superior mesenteric artery, Doppler, fetus, reference ranges, hemodynamics

Correspondence: Cathrine Ebbing MD
Department of Obstetrics and Gynecology,
Haukeland University Hospital, N-5021 Bergen, Norway
Fax: +47 55974968
Tel: +47 55974200 and private +47 99730026
E-mail:cathrine.ebbing@molmed.uib.no and cathrine.ebbing@helse-bergen.no

Professor, Svein Rasmussen MD PhD
Department of Obsterics and Gynecology,
Haukeland University Hospital, N-5021 Bergen, Norway
Tel: +47 55974200 and private +47 55200067.

E-mail: Svein.Rasmussen@mfr.uib.no

Professor Keith M. Godfrey BM PhD FRCP
Professor of Epidemiology & Human Development and Deputy Director, Centre for Developmental Origins of Health & Disease
MRC Epidemiology Resource Centre
University of Southampton
Southampton General Hospital, Mailpoint 95
Southampton SO16 6YD, UK
Tel: +44 (0)23 80777624
Fax: +44 (0)23 80704021
E-mail: kmg@mrc.soton.ac.uk

Professor Mark Hanson DPhil
British Heart Foundation Professor of Cardiovascular Science
Director, Institute of Developmental Sciences
Director, Division of Developmental Origins of Health & Disease,
University of Southampton
Mailpoint 887
Southampton General Hospital
SO16 6YD, UK
Tel: +44 2380 798421
Fax + 44 2380 786933
Email: m.hanson@soton.ac.uk

Professor Torvid Kiserud MD PhD
Department of Obsterics and Gynecology,
Haukeland University Hospital, N-5021 Bergen, Norway
Tel:+47 55974200 and private +47 98464110 Fax: +47 55974968
E-mail: torvid.kiserud@kk.uib.no

ABSTRACT

The superior mesenteric artery (SMA) supplies most of the gut and is an important contribution to portal liver perfusion in postnatal life. Less is known of its functional role during fetal life. Based on 589 serial Doppler ultrasound measurements in 161 low-risk pregnancies we established longitudinal reference ranges for SMA blood flow velocities and pulsatility index (PI) for gestational weeks 21-39. Using ductus venosus peak velocity to represent port-caval pressure gradient and umbilical venous flow to represent portal flow, we found that low portal pressure and flow were associated with low SMA impedance. SMA PI correlated weakly with the hepatic and splenic artery PI and showed co-variation with umbilical and cerebral artery PIs. Thus, the SMA not only perfuses the fetal gut, but is also actively involved in the regulation of fetal liver perfusion, which is believed to be of importance for both fetal and postnatal development.

Word count: 146

INTRODUCTION

During postnatal life the portal vein perfuses the entire liver. Prenatally, splanchnic blood through the main portal stem constitutes only 15% of the total venous liver perfusion, the major source being the umbilical vein (85%).[1,2] These recent data from human fetuses indicate that splanchnic blood is almost exclusively assigned for the right liver lobe while the oxygenated blood from the umbilical vein perfuses the entire left lobe and additionally blends in with the deoxygenated splanchnic blood in the right lobe. One third (1/5 near term) of the combined ventricular output perfuse the placenta,[3] but as much as 75-85% of the venous return from the placenta is distributed to the fetal liver, signifying a high developmental priority, and this is supported by experimental data.[4,5] Increased umbilical liver perfusion in fetal lambs leads to augmented liver cell proliferation, increased IGF 1 and 2 production, and increased growth of other organs, while a reduced perfusion has opposite effects.[6]

The liver circulation includes blood from the hepatic artery, directly connected to the liver tissue, and the splenic and mesenteric arteries, indirectly connected to the portal vein through the spleen and gut. We have recently found evidence that the hepatic artery buffer response (i.e. an adenosine-mediated arterial vasodilatation caused by a drop in portal perfusion[7]) is active in human fetuses during the second half of pregnancy.[8]

The superior mesenteric artery (SMA) is a prominent contributor to portal flow and liver perfusion, represents also a circulatory bed of considerable capacity [9] and shows substantial variation induced by meals,[10] but with no steal phenomenon from the cerebral circulation.[11] Experimentally, the fetal SMA shows vasoconstriction as part of the general redistribution response to hypoxia or hypovolemia.[12,13] If sustained, such hypoperfusion of the gut is associated with an increased risk of necrotising enterocolitis in the neonatal period.[14] With this background we speculate that Doppler recording of the SMA is a

potentially useful method in the evaluation of fetal hemorrhage, anemia, hypoxemia and placental compromise, but its hemodynamic role in the human fetal circulation is not known.

Thus, the objectives of the present study were 1) to establish longitudinal reference ranges for the blood flow velocities and pulsatility index (PI_{SMA}) for the SMA, and 2) to test the hypothesis that the SMA is functionally linked to the port-caval pressure gradient and umbilical flow and, on the arterial side, related to the splenic, middle cerebral and umbilical artery hemodynamics.

METHODS

Subjects

The present study is part of a prospective longitudinal study of the fetal cerebral, umbilical and splanchnic circulation. Here we present the results of the superior mesenteric artery hemodynamics. The participants were 161 women with low-risk pregnancies recruited after written consent provided gestational age had been assessed by ultrasound at 17-20 weeks of gestation.[15] Exclusion criteria were twin pregnancy, fetal anomaly, history of pregnancy complications (e.g. pregnancy induced hypertension, fetal growth restriction and abruptio placentae), or any general chronic disease. Each woman was scheduled for examination 3-5 times, at 3-5 weeks intervals. Complications in pregnancy, birthweight, Apgar score, gestational age at delivery, gender and congenital abnormalities were noted.

Measurements

Doppler ultrasound measurements were recorded using a 2-5, 2-7 or 4-8 MHz abdominal transducer (Voluson730 Expert, GE Medical systems, Kretz Ultrasoud, Zipf, Austria) with the high-pass filter set to 70 Hz. Mechanical and thermal indices were <1.1 and <0.9, respectively, in the majority of the sessions and always <1.9 and <1.5, respectively.

The fetal abdomen was insonated in a sagittal or horizontal direction using colour Doppler to visualise the SMA as the second of the unpaired branches of the abdominal aorta,

directed anterior and caudal (Figure 1). The blood flow velocity was recorded close to its origin using pulsed Doppler with median sample volume 4 mm (range 1-9mm).

The port-caval (i.e. umbilico-caval) pressure gradient drives the venous perfusion of the liver. The blood velocity in the port-caval shunt ductus venosus is a direct representation of this pressure gradient.[16] The ductus venosus peak blood velocity was recorded [17] and included in the analysis to determine the effect of port-caval pressure on PI_{SMA}.

The umbilical venous flow (Q_{UV}) and hepatic artery (HA) was assessed as described previously.[8] Prenatally the left portal vein (LPV) connects the UV to the portal circulation, representing a watershed between the two circuits.[18,19] The time-averaged maximum velocity of the LPV ($V_{LPVtamx}$) is a direct reflection of this watershed and we used it to assess whether a shift of venous liver perfusion was associated with PI_{SMA} changes.[20] The splenic artery (SA) was visualised in a horizontal view of the fetal abdomen, and PI obtained from the proximal part of the vessel.

In addition to these local regulatory links, we tested whether PI_{SMA} had any functional link to other essential sections of the fetal circulation, i.e. the umbilical and cerebral circulation, using the PI_{UA} and PI_{MCA}. [21,22]

All insonations for Doppler measurements were aligned in the direction of the vessel, and the angle of interrogation was always kept $\leqq$30 degrees. When this angle was not zero, the Doppler shift was corrected accordingly. The recordings were acquired during fetal quiescence over at least 3 uniform heart cycles to determine systolic peak and time averaged maximum velocity and PI. Head and abdominal circumferences and femur length were used for the estimation of fetal weight.[23]

Statistics

Multilevel modelling was used in order to calculate mean and centiles for the SMA systolic peak and time averaged maximum velocity and PI by gestational ages. To achieve

normal distribution of the outcome variables, we used power transformation. The outcome variables were regressed against gestational age using fractional polynomials. The 2.5, 5, 10 and 25th centiles were calculated by subtracting 1.96 standard deviation (SD), 1.645 SD, 1.282 SD, and 0.674 SD from the mean, respectively. The 97.5, 95, 90 and 75th centiles were calculated by adding the respective multiples of the SD to the mean. The 95% confidence intervals of the mean, 5^{th} and 95^{th} centiles were derived.

To assess the effect of $V_{DV\text{-}ps}$, $V_{LPV\text{-}tamx}$, Q_{UV}, PI_{MCA} and PI_{UA} on PI in the SMA, we grouped these measurements in three categories ($<10^{th}$ centile, $10–90^{th}$ centile, and $>90^{th}$ centile) assuming that responses occur more commonly in extreme conditions. The variables were included in the multilevel regression models describing the mean PI_{SMA}. Indicator variables with significant improvement in the goodness of fit to the models, as assessed by the deviance statistics (χ^2 with p <0.05), were considered to significantly influence the outcome variables. Similarly, gender effects on SMA velocities and PI, were assessed including gender in the regression models. Associations of SMA (PI_{SMA}) with splenic and hepatic artery (PI_{SA} and PI_{HA}), were assessed by Pearson correlation analyses.

Intra- and inter-observer reproducibilities were expressed as intra-class and inter-class correlation coefficients based on repeat observations in 17 and 14 participants, respectively.

The statistical analysis was performed using SPSS (Statistical Package for the Social Sciences, SPSS Inc, Chicago, IL) and the MlWin program (MlWin, Centre for Multilevel Modelling, University of Bristol, UK).

The Regional Committee for Medical Research Ethics approved the study protocol (REK Vest no 203.03).

RESULTS

Median gestational age at delivery was 40 weeks+3 days (range 35+3 to 42+4 weeks). The caesarean section rate (10.6 %) and birth weights (median 3700 g, range 2260-4980) were

similar to those of the general population (caesarean rate being 11.8%). Five women (3.1%) developed pre-eclampsia (further population characteristics have been detailed previously)[8,24].

We obtained 589 measurements of the SMA in a total of 633 sessions (93% success rate). Unfavourable fetal position and fetal movements were reasons for not obtaining measurements. The reproducibility study showed intra-class correlation coefficients of 98, 95 and 94% for the $V_{SMA\text{-}ps}$, $V_{SMA\text{-}tamx}$, and PI_{SMA}, respectively. The corresponding values for inter-observer variation were 94, 85 and 75%.

The abdominal aorta, renal and celiac arteries were anatomical landmarks for identifying the SMA. Median angle correction of the Doppler insonation was 16° (range 0-30). The $V_{SMA\text{-}ps}$, $V_{SMA\text{-}tamx}$ and PI_{SMA} with fitted mean and reference intervals are presented in Figure 2. The corresponding gestational age-specific centiles are presented in tables 1-3. Terms for calculating conditional ranges for repeat measurements of the SMA are presented in the appendix.

Gender had no effect on $V_{SMA\text{-}ps}$ when corrected for estimated fetal weight, but female fetuses had lower $V_{SMA\text{-}tamx}$ (1%, $p<0.0001$) and higher PI_{SMA} (2%, $p<0.0001$) than males.

We found a relatively weak correlation between the SMA (PI_{SMA}) and the splenic and hepatic artery (PI_{SA} and PI_{HA}), r=0.30 (95%CI 0.22-0.37) and r=0.39 (95%CI 0.27-0.51) respectively, indicating largely independent local regulation of these vessels.

When examining the hypothesis that port-caval pressure gradient (expressed by the V_{DVps}) influences SMA vasoactivity (expressed by the PI_{SMA}), we found that those with the lowest port-caval pressure (V_{DVps} <10^{th} centile) had evidence of vasodilation (i.e. lower PI_{SMA}) ($p<0.0001$), but the effect was small (PI_{SMA} variation 0.02-0.03). Vasodilatation (i.e. low PI_{SMA}) was also linked to Q_{UV} < 10^{th} centile ($p<0.0001$) and a right-shift in umbilical flow distribution to the liver, i.e. $V_{LPVtamx}$ >90^{th} centile.

PI_{SMA} co-varied with PI_{UA} and PI_{MCA} ($p<0.0001$) indicating some common hemodynamic determinants for the mesenteric, cerebral and placental vasculature.

DISCUSSION

In this study we provide new longitudinal reference ranges suitable for single and serial measurements of the fetal SMA and have shown that this artery is functionally linked to the port-caval pressure gradient and liver perfusion. Keeping in mind that during prenatal life it is essentially the umbilical blood that perfuses the liver and that the main portal stem provides a modest 15% of hepatic venous blood flow, we now can draw a more complete map of the fetal liver circulation that includes differential roles of the hepatic, splenic and superior mesenteric arteries (Figure 3). The SMA represents an important source of blood to the portal system, but seems modestly involved in the regulation of portal pressure and fetal liver perfusion under physiological conditions. The splenic artery, however, seems more tightly linked to compensate portal pressure reduction (Unpublished data). The hepatic artery operates differently by increasing arterial flow directly to the sinusoids when portal perfusion is low.[7,8] Our data suggest that the regulation of the three arteries is relatively independent from each other, which is in line with studies in postnatal life.[25,26]

In addition to showing regulatory adjustments according to the port-caval pressure gradient (i.e. V_{DVps}) and umbilical flow, our present and previous results show that these arteries are also linked to the more subtle internal distribution of umbilical blood in the liver as expressed by the Doppler recording in the left portal vein, which reflects the watershed between the left and right lobes. Recent data suggest an extensive functional differentiation between the left and right liver lobe in the developing fetus and that maternal diet and body composition modifies umbilical liver perfusion.[27,28] It seems plausible that also the mesenteric, splenic and hepatic arteries are engaged in the finer circulatory tuning of the fetal liver development, possibly with long-term consequences.

SMA hemodynamics shows significant co-variation with cerebral and placental hemodynamics, probably signifying that these sections of the fetal circulation have also common determinants (e.g. blood pressure).

We found that peak systolic and time averaged maximum flow velocities and PI in the SMA increased with gestational age (Figure 2). In general, increasing velocities are related to increased volume flow [29] and, in our case, this confirms that intestinal perfusion rises towards term, which is in agreement with recent studies of the main stem of the portal system in human fetuses.[30]

When redistribution causes lower mesenteric perfusion, the intestinal tissues respond by increasing oxygen extraction, keeping oxygen consumption relatively constant, but consequently the oxygen tension in the portal venous blood is reduced.[31,32] We speculate that under such circumstances, redistribution from the mesenteric to the splenic and hepatic vascular beds occurs, possibly optimising the oxygen delivery to the liver. Similar results are reported from experimental animal studies and a study of neonates.[24,33] In line with this is the finding that growth restricted fetuses with compromised umbilical circulation and elevated PI_{SMA} before birth are more likely to develop necrotising enterocolitis.[34] Similarly, SGA neonates more frequently show a high resistance pattern in the SMA compared with normally grown infants, possibly reflecting a persistent SMA pattern from prenatal life.[25,35-37]

Thus, there are good reasons for a more detailed evaluation of the splanchnic circulation before birth. This conclusion is supported by previous studies of fetuses with gastrochisis and placental compromise and smaller series of normal fetuses.[34,38,39] We believe that the present longitudinal reference ranges based on a high number of observations form an improved basis for such future clinical assessment.

Reference List

1. Haugen G, Kiserud T, Godfrey K, Crozier S, Hanson M. Portal and umbilical venous blood supply to the liver in the human fetus near term. Ultrasound Obstet Gynecol 2004;24:599-605.

2. Kessler J, Rasmussen S, Godfrey K, Hanson M, Kiserud T. Longitudinal study of umbilical and portal venous blood flow to the fetal liver: low pregnancy weight gain is associated with preferential supply to the left fetal liver lobe. Pediatr Res 2007;In press. DOI:10.1203/PDR.0b013e318163a1de

3. Kiserud T, Ebbing C, Kessler J, Rasmussen S. Fetal cardiac output, distribution to the placenta and impact of placental compromise. Ultrasound Obstet Gynecol 2006;28:126-136.

4. Bellotti M, Pennati G, De Gasperi C, Battaglia FC, Ferrazzi E. Role of ductus venosus in distribution of umbilical blood flow in human fetuses during second half of pregnancy. Am J Physiol-Heart Physiol 2000;279:H1256-H1263.

5. Kiserud T, Rasmussen S, Skulstad S. Blood flow and the degree of shunting through the ductus venosus in the human fetus. Am J Obstet Gynecol 2000;182:147-153.

6. Tchirikov M, Kertschanska S, Sturenberg HJ, Schroder HJ. Liver blood perfusion as a possible instrument for fetal growth regulation. Placenta 2002;23:S153-S158.

7. Lautt WW. The 1995 Ciba-Geigy Award Lecture. Intrinsic regulation of hepatic blood flow. Can J Physiol and Pharm 1996;74:223-233.

8. Ebbing C, Rasmussen S, Godfrey K.M, Hanson M.A., Kiserud T. Hepatic artery hemodynamics suggest operation of a buffer response in the human fetus. Reproductive Sciences 2008 (in press).

9. Reilly PM, Wilkins KB, Fuh KC, Haglund U, Bulkley GB. The mesenteric hemodynamic response to circulatory shock: An overview. Shock 2001;15:329-343.

10. Perko MJ. Duplex ultrasound for assessment of superior mesenteric artery blood flow. Eur J Vasc Surg 2001;21:106-117.

11. Martinussen M, Brubakk AM, Linker DT, Vik T, Yao AC. Mesenteric Blood-Flow Velocity and Its Relation to Circulatory Adaptation During the First-Week of Life in Healthy Term Infants. Pediatr Res 1994;36:334-339.

12. Jensen A, Hanson MA. Circulatory responses to acute asphyxia in intact and chemodenervated fetal sheep near term. Reprod Fertil Dev 1995;7:1351-1359.

13. Quaedackers JS, Roelfsema V, Heineman E, Gunn AJ, Bennet L. The role of the sympathetic nervous system in postasphyxial intestinal hypoperfusion in the pre-term sheep fetus. Journal of Physiol-London 2004;557:1033-1044.

14. Murdoch EM, Smith GCS, Sinha AK, Shanmugalingam ST, Kempley ST. Neonatal necrotizing enterocolitis is associated with high resistance flow in the superior mesenteric artery on day 1 of life in preterm infants. Early Hum Dev 2006;82:618-619.

15. Johnsen SL, Rasmussen S, Sollien R, Kiserud T. Fetal age assessment based on ultrasound head biometry and the effect of maternal and fetal factors. Acta Obstet Gynecol Scand 2004;83:716-723.

16. Kiserud T, Hellevik LR, Eiknes SH, Angelsen BAJ, Blaas HG. Estimation of the pressure-gradient across the fetal ductus venosus based on doppler velocimetry. Ultrasound Med Biol 1994;20:225-232.

17. Kiserud T, Eiknes SH, Blaas HGK, Hellevik LR. Ultrasonographic Velocimetry of the Fetal Ductus Venosus. Lancet 1991;338:1412-1414.

18. Kilavuz O, Vetter K, Kiserud T, Vetter P. The left portal vein is the watershed of the fetal venous system. J Perinat Med 2003;31:184-187.

19. Kiserud T, Kilavuz O, Hellevik LR. Venous pulsation in the fetal left portal branch: the effect of pulse and flow direction. Ultrasound Obstet Gynecol 2003;21:359-364.

20. Kessler J, Rasmussen S., Kiserud T. The left portal vein as an indicator of watershed in the fetal circulation: development during the second half of pregnancy and a suggested method of evaluation. Ultrasound Obstet Gynecol 2007;30:757-764.

21. Acharya G, Wilsgaard T, Berntsen GKR, Maltau JM, Kiserud T. Doppler-derived umbilical artery absolute velocities and their relationship to fetoplacental volume blood flow: a longitudinal study. Ultrasound Obstet Gynecol 2005;25:444-453.

22. Mari G, Zimmermann R, Moise KJ, Deter RL. Correlation between middle cerebral artery peak systolic velocity and fetal hemoglobin after 2 previous intrauterine transfusions. Am J Obstet Gynecol 2005;193:1117-1120.

23. Combs CA, Jaekle RK, Rosenn B, Pope M, Miodovnik M, Siddiqi TA. Sonographic Estimation of Fetal Weight Based on A Model of Fetal Volume. Obstet Gynecol 1993;82:365-370.

24. Ebbing C., Rasmussen S., Kiserud T. Middle cerebral artery blood flow velocities and pulsatility index and the cerebroplacental ratio: longitudinal reference ranges and terms for serial measurements. Ultrasound Obstet Gynecol 2007;30:287-296.

25 Coombs RC, Morgan MEI, Durbin GM, Booth IW, Mcneish AS. Abnormal Gut Blood-Flow Velocities in Neonates at Risk of Necrotizing Enterocolitis. J Pediatr Gastroenterol Nutr 1992;15:13-19.

26. Murdoch EM, Sinha AK, Shanmugalingam ST, Smith GCS, Kempley ST. Doppler flow velocimetry in the superior mesenteric artery on the first day of life in preterm infants and the risk of neonatal necrotizing enterocolitis. Pediatrics 2006;118:1999-2003.

27. Perko MJ, Nielsen HB, Skak C, Clemmesen JO, Schroeder TV, Secher NH. Mesenteric, coeliac and splanchnic blood flow in humans during exercise. J Physiol 1998;513:907-913.

28. Cox LA, Schlabritz-Loutsevitch N, Hubbard GB, Nijland MJ, McDonald TJ, Nathanielsz PW. Gene expression profile differences in left and right liver lobes from mid-gestation fetal baboons: a cautionary tale. J Physiol 2006;572:59-66.

29. Haugen G, Hanson M, Kiserud T, Crozier S, Inskip H, Godfrey KM. Fetal liver-sparing cardiovascular adaptations linked to mother's slimness and diet. Circ Res 2005;96:12-14.

30. Kessler J, Rasmussen S, Kiserud T. The fetal portal vein: normal blood flow development during the second half of human pregnancy. Ultrasound Obstet Gynecol 2007;30:52-60.

31. Ceppa EP, Fuh KC, Bulkley GB, Gregory B. Mesenteric hemodynamic response to circulatory shock. Curr Opin Crit Care 2003;9:127-132.

32. Jakob SM. Clinical review: Splanchnic ischaemia. Crit Care 2002;6:306-312.

33. Jakob SM, Tenhunen JJ, Heino A, Pradl R, Alhava E, Takala J. Splanchnic vasoregulation during mesenteric ischemia and reperfusion in pigs. Shock 2002;18:142-147.

34. Korszun P, Dubiel M, Breborowicz G, Danska A, Gudmundsson S. Fetal superior mesenteric artery blood flow velocimetry in normal and high-risk pregnancy. J Perinat Med 2002;30:235-241.

35. Kempley ST, Gamsu HR, Vyas S, Nicolaides K. Effects of intrauterine growth-retardation on postnatal visceral and cerebral blood-flow velocity. Arc Dis Child 1991;66:1115-1118.

36. Martinussen M, Brubakk AM, Vik T, Yao AC. Relationship between intrauterine growth retardation and early postnatal superior mesenteric artery blood flow velocity. Biol Neonate 1997;71:22-30.

37. Robel-Tillig E, Vogtmann C, Bennek J. Prenatal hemodynamic disturbances - Pathophysiological background of intestinal motility disturbances in small for gestational age infants. Eur J Pediatr Surg 2002;12:175-179.

38. Abuhamad AZ, Mari G, Cortina RM, Croitoru DP, Evans AT. Superior mesenteric artery Doppler velocimetry and ultrasonographic assessment of fetal bowel in gastroschisis: A prospective longitudinal study. Am J Obstet Gynecol 1997;176:985-990.

39. Achiron R, Orvieto R, Lipitz S, Yagel S, Rotstein Z. Superior mesenteric artery blood flow velocimetry: Cross-sectional Doppler sonographic study in normal fetuses. J Ultrasound Med 1998;17:769-773.

Appendix

Systolic peak velocity V_{SMAps}

An actual transformed V_{SMAps} observation may be expressed by the regression mean as a function of gestational age (GA) in weeks and residuals as

$y_{ij} = \hat{\beta}_0 + e_{0ij} + \hat{\beta}_1 GA_{ij} + \hat{\beta}_2 GA_{ij}^2 + u_{2j}$, where $\hat{\beta}_0 = -2.19094$,

$\hat{\beta}_1 = 0.4448166$, and $\hat{\beta}_2 = -0.0055396$, and e_{0ij} and u_{0j} residuals, and $_i$ denotes

level 1 (observation) and $_j$ level 2 (fetus)

1) Unconditional mean and variance
V_{SMAps} was transformed to the 0.459 power.

Transformed mean= μ
$= -2.190914 + 0.4448166\ GA - 0.0055396\ GA^2$
which may be "backtransformed" as $\mu^{(1/0.459)}$

Variance
$=\sigma^2$
$= \hat{\sigma}_{e0}^2 + \sigma_{u2}^2$
$= 0.2404756 + 0.00000007220807\ GA^4$

2) Unconditional reference interval is given by
$= \mu + \hat{z}\sigma$,

where σ is the standard deviation and $\hat{z} = -1.96, -1.645, -1.282, -0.674, 0.674, 1.282, 1.645$, and

1.96 for the $2.5^{th}, 5^{th}, 10^{th}, 25^{th}, 50^{th}, 75^{th}, 90^{th}, 95^{th}$, and 97.5^{th} percentiles, respectively.

3) Conditional mean and variance
The covariance between the first and a later observation (at gestational ages GA1 and GA2) is set as the level-2 covariance as the level-1 covariance is assumed to be zero. The covariance is given by

$\sigma_{12} = \sigma_{u2}^2 GA1^2\ GA2^2$

$= 0.0000000722\ 0807\ GA1^2\ GA2^2$

Conditional mean $\mu_{2|1}$ is given by
$\mu_2 + (y_1 - \mu_1)\sigma_{12} / \sigma_1^2$
were μ_2 and μ_1 are means at GA_2 and GA_1, y_1 is the observation at GA_1,
and σ_1^2 the variance at GA_1

Conditional variance is given by

$\sigma^2_{2|1}$
$= \sigma^2_2 - \sigma^2_{12} / \sigma^2_1$

4) Conditional reference interval
$\mu_{2|1} + z\ \sigma_{2|1}$

Pulsatility index PI_{SMA}
An actual transformed PI_{SMA} observation may be expressed by the regression mean as a function
of gestational age (GA) in weeks and residuals as

$$y_{ij} = \hat{\beta}_0 + u_{0j} + e_{0ij} + \hat{\beta}_1 GA_{ij} + u_{1j} + \hat{\beta}_2 GA^2_{ij}, \text{where} \hat{\beta}_0 = 0.2424218,$$

$\hat{\beta}_1 = 0.0779139$, and $\hat{\beta}_2 = -0.001147983$, and u_{0j}, e_{0ij}, and u_{1j} residuals, and $_i$ denotes

level 1 (observation) and $_j$ level 2 (fetus)

1) Unconditional mean and variance
PI_{SMA} was transformed to the 0.503 power.
Transformed mean= μ
=0.2424218+0.0779139 GA –0.001147983 GA^2 which may be ”backtransformed” as $\mu^{(1/0.503)}$

Variance
$=\sigma^2$
$= \hat{\sigma}^2_{e0} + \hat{\sigma}^2_{u0} + 2\hat{\sigma}_{u01} GA + \hat{\sigma}^2_{u1} GA^2$
$=0.03710171 - 0.001855088\ GA + 0.000036501\ GA^2$
2) Unconditional reference interval is given by

$= \mu + \hat{z}\sigma,$
where σ is the standard deviation and $\hat{z} = -1.96, -1.645, -1.282, -0.674, 0.674, 1.282, 1.645,$ and 1.96 for the $2.5^{th}, 5^{th}, 10^{th}, 25^{th}, 50^{th}, 75^{th}, 90^{th}, 95^{th},$ and 97.5^{th} percentiles, respectively.

3) Conditional mean and variance

The covariance between the first and a later observation (at gestational ages GA1 and GA2) is set as the level-2 covariance as the level-1 covariance is assumed to be zero. The covariance is given by

$$\sigma_{12} = \hat{\sigma}^2_{u0} + 2\hat{\sigma}_{u01}(GA1 + GA2) + \hat{\sigma}^2_{u1} GA1\, GA2$$

$$= 0.02603667 + 0.000927544\,(GA1 + GA2) + 0.000036501\, GA1\, GA2$$

Conditional mean $\mu_{2|1}$ is given by
$\mu_2 + (y_1 - \mu_1)\sigma_{12} / \sigma^2_1$
were μ_2 and μ_1 are means at GA_2 and GA_1, y_1 is the observation at GA_1,
and σ^2_1 the variance at GA_1; in this case the variance is independent of gestational age.

Conditional variance is given by

$\sigma^2_{2|1}$
$= \sigma^2_2 - \sigma^2_{12} / \sigma^2_1$

4) Conditional reference interval

$\mu_{2|1} + z\ \sigma_{2|1}$

Time averaged maximum velocity $V_{SMAtamx}$

An actual transformed $V_{SMAtamx}$ observation may be expressed by the regression mean as a function of gestational age (GA) in weeks and residuals as

$$y_{ij} = \hat{\beta}_0 + u_{0j} + e_{0ij} + \hat{\beta}_1 \ln(GA)_{ij} + \hat{\beta}_2 GA_{ij}^{0.5}, \text{where} \hat{\beta}_0 = -4.178232,$$

$\hat{\beta}_1 = 3.790669$, and $\hat{\beta}_2 = -1.080868$, and u_{0j} and e_{0ij} residuals, and $_i$ denotes level 1 (observation) and $_j$ level 2 (fetus)

1) Unconditional mean and variance

$V_{SMAtamx}$ was transformed to the 0.338 power.

Transformed mean= μ
= –4.178232+3.790669 ln(GA) –1.080868 $GA^{0.5}$
which may be ”backtransformed” as $\mu^{(1/0.338)}$

Variance

$= \hat{\sigma}^2$

$= \hat{\sigma}^2_{e0} + \hat{\sigma}^2_{u0}$

=0.03200046 + 0.005569469 =0.037569929

2) Unconditional reference interval is given by

$= \mu + \hat{z}\sigma,$

where σ is the standard deviation and $\hat{z} = -1.96, -1.645, -1.282, -0.674, 0.674, 1.282, 1.645,$ and 1.96 for the $2.5^{th}, 5^{th}, 10^{th}, 25^{th}, 50^{th}, 75^{th}, 90^{th}, 95^{th},$ and 97.5^{th} percentiles, respectively.

3) Conditional mean and variance

The covariance between the first and a later observation (at gestational ages GA1 and GA2) is set as the level-2 covariance as the level-1 covariance is assumed to be zero. The covariance is given by

$\sigma_{12} = \hat{\sigma}^2_{u0}$

$= 0.005569464$

Conditional mean $\mu_{2|1}$ is given by

$\mu_2 + (y_1 - \mu_1)\sigma_{12} / \sigma_1^2$
were μ_2 and μ_1 are means at GA_2 and GA_1, y_1 is the observation at GA_1,
and σ_1^2 the variance at GA_1; in this case the variance is independent of gestational age.

Conditional variance is given by
$\sigma_{2|1}^2$
$= \sigma_2^2 - \sigma_{12}^2 / \sigma_1^2$

4) Conditional reference interval
$\mu_{2|1} + z \sigma_{2|1}$

Table 1 Longitudinal reference ranges for the superior mesenteric artery peak systolic velocity (cm/s) based on 589 observations in 161 low-risk pregnancies

Gestation (weeks)	**Centile**								
	50	**2.5**	**5**	**10**	**25**	**75**	**90**	**95**	**97.5**
21	**29**	17	19	21	25	34	39	42	44
22	**32**	20	21	24	27	37	42	45	48
23	**35**	22	24	26	30	40	45	49	52
24	**38**	24	26	28	33	43	49	52	55
25	**40**	26	28	31	35	46	52	56	59
26	**43**	28	30	33	37	49	55	59	62
27	**46**	30	32	35	40	52	58	62	65
28	**48**	32	34	37	42	55	61	65	69
29	**50**	33	36	39	44	57	64	68	72
30	**53**	35	37	40	46	60	67	71	75
31	**55**	36	39	42	48	62	69	73	77
32	**56**	37	40	43	49	64	71	76	80
33	**58**	38	41	45	51	66	73	78	82
34	**60**	39	42	46	52	68	75	80	85
35	**61**	40	43	47	53	69	77	82	87
36	**62**	40	44	47	54	70	79	84	88
37	**63**	41	44	48	55	71	80	85	90
38	**63**	41	44	48	55	72	81	86	91
39	**64**	41	44	48	55	73	82	87	92

Table 2 Longitudinal reference ranges for the superior mesenteric artery time averaged maximum velocity (cm/s) based on 589 observations in 161 low-risk pregnancies.

Gestation (weeks)	**Centiles**								
	50	**2.5**	**5**	**10**	**25**	**75**	**90**	**95**	**97.5**
21	**13**	8	9	10	11	16	18	19	21
22	**15**	9	10	11	12	17	19	21	22
23	**15**	10	10	11	13	18	20	22	23
24	**16**	10	11	12	14	19	22	23	25
25	**17**	11	12	13	15	20	23	24	26
26	**18**	11	12	14	16	21	24	25	27
27	**19**	12	13	14	16	22	24	26	28
28	**20**	13	14	15	17	22	25	27	29
29	**20**	13	14	15	18	23	26	28	30
30	**21**	14	15	16	18	24	27	29	30
31	**22**	14	15	16	19	25	28	30	31
32	**22**	14	16	17	19	25	28	30	32
33	**23**	15	16	17	20	26	29	31	33
34	**23**	15	16	18	20	26	29	31	33
35	**23**	15	17	18	20	27	30	32	34
36	**24**	16	17	18	21	27	30	32	34
37	**24**	16	17	19	21	28	31	33	35
38	**24**	16	17	19	21	28	31	33	35
39	**25**	16	18	19	22	28	31	34	35

Table 3 Longitudinal reference ranges for the superior mesenteric artery pulsatility index based on 589 observations in 161 low-risk pregnancies

Gestation (weeks)	Centiles								
	50	**2.5**	**5**	**10**	**25**	**75**	**90**	**95**	**97.5**
21	1.88	1.29	1.38	1.48	1.66	2.10	2.31	2.45	2.57
22	1.95	1.36	1.45	1.56	1.74	2.18	2.40	2.53	2.65
23	2.03	1.43	1.52	1.63	1.82	2.26	2.48	2.61	2.73
24	2.10	1.50	1.59	1.69	1.88	2.33	2.55	2.69	2.81
25	2.16	1.55	1.64	1.75	1.94	2.40	2.62	2.76	2.88
26	2.22	1.60	1.69	1.80	2.00	2.46	2.68	2.82	2.95
27	2.27	1.64	1.73	1.85	2.04	2.51	2.74	2.88	3.01
28	2.32	1.67	1.77	1.88	2.08	2.56	2.79	2.93	3.06
29	2.35	1.70	1.80	1.91	2.12	2.60	2.84	2.98	3.11
30	2.38	1.72	1.82	1.94	2.14	2.64	2.87	3.02	3.15
31	2.41	1.73	1.83	1.95	2.16	2.66	2.91	3.06	3.19
32	2.42	1.73	1.84	1.96	2.17	2.68	2.93	3.09	3.22
33	2.43	1.73	1.84	1.96	2.18	2.70	2.95	3.11	3.25
34	2.43	1.72	1.83	1.95	2.17	2.70	2.96	3.12	3.26
35	2.43	1.70	1.81	1.94	2.16	2.70	2.97	3.13	3.28
36	2.41	1.68	1.79	1.92	2.15	2.70	2.97	3.13	3.28
37	2.39	1.65	1.76	1.89	2.12	2.68	2.96	3.13	3.28
38	2.37	1.61	1.72	1.85	2.09	2.66	2.94	3.11	3.27
39	2.33	1.56	1.68	1.81	2.05	2.63	2.92	3.09	3.25

LEGENDS

Figure 1: Colour Doppler image of the fetal superior mesenteric artery. The Doppler gate is placed over the proximal part of the vessel.

Figure 2: Longitudinal reference ranges for the superior mesenteric artery systolic peak velocity ($V_{SMA\text{-}ps}$) (Panel A), time averaged maximum velocity ($V_{SMA\text{-}tamx}$) (Panel B), and pulsatility index (PI_{SMA}) (Panel C) with fitted 5^{th}, 50^{th} and 95^{th} centiles and 95% confidence limits for the centiles based on 589 observations.

Figure 3: The umbilical vein (UV) is the dominant supplier of blood for perfusion of the fetal liver. The ductus venosus (DV) partially regulates this and its blood velocity reflects the port-caval pressure gradient. The superior mesenteric artery (SMA) and the splenic artery (SA) are less prominent contributors to the liver perfusion through their capillary beds and main portal stem (MPS). When portal flow is low, the hepatic artery (HA) responds with an increased direct flow to the liver tissue.

Figure 1

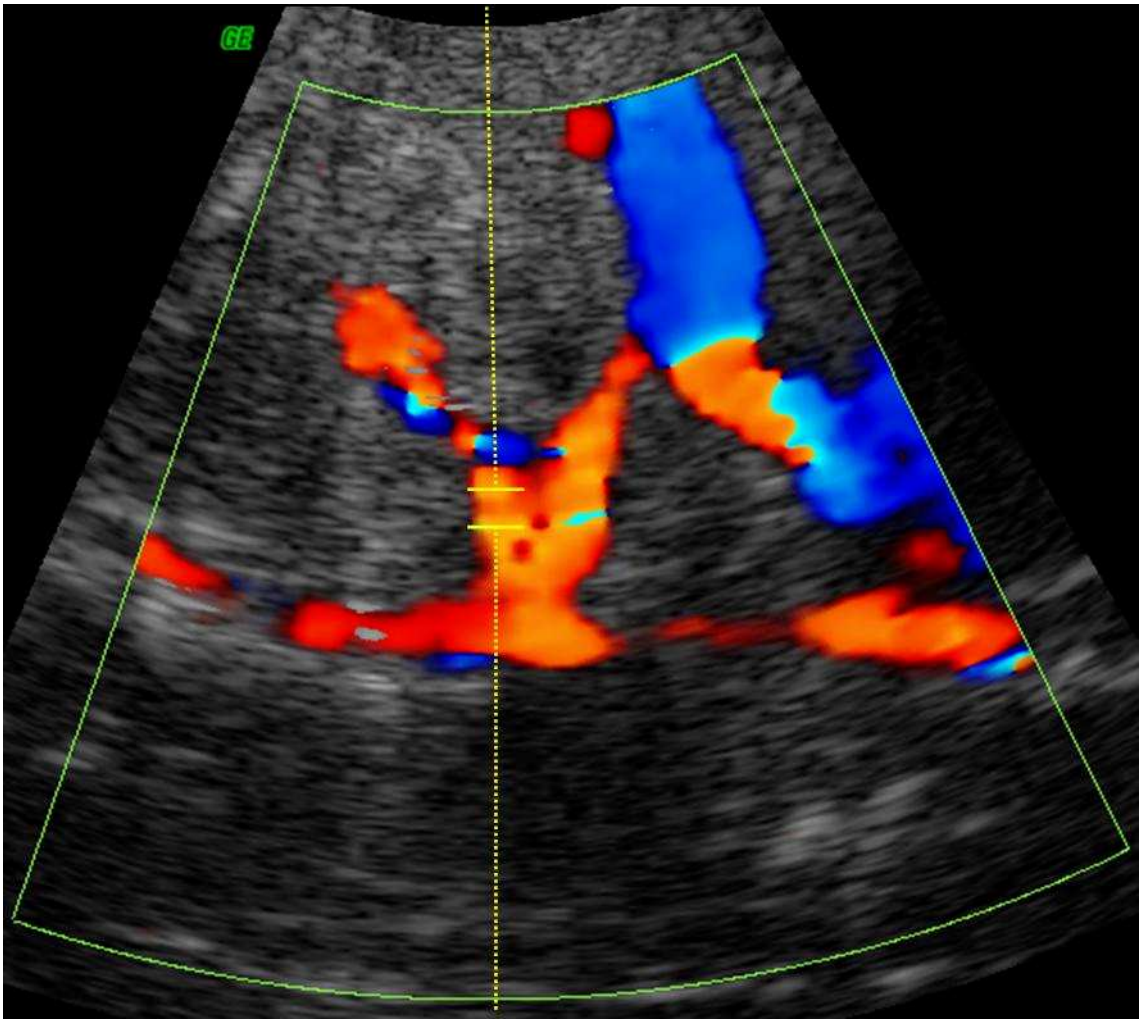

Figure 2

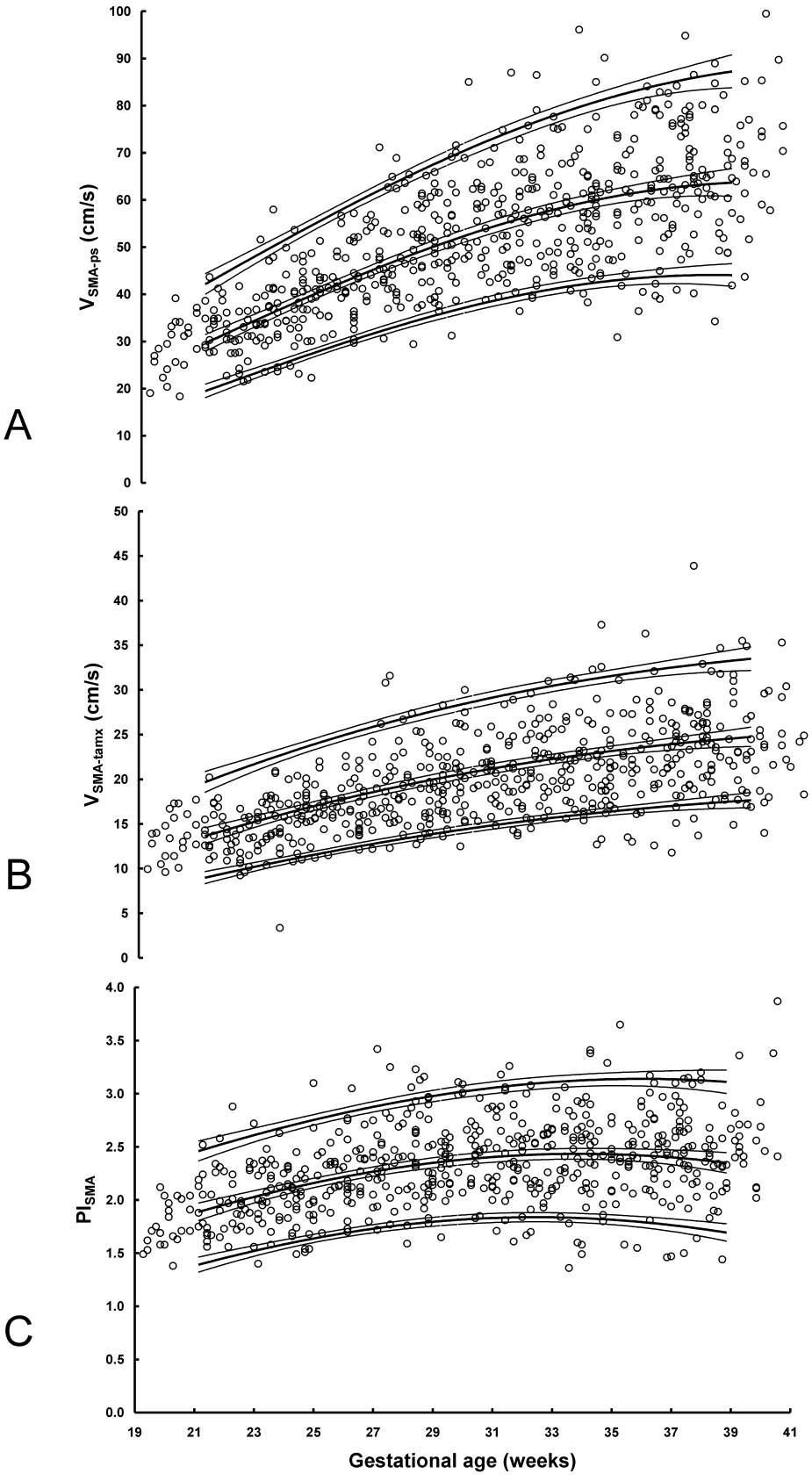

Figure 3

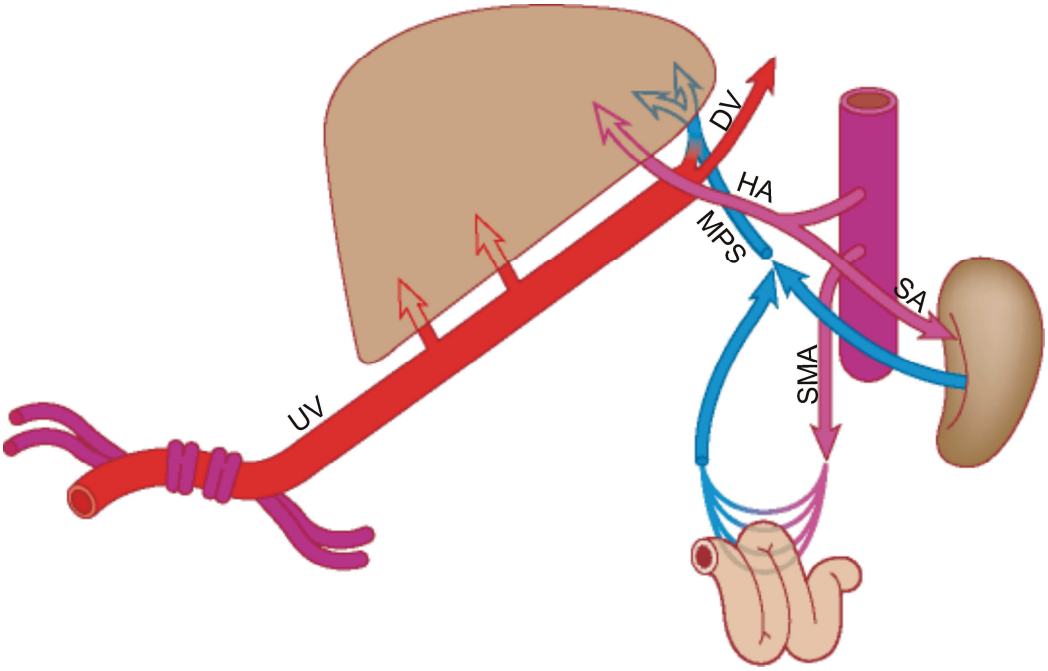

Article IV

Ultrasound Obstet Gynecol 2007; **30**: 287–296
Published online in Wiley InterScience (www.interscience.wiley.com). **DOI:** 10.1002/uog.4088

Middle cerebral artery blood flow velocities and pulsatility index and the cerebroplacental pulsatility ratio: longitudinal reference ranges and terms for serial measurements

C. EBBING*†, S. RASMUSSEN*†‡ and T. KISERUD*†

**Department of Clinical Medicine, University of Bergen, †Department of Obstetrics and Gynecology, Haukeland University Hospital and ‡Medical Birth Registry of Norway, Locus of Registry Based Epidemiology, University of Bergen and the Norwegian Institute of Public Health, Bergen, Norway*

KEYWORDS: blood flow; cerebroplacental ratio; Doppler; fetus; middle cerebral artery; reference ranges

ABSTRACT

Objectives *To establish reference ranges suitable for serial assessments of the fetal middle cerebral (MCA) and umbilical (UA) artery blood flow velocities, pulsatility index (PI) and cerebroplacental pulsatility ratio and to provide terms for calculating conditional reference intervals suitable for individual serial measurements.*

Methods *This was a longitudinal study of 161 singleton pregnancies. Using Doppler ultrasound, MCA and UA blood velocities and PI were determined three to five times at 3–5-week intervals over a gestational age range of 19–41 weeks. Polynomial regression lines for the 95th, 50th and 5th percentiles were calculated for the peak systolic velocity (PSV), time-averaged maximum velocity (TAMXV), PI and cerebroplacental ratio. Terms for calculating conditional reference intervals were established.*

Results *Based on 566 observations our new longitudinal reference ranges for fetal middle cerebral PSV, TAMXV and PI provided terms for calculating conditional reference intervals (i.e. predicting expected 95% confidence limits based on a previous measurement), and correspondingly for the cerebroplacental ratio ($n = 550$). The reference ranges were at some variance with those of previous cross-sectional studies. The narrow 95% confidence limits for the 5th and 95th percentiles ensured reliable ranges.*

Conclusions *We have established longitudinal reference ranges appropriate for the serial assessment of MCA blood velocities and PI and cerebroplacental ratio. Particularly the terms for calculating conditional ranges based on a previous observation make this system more appropriate for longitudinal monitoring than are cross-sectional data.*

INTRODUCTION

Evaluation of the cerebral blood flow in the fetus has become an integrated part of the assessment of high-risk pregnancies. The middle cerebral artery (MCA) has been studied extensively, and its Doppler recordings are incorporated regularly into the management of fetuses at risk of developing placental compromise and fetal anemia. In cases of intrauterine growth restriction (IUGR), clinical management is based primarily on the waveform analysis, i.e. the pulsatility index (PI), a low PI reflecting redistribution of cardiac output to the brain[1,2]. MCA peak systolic velocity (PSV) is used mainly for the prediction and management of fetal anemia[3–5]. However, high MCA-PSV has been shown to predict perinatal mortality better than does low MCA-PI in a group of IUGR fetuses[6]. The surveillance of fetuses at risk usually requires serial Doppler measurements, including that of the MCA.

The use of such parameters depends on appropriate reference ranges[7]. However, while several cross-sectional reference ranges are now in use[8–10], these are less suitable for serial observations because the appropriate reference ranges for serial measurements require longitudinal data[11]. A few longitudinal studies have been published, but they suffer from too few participants, or lack ranges for commonly used parameters, and none has developed conditional terms for repeat measurements[12–14].

Combining the Doppler waveform analysis of the MCA with that of the umbilical artery (UA) by a common cerebroplacental ratio, i.e. the ratio of their

Correspondence to: Dr C. Ebbing, Department of Obstetrics and Gynecology, Haukeland University Hospital, N-5021 Bergen, Norway (e-mail: cathrine.ebbing@molmed.uib.no)

Accepted: 13 June 2007

pulsatility indices has been suggested as a useful clinical simplification[15]. A low cerebroplacental ratio reflects redistribution of the cardiac output to the cerebral circulation and has been shown to improve accuracy in predicting adverse outcome compared with MCA or UA Doppler alone[16–20]. The ratio has increasingly been incorporated in the surveillance of the fetus at risk by repeating the assessment at intervals[21–23]. Reference ranges currently in use for the cerebroplacental ratio assessment[21,24–26] are based on cross-sectional studies and thus suitable for single observations[27,28]. For serial assessments, however, the reference ranges should be based on studies with a longitudinal design[11].

The purpose of this study was therefore to establish new longitudinal reference ranges for MCA and UA Doppler velocities and PI and the cerebroplacental ratio, and to provide terms for calculating conditional reference intervals suitable for individual serial measurements.

METHODS

The study population of 161 women was recruited from the low-risk population to a prospective longitudinal observational study of the cerebral, splanchnic and umbilical arterial circulation. Here we present the results of the MCA, UA and the cerebroplacental ratio part of that project. The regional committee for medical research ethics approved the study protocol (REK Vest no. 203.03), and all participants gave prior informed written consent. Gestational age was assessed by ultrasound head biometry at 17–20 weeks of gestation[29]. Multiple pregnancy, fetal abnormalities, obstetric history of previous complications such as pregnancy-induced hypertension, IUGR and placental abruption excluded participation, as did the presence of diabetes or any general chronic disease. None of the fetuses was at risk of developing anemia. Each woman was examined three to five times, at 3–5-week intervals over a gestational age range of 19–41 weeks. Complications in pregnancy and birth, birth weight, placental weight, Apgar score, age, gender and mode of delivery were noted. A pediatrician examined the neonates once during the first 3 postnatal days, and any abnormality was noted.

Doppler ultrasound measurements were recorded using a 2–5, 4–8 or 2–7-MHz transabdominal transducer (Voluson 730 Expert, GE Medical systems, Kretz Ultrasound, Zipf, Austria). The high-pass filter was set to 70 Hz and in the majority of the sessions the mechanical and thermal indices were below 1.1 and 0.9, respectively, and they were always kept below 1.9 and 1.5. The MCA was visualized using color flow mapping in an axial section of the brain. The Doppler beam was directed along the MCA, and the sample volume (median, 3 mm; mean, 3.5 mm; range, 1–7 mm) was placed over the proximal section where the MCA emerges from the circle of Willis. When the MCA in the near field could not be interrogated, we used the MCA of the opposite side. The recordings were acquired in the absence of fetal breathing or body movements over at least three uniform heart cycles. The Doppler waveforms were traced automatically, the PSV and time-averaged maximum velocity (TAMXV) were determined, and the PI was calculated according to Gosling and King[30].

The waveforms from the UA were obtained in a free-floating loop of the umbilical cord using a corresponding technique with the insonation in alignment with the direction of the vessel. The velocities and PI were entered into the statistics and the cerebroplacental ratio was calculated as the ratio of the MCA- and UA-PI.

The number of participants needed to construct percentiles based on cross-sectional collected data (Nc) has been calculated to be about 15 per gestational week[31]. The corresponding number for a longitudinally designed study (Nl) is Nc/D, were D is the 'design factor', which has been calculated as 2.3 in studies on fetal size[7]. Thus, observations over 20 weeks correspond to Nc = 300 and Nl = 130. An anticipated overall success rate of 80% for Doppler measurements increased the study group to 160 participants. Multilevel modeling was used in order to calculate mean and percentiles for the MCA Doppler velocities and PI according to gestational age. To achieve normal distribution of outcome variables, we used Box–Cox power transformation. Fractional polynomial regression models[11] were fitted to the data in order to construct mean curves for PSV, TAMXV and PI according to gestational age. We used multilevel modeling, where the first level was the variance between measurements within the same fetus and the second was the variance between the participating women. The choice of fixed and random components in the models was based on gain in likelihood. The confidence interval of the mean was calculated from the standard error (SE) of the mean. To obtain approximate SEs around the 5th and 95th percentiles, transformed observations ± 1.645 SD were regressed against gestational age. The regression lines equaled the 5th and 95th percentiles. The SE of the regression lines was used to obtain 95% confidence intervals around the 5th and 95th percentiles. The longitudinal design provided the necessary information for establishing terms for conditional reference values; i.e. for calculating the expected value and reference ranges conditional on a previous measurement[11]. Briefly, the conditional reference interval is calculated from the conditional mean and variance and the level-2 covariance; the level-1 covariance is assumed to be zero[11]. Formulae for conditional means and SDs are presented in Appendix S1 online. The intraobserver and interobserver variations were calculated with a paired sample *t*-test on the basis of 20 and 14 observations, respectively. The statistical analysis was carried out using SPSS (Statistical Package for the Social Sciences, SPSS Inc, Chicago, IL, USA) and the MlWin program (MlWin, Centre for Multilevel Modelling, University of Bristol, Bristol, UK).

RESULTS

Measurements were obtained from all 161 participants: one woman had one set of measurements, two had two

Table 1 Characteristics of the study population ($n = 161$)

Characteristic	*Median (range) or %*
Maternal age at inclusion (years)	29 (20–40)
Parity	1 (0–5)
Para 0 (%)	48.4
BMI at first visit (kg/m^2)	22.9 (18.1–40.8)
Smokers (%)	2.5
Gestational age at delivery (weeks)	40.4 (35.4–42.6)
Mode of delivery spontaneous (%)	77
Induction of labor (%)	5.6
Vacuum extraction (%)	3.7
Forceps (%)	3.1
Cesarean section (%)	10.6
Placental weight (g)	720 (350–1200)
Birth weight (g)	3700 (2260–4980)
Apgar score at 5 min < 7 (%)	0.62

BMI, body mass index.

sets, 18 had three, 126 had four and 14 had five. The median fetal age at first examination in the study was 23.3 (range, 19.3–28.4) weeks. Characteristics of the study population are presented in Table 1. All except three women were Caucasian. Two pregnancies were the result of *in-vitro* fertilization. Five women developed pre-eclampsia (3.1%) and three women delivered preterm (gestational age, 35–36 weeks). One fetus developed a supraventricular arrhythmia shortly before term, and another proved to have a single umbilical artery. There were 80 female and 81 male neonates. Participants who developed complications after enrolment in the study were not excluded.

We obtained measurements of the MCA in 604 of 633 sessions, giving a success rate of 95.4%. Measurements that required an angle correction larger than 10° were not included in the statistics. No angle correction was required in 540 recordings and in 26 the angle correction was $\leq 10°$, leaving 566 observations for statistical analysis. Unfavorable fetal position or movements were the reasons for not achieving an acceptable measurement.

The results showed notable individual variation with gestational age (Figure S1, available online). The results of the MCA-PSV and PI with fitted mean and reference intervals are presented in Figures 1 and 2. The corresponding gestational age-specific reference values for the 2.5th, 5th, 10th, 25th, 50th, 75th, 90th, 95th and 97.5th percentiles are presented in Tables 2 and 3 (Table S1 and Figure S2 for the TAMXV are available online). MCA velocities increased throughout the second half of pregnancy. The PSV increased less during the last 10 weeks compared with the TAMXV, resulting in a continuous decline in PI in the last 10 weeks of gestation. This gave the PI reference curve an inverted U-shape with a turning point at 30 weeks (Figure 2).

Terms for calculating conditional mean, SD and ranges are presented in Appendix S1 online. A clinical case illustrates the use of conditional ranges in serial measurements in Figure 3. A spreadsheet for calculating conditional mean and ranges (see Figure 3b) can be downloaded from the UOG website (Spreadsheet S1).

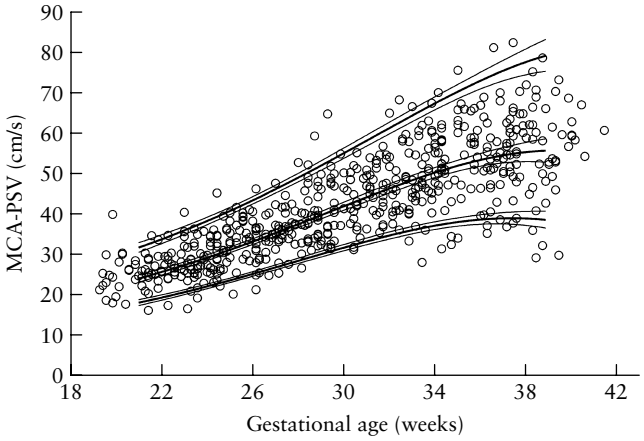

Figure 1 Peak systolic velocity (PSV) in the middle cerebral artery (MCA) in 161 low-risk pregnancies (566 observations) with 5th, 50th and 95th percentiles (thick lines) and their corresponding 95% CI (thin lines).

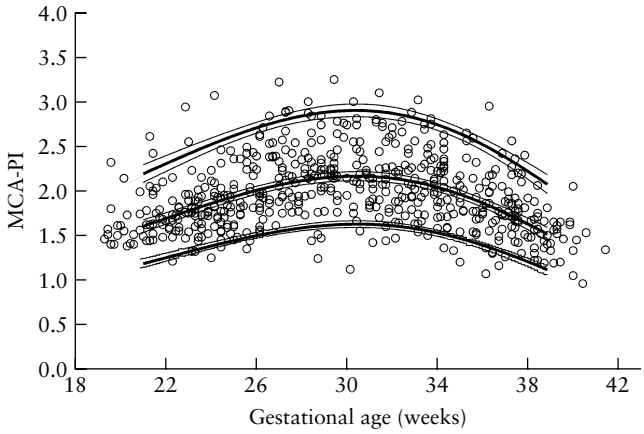

Figure 2 Pulsatility index (PI) in the middle cerebral artery (MCA) in 161 low-risk pregnancies (566 observations) with 5th, 50th and 95th percentiles (thick lines) and their corresponding 95% CI (thin lines).

The intra- and interobserver study showed acceptable reproducibility (Table 4).

We obtained 611 recordings of the UA velocity, and 550 complete sets of both MCA and UA observations. The angle of insonation of the UA was zero degrees in 582 observations and the median was 2 degrees in the remaining 29 (range 1–17). The UA-PI declined linearly from mean 1.15 at 21 weeks to 0.77 at 39 weeks (Figure 4). Individual observations of the umbilical artery peak systolic and time averaged maximum velocities and calculated 5th, 50th and 95th percentiles with 95% CI are presented in Figures 5 and 6.

The cerebroplacental ratio increased from mean 1.41 at 21 weeks of gestation to a peak 2.36 at 33 weeks, and then decreased to 1.97 at 39 weeks (Figure 7). The 95% CI for the 5th percentile at 21 and 39 weeks were 0.84–0.96 and 1.12–1.40 respectively, and correspondingly for the 95th percentile 2.00–2.23 and 2.74–3.07. Gestational age specific values for the 2.5th, 5th, 10th, 50th, 75th, 90th, 95th and 97.5th percentiles for the cerebroplacental ratio are presented in Table 5. In Figure 8 a clinical example

Table 2 Longitudinal reference ranges for the middle cerebral artery peak systolic velocity (in cm/s) based on 566 observations in 161 low-risk pregnancies

GA (weeks)	*Percentile*								
	2.5th	*5th*	*10th*	*25th*	*50th*	*75th*	*90th*	*95th*	*97.5th*
21	17.14	18.12	19.31	21.46	24.09	27.00	29.90	31.75	33.45
22	18.34	19.37	20.63	22.91	25.69	28.77	31.83	33.79	35.57
23	19.62	20.72	22.05	24.47	27.41	30.67	33.90	35.97	37.86
24	20.98	22.15	23.56	26.12	29.25	32.70	36.12	38.31	40.31
25	22.41	23.65	25.16	27.87	31.19	34.85	38.48	40.80	42.91
26	23.89	25.21	26.82	29.70	33.22	37.11	40.96	43.42	45.67
27	25.43	26.83	28.53	31.60	35.34	39.47	43.56	46.18	48.56
28	26.98	28.47	30.28	33.54	37.52	41.92	46.27	49.05	51.59
29	28.53	30.11	32.04	35.51	39.74	44.42	49.06	52.03	54.73
30	30.04	31.73	33.77	37.47	41.98	46.97	51.91	55.08	57.97
31	31.49	33.28	35.46	39.39	44.19	49.51	54.79	58.18	61.27
32	32.83	34.73	37.04	41.22	46.34	52.02	57.67	61.30	64.61
33	34.02	36.04	38.49	42.94	48.39	54.46	60.50	64.39	67.94
34	35.02	37.16	39.76	44.48	50.29	56.77	63.24	67.41	71.22
35	35.79	38.05	40.80	45.81	51.99	58.90	65.83	70.31	74.41
36	36.29	38.66	41.57	46.86	53.43	60.81	68.22	73.02	77.43
37	36.48	38.97	42.02	47.60	54.56	62.41	70.34	75.49	80.23
38	36.33	38.92	42.12	47.99	55.34	63.67	72.13	77.64	82.73
39	35.82	38.51	41.83	47.97	55.70	64.52	73.52	79.41	84.85

GA, gestational age.

Table 3 Longitudinal reference ranges for the middle cerebral artery pulsatility index based on 566 observations in 161 low-risk pregnancies

GA (weeks)	*Percentile*								
	2.5th	*5th*	*10th*	*25th*	*50th*	*75th*	*90th*	*95th*	*97.5th*
21	1.12	1.18	1.26	1.41	1.60	1.82	2.04	2.19	2.33
22	1.18	1.25	1.33	1.49	1.69	1.92	2.15	2.30	2.45
23	1.24	1.32	1.41	1.57	1.78	2.01	2.25	2.41	2.56
24	1.31	1.38	1.47	1.64	1.86	2.10	2.35	2.52	2.67
25	1.36	1.44	1.54	1.71	1.94	2.19	2.45	2.62	2.78
26	1.42	1.50	1.60	1.78	2.01	2.26	2.53	2.71	2.87
27	1.46	1.55	1.65	1.83	2.06	2.33	2.60	2.78	2.95
28	1.50	1.58	1.69	1.88	2.11	2.38	2.66	2.84	3.01
29	1.53	1.61	1.71	1.91	2.15	2.42	2.70	2.88	3.05
30	1.54	1.62	1.73	1.92	2.16	2.44	2.72	2.90	3.07
31	1.54	1.62	1.73	1.92	2.16	2.43	2.71	2.90	3.07
32	1.52	1.61	1.71	1.90	2.14	2.41	2.69	2.87	3.04
33	1.49	1.58	1.68	1.87	2.10	2.37	2.64	2.82	2.98
34	1.45	1.53	1.63	1.81	2.04	2.30	2.57	2.74	2.90
35	1.39	1.47	1.56	1.74	1.96	2.21	2.47	2.64	2.80
36	1.32	1.39	1.48	1.65	1.86	2.11	2.36	2.52	2.67
37	1.23	1.30	1.39	1.55	1.75	1.98	2.22	2.38	2.52
38	1.14	1.20	1.29	1.44	1.63	1.85	2.07	2.22	2.36
39	1.04	1.10	1.18	1.32	1.49	1.70	1.91	2.05	2.18

GA, gestational age.

of a high-risk pregnancy illustrates the calculation of conditional mean and ranges based on the first examination. All equations and terms are listed in the Appendix S2, and a spreadsheet for practical use is available online (Spreadsheet S2).

DISCUSSION

We have established longitudinal reference ranges for the MCA-PSV, -TAMXV and -PI and the cerebroplacental ratio suitable for use with serial measurements for fetal surveillance. We have also provided terms for calculating conditional reference ranges needed for such longitudinal monitoring (Appendix S1 and S2 online). In practical terms, this means that the expected 50th percentile and corresponding ranges can be adjusted according to the previous observation, as shown in the examples in Figures 3 and 8. Typically, the conditional 50th percentile is shifted in the same direction as the index value, and

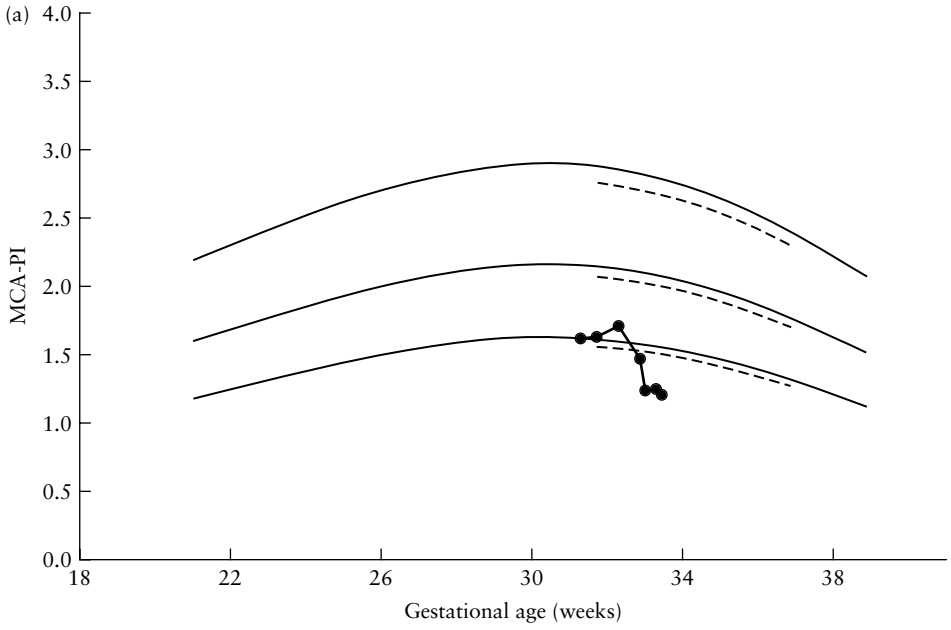

(b) PI

Type:			Unconditional percentiles								
	weeks	days	50	2.5	5	10	25	75	90	95	97.5
GA 1st visit:	31	2	2.16	1.54	1.62	1.73	1.92	2.43	2.71	0.92	3.06
PI 1st visit: 1.62											
GA today:	31	5	2.15	1.53	1.61	1.72	1.91	2.42	2.70	2.88	3.05
			Conditional percentiles								
			50	2.5	5	10	25	75	90	95	97.5
			2.07	1.48	1.56	1.66	1.84	2.33	2.59	2.76	2.92

Figure 3 (a) Serial measurements of pulsatility index (PI) in the middle cerebral artery (MCA) in a fetus under surveillance for intrauterine growth restriction (●), conditional mean and reference interval (5th and 95th percentiles) calculated from the first measurement (– – –) and unconditional 5th, 50th and 95th percentiles (——). (b) Spreadsheet for the calculation of unconditional and conditional mean and percentiles. In this example, the conditional mean and ranges for week 31 + 5 were calculated based on the measurement at 31 + 2 weeks. 1st visit, values from previous measurements; GA, gestational age.

Table 4 Intra- and interobserver variation in middle cerebral artery flow velocities and pulsatility index

	Paired differences									
				95% CI					*LOA*	
	Mean	*SD*	*SEM*	*Lower*	*Upper*	t	*d.f.*	P*	*Lower*	*Upper*
Intraobserver variation										
PSV	−0.24	1.14	0.26	−0.78	−0.31	−0.90	18	0.380	−2.47	2.00
TAMXV	−0.16	0.79	0.18	−0.54	0.22	−0.88	18	0.390	−1.71	1.39
PI	0.00	0.12	0.03	−0.06	0.06	0.04	18	0.970	−0.24	0.24
Interobserver variation										
PSV	1.46	7.44	1.99	−2.84	5.75	0.73	13	0.477	−13.13	16.04
TAMXV	0.29	2.98	0.80	−1.43	2.01	0.36	13	0.724	−5.55	6.13
PI	0.05	0.43	0.11	−0.20	0.30	0.43	13	0.674	−0.79	0.89

*Two-tailed significance. d.f., degrees of freedom; LOA, limits of agreement; PI, pulsatility index; PSV, peak systolic velocity; SEM, standard error of the mean; *t*, test value of the paired *t*-test; TAMXV, time-averaged maximum velocity.

the ranges are narrower compared with the unconditional ones. This provides an objective method of assessing changes in blood flow, which cross-sectional percentiles cannot achieve with validity.

The reference ranges we have established for the MCA differ slightly from those of cross-sectional studies. Our PSV values are slightly lower compared with those of Kurmanavicius *et al.*[9], especially after 34 weeks of gestation (Figure 9). Compared with Mari *et al.*[10], our mean values are higher from the 28th to the 35th week of gestation. Our finding that the increase in velocity is blunted after 36 weeks of gestation is in line with

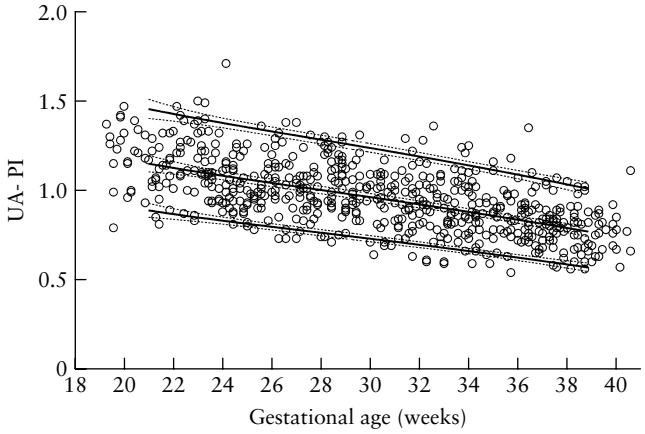

Figure 4 Umbilical artery pulsatility index (UA-PI) (free loop) in 161 low-risk pregnancies (611 observations) with 5th, 50th and 95th percentiles (solid lines) and their corresponding 95% CI (dashed lines).

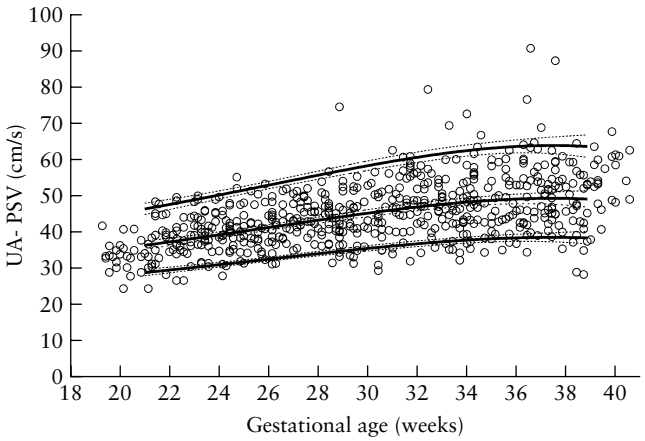

Figure 5 Umbilical artery peak systolic velocity (UA-PSV) (free loop) in 161 low-risk pregnancies (611 observations) with 5th, 50th and 95th percentiles (solid lines) and their corresponding 95% CI (dashed lines).

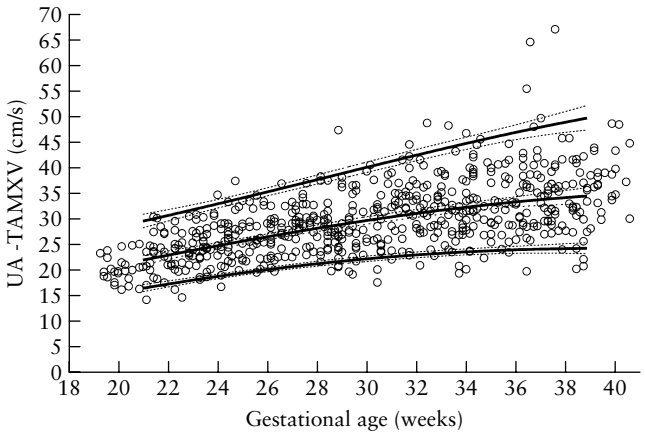

Figure 6 Umbilical artery time averaged maximum velocity (UA-TAMXV) (free loop) in 161 low-risk pregnancies (611 observations) with 5th, 50th and 95th percentiles (solid lines) and their corresponding 95% CI (dashed lines).

another small longitudinal study[14], and probably reflects a physiological reduction of vascular impedance.

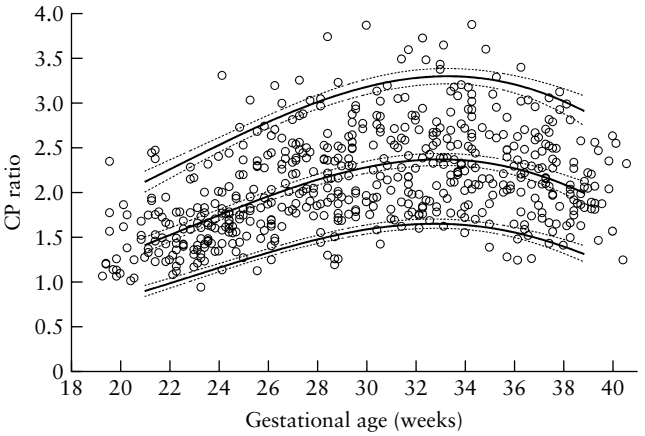

Figure 7 Cerebroplacental ratio (CP ratio) in 161 low-risk pregnancies (550 observations) with 5th, 50th and 95th percentiles (solid lines) and their corresponding 95% CI (dashed lines).

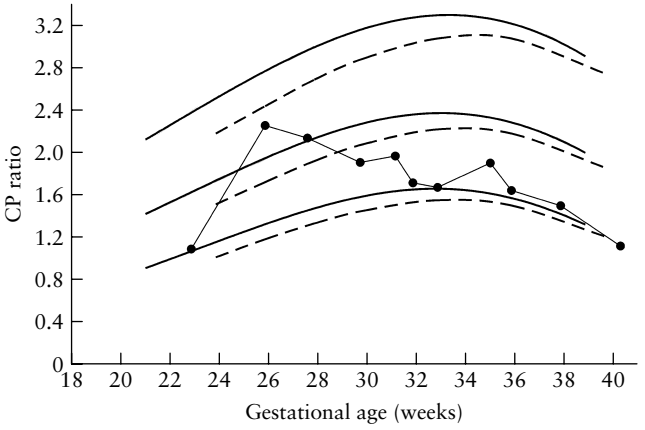

Figure 8 Serial measurements of the cerebroplacental ratio (CP ratio) in a pregnancy at risk of intrauterine growth restriction (●). Based on Doppler measurements and cardiotocography she was delivered acutely at term of a girl weighing < 2.5th percentile (2250 g). Conditional percentiles (– – –) were calculated from the first observation at gestational age 22.9 weeks. Unconditional reference ranges are also shown (——). The necessary terms for calculating the conditional mean and ranges are found in Appendix S2, and a spreadsheet for practical use is available online.

The method of using multiples of the median for the MCA-PSV has been extremely successful in identifying fetal anemia using single observations[5]. To further improve surveillance, Detti *et al.*[32] suggested the steepness of a regression line constructed from three successive measurements would indicate the severity of the development. However, to take full advantage of serial measurements, the calculation of longitudinally conditioned ranges, such as in our present study, offers a more statistically sound basis for predicting a deviation from normal development.

Our parabolic curves for PI in the MCA are higher than are those of Bahlmann[8], and somewhat lower than are those of Mari and Deter[2] (Figure 10). However, all the compared reference curves had similar values for the last weeks of pregnancy. Study methodology was expected to cause differences between our results

Table 5 Longitudinal reference ranges for the cerebroplacental Doppler ratio (formed as a ratio of the middle cerebral and umbilical artery pulsatility index) based on 550 observations in 161 low-risk pregnancies

GA (weeks)	*Percentile*								
	2.5th	*5th*	*10th*	*25th*	*50th*	*75th*	*90th*	*95th*	*97.5th*
21	0.82	0.90	1.00	1.18	1.41	1.67	1.94	2.11	2.27
22	0.90	0.98	1.09	1.28	1.52	1.79	2.07	2.25	2.42
23	0.98	1.07	1.18	1.38	1.63	1.92	2.20	2.39	2.56
24	1.06	1.16	1.27	1.48	1.74	2.04	2.33	2.52	2.70
25	1.14	1.24	1.36	1.58	1.85	2.15	2.46	2.65	2.83
26	1.22	1.32	1.45	1.67	1.95	2.26	2.58	2.78	2.96
27	1.30	1.40	1.53	1.76	2.05	2.37	2.69	2.90	3.08
28	1.37	1.47	1.60	1.84	2.14	2.46	2.79	3.00	3.19
29	1.42	1.53	1.67	1.91	2.21	2.55	2.88	3.09	3.29
30	1.47	1.58	1.72	1.97	2.28	2.62	2.95	3.17	3.37
31	1.51	1.62	1.76	2.01	2.32	2.67	3.01	3.23	3.43
32	1.53	1.64	1.78	2.04	2.35	2.70	3.05	3.27	3.47
33	1.53	1.65	1.79	2.05	2.36	2.72	3.07	3.29	3.49
34	1.52	1.63	1.78	2.04	2.35	2.71	3.06	3.29	3.49
35	1.49	1.60	1.74	2.00	2.32	2.68	3.03	3.26	3.46
36	1.44	1.55	1.69	1.95	2.27	2.62	2.97	3.20	3.41
37	1.37	1.48	1.62	1.88	2.19	2.54	2.89	3.12	3.33
38	1.29	1.40	1.53	1.78	2.09	2.44	2.79	3.01	3.22
39	1.19	1.29	1.43	1.67	1.97	2.31	2.66	2.88	3.09

GA, gestational age.

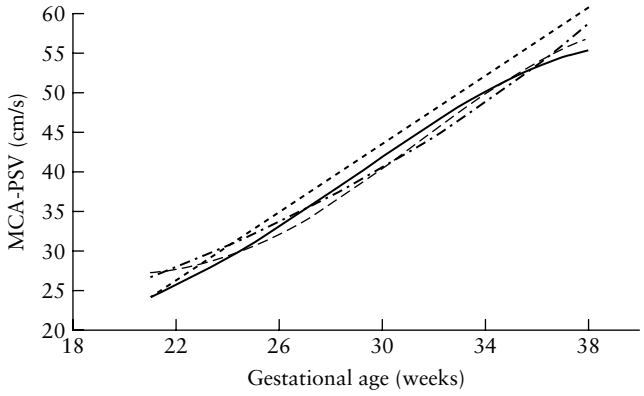

Figure 9 Mean peak systolic velocity (PSV) in the middle cerebral artery (MCA) in our present longitudinal study (——) compared with that in the cross-sectional studies of Kurmanavicius *et al.*[9] (·····), Mari *et al.*[10] (·–·–) and Bahlmann[8] (– – –).

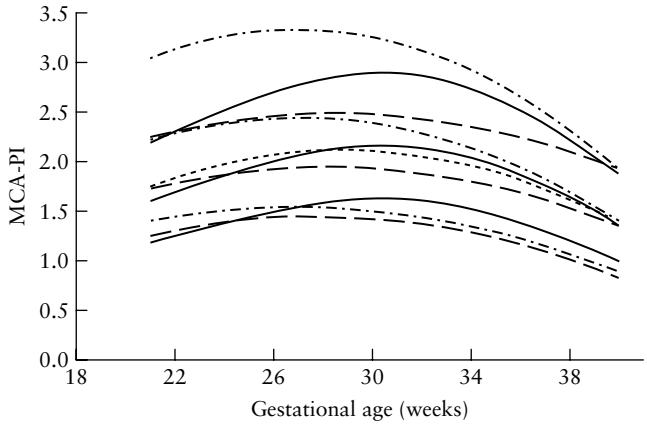

Figure 10 Reference ranges (5th, 50th and 95th percentiles) for pulsatility index (PI) in the middle cerebral artery (MCA) in our present longitudinal study (——) compared with those in the cross-sectional studies of Bahlmann[8] (— –), Mari and Deter[2] (mean and predicted values, ·–·–) and Baschat[25] (mean, - - - -).

and those of others. The study on MCA-PSV by Mari *et al.*[10] was retrospective and included 135 participants at 15–42 gestational weeks, whilst the study by Mari and Deter[2] on PI included 128 participants, which, according to Royston and Altman[7], is too small a number from which to construct reliable reference ranges. The study by Kurmanavicius *et al.*[9] on MCA-PSV had few observations for the last weeks of pregnancy, whilst Bahlmann[8] had few observations in the early weeks and excluded fetuses with biometric parameters of the head and abdomen outside the 90% reference interval. The 95% CIs for the 5th, 50th and 95th percentiles presented here (Figures 1 and 2) assured reliable ranges for clinical use, both for single measurements and for longitudinal surveillance, provided that the same technique of measurement is applied.

The variability of velocities and indices has been shown to be larger and the PI higher in the distal portion compared with the proximal third of the MCA[33–36]. We therefore standardized our technique to record at the origin of the vessel at the circle of Willis, and we recommend an insonation aligned accurately along the vessel. In our hands, this technique gave reproducible results, with no difference between observers and acceptable limits of agreement (Table 4). We measured TAMXV because this parameter is robust and is influenced less by interference compared with weighted mean velocity[37]. A retrospective study by Bartha *et al.*[38] showed that time-averaged weighted mean velocity is altered earlier than is PSV when

anemia develops. We assume that TAMXV could be a corresponding useful parameter for surveillance of fetuses at risk of anemia.

Our longitudinal reference ranges for the cerebroplacental ratio are suitable both for single observations (Figure 7 and Table 5) and for serial measurements (when using the corresponding terms as shown in Figure 8). The number of included participants and observations ensured reliable ranges as reflected in the narrow 95% CI for the 5th, 50th and 95th percentiles (Figure 7). Our results differ somewhat from reference curves based on cross-sectional data (Figure 11)[21,24,25]. Low numbers of observations (82)[21], or unknown method of the MCA measurement[24], and different site of MCA recording (i.e. distal section of the vessel[25] rather than the recommended proximal site,[33,36,39]) may have contributed to the variation between curves. The difference in design and analysis was also expected to cause visible differences. When comparing our results of the UA velocities with those of another longitudinal study with corresponding design and insonation technique[40] we found minor differences, while the results of the UA-PI were identical, which was a reassuring external validation.

Different approaches have been applied in order to interpret cerebroplacental ratio results, a fixed cut-off at = 1.08[16] or cross-sectional reference ranges according to gestational age[21,24,25]. Curiously, one study showed that the use of a uniform cut-off for the second half of pregnancy (Figure 11) predicts adverse outcome equally well compared with using reference ranges according to gestational age[23]. Cerebroplacental ratio performs differently before and after 34 weeks of gestation[21,23], which may reflect differences in physiologic responses with advancing development. We believe that by introducing our new longitudinal reference ranges and individually calculated conditional ranges for repeat observations, the clinical application of the cerebroplacental ratio is more in line with physiologic development.

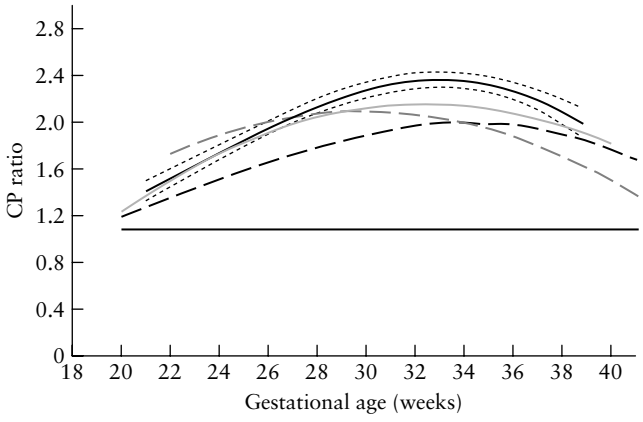

Figure 11 The 50th percentile for the cerebroplacental ratio (CP ratio) established in the present longitudinal study (——) with 95% CI (·····) compared with cross-sectional studies: Baschat and Gembruch[25] (——), Arduini and Rizzo[24] (– – –), Bahado-Singh *et al.*[21] (— — —), and categorical cut-off 1.08 (——) according to Gramellini *et al.*[16].

The hypoxic index (amplitude of flow redistribution × duration in days) was introduced by Arbeille *et al.* in order to describe the cumulative intensity and duration of hypoxia or redistribution of flow to the brain in fetuses at risk[41]. The approach seems intricate and time-consuming. Our alternative, using a spreadsheet to calculate conditional ranges for repeat assessments of the cerebroplacental ratio appears quicker and is individually adjusted.

Our aim was to construct reference ranges for the second half of pregnancy. However, we obtained insufficient numbers of observations for constructing reliable ranges for gestational age below 21 and above 39 weeks (Figures 1, 2 and 7). A considerably larger study population would be needed to cover the period of 40–42 weeks of gestation adequately, a period when a substantial proportion of the women has delivered. We also aimed to examine each participant at least three times, but one woman had only one examination, and two had two examinations. Nevertheless, the study population showed overall excellent compliance.

The question may be raised as to whether our reference ranges were applicable to the background population. The study was based on a population that was at low risk. The gestational age at delivery (median, 40.4 weeks), average birth weight (mean 3660 g[42]) and Cesarean section rate (approximately 12%) were in accordance with that of the background population. By not excluding participants who developed complications, we avoided selection towards the supernormal and believe that our reference ranges can be applied in a general population.

It can be argued that the study population was rather uniformly of Nordic ethnicity and that the reference ranges may not be equally applicable in different ethnic populations. Apart from birth weight and placental size, it has been shown that the effect of ethnic and socioeconomic differences is likely to be small[43]. Since our data are longitudinally designed, conditional reference ranges can be calculated for any fetus based on a previous measurement.

In short, we have established new reference ranges for MCA-PSV, -TAMXV and -PI as well as for the cerebroplacental ratio based on longitudinal observations and have provided terms for calculating the conditional reference ranges that are needed for longitudinal monitoring.

ACKNOWLEDGMENT

The study was supported financially by the Western Norway Regional Health Authority (Grant no 911160).

REFERENCES

1. Wladimiroff JW, Tonge HM, Stewart PA. Doppler ultrasound assessment of cerebral blood-flow in the human-fetus. *Br J Obstet Gynaecol* 1986; **93**: 471–475.
2. Mari G, Deter RL. Middle cerebral-artery flow velocity waveforms in normal and small-for-gestational-age fetuses. *Am J Obstet Gynecol* 1992; **166**: 1262–1270.

3. Zimmermann R, Durig P, Carpenter RJ, Mari G. Longitudinal measurement of peak systolic velocity in the fetal middle cerebral artery for monitoring pregnancies complicated by red cell alloimmunisation: a prospective multicentre trial with intention-to-treat. *BJOG* 2002; **109**: 746–752.
4. Oepkes D, Seaward PG, Vandenbussche FPHA, Windrim R, Kingdom J, Beyene J, Kanhai HH, Ohlsson A, Ryan G; DIAMOND Study Group. Doppler ultrasonography versus amniocentesis to predict fetal anemia. *N Engl J Med* 2006; **355**: 156–164.
5. Mari G. Noninvasive diagnosis by Doppler ultrasonography of fetal anemia due to maternal red-cell alloimmunization. *N Engl J Med* 2000; **342**: 9–14.
6. Mari G, Hanif F, Kruger M, Cosmi E, Santolaya-Forgas J, Treadwell M. Middle cerebral artery peak systolic velocity: a new Doppler parameter in the assessment of growth restricted fetuses. *Ultrasound Obstet Gynecol* 2007; **29**: 310–316.
7. Royston P, Altman DG. Design and analysis of longitudinal studies of fetal size. *Ultrasound Obstet Gynecol* 1995; **6**: 307–312.
8. Bahlmann F. Blood flow velocity waveforms of the fetal middle cerebral artery in a normal population: reference values from 18 weeks to 42 weeks of gestation. *J Perinat Med* 2002; **30**: 490–501.
9. Kurmanavicius J, Streicher A, Wright EM, Wisser J, Muller R, Royston P, Huch R, Huch A, Zimmermann R. Reference values of fetal peak systolic blood flow velocity in the middle cerebral artery at 19–40 weeks of gestation. *Ultrasound Obstet Gynecol* 2001; **17**: 50–53.
10. Mari G, Adrignolo A, Abuhamad AZ, Pirhonen J, Jones DC, Ludomirsky A, Copel JA. Diagnosis of fetal anemia with Doppler ultrasound in the pregnancy complicated by maternal blood-group immunization. *Ultrasound Obstet Gynecol* 1995; **5**: 400–405.
11. Royston P. Calculation of unconditional and conditional reference intervals for fetal size and growth from longitudinal measurements. *Stat Med* 1995; **14**: 1417–1436.
12. Arstrom K, Eliasson A, Hareide JH, Marsal K. Fetal blood velocity waveforms in normal pregnancies – a longitudinal-study. *Acta Obstet Gynecol Scand* 1989; **68**: 171–178.
13. Harrington K, Carpenter RG, Nguyen M, Campbell S. Changes observed in Doppler studies of the fetal circulation in pregnancies complicated by preeclampsia or the delivery of a small-for-gestational-age baby. 1. Cross-sectional analysis. *Ultrasound Obstet Gynecol* 1995; **6**: 19–28.
14. Meerman RJ, Vanbel F, Vanzwieten PHT, Oepkes D, Denouden L. Fetal and neonatal cerebral blood velocity in the normal fetus and neonate – a longitudinal Doppler ultrasound study. *Early Hum Dev* 1990; **24**: 209–217.
15. Arbeille P, Roncin A, Berson M, Patat F, Pourcelot L. Exploration of the fetal cerebral blood-flow by duplex doppler linear-array system in normal and pathological pregnancies. *Ultrasound Med Biol* 1987; **13**: 329–337.
16. Gramellini D, Folli MC, Raboni S, Vadora E, Merialdi A. Cerebral-umbilical Doppler ratio as a predictor of adverse perinatal outcome. *Obstet Gynecol* 1992; **79**: 416–420.
17. Harrington K, Thompson MO, Carpenter RG, Nguyen M, Campbell S. Doppler fetal circulation in pregnancies complicated by pre-eclampsia or delivery of a small for gestational age baby: 2. Longitudinal analysis. *Br J Obstet Gynaecol* 1999; **106**: 453–466.
18. Hershkovitz R, Kingdom JCP, Geary M, Rodeck CH. Fetal cerebral blood flow redistribution in late gestation: identification of compromise in small fetuses with normal umbilical artery Doppler. *Ultrasound Obstet Gynecol* 2000; **15**: 209–212.
19. Sterne G, Shields LE, Dubinsky TJ. Abnormal fetal cerebral and umbilical Doppler measurements in fetuses with intrauterine growth restriction predicts the severity of perinatal morbidity. *J Clin Ultrasound* 2001; **29**: 146–151.
20. Vergani P, Roncaglia N, Locatelli A, Andreotti C, Crippa I, Pezzullo JC, Ghidini A. Antenatal predictors of neonatal outcome in fetal growth restriction with absent end-diastolic flow in the umbilical artery. *Am J Obstet Gynecol* 2005; **193**: 1213–1218.
21. Bahado-Singh RO, Kovanci E, Jeffres A, Oz U, Deren O, Copel J, Mari G. The Doppler cerebroplacental ratio and perinatal outcome in intrauterine growth restriction. *Am J Obstet Gynecol* 1999; **180**: 750–756.
22. Hecher K, Spernol R, Stettner H, Szalay S. Potential for diagnosing imminent risk to appropriate-for-gestational-age and small-for-gestational-age fetuses by Doppler sonographic examination of umbilical and cerebral arterial blood-flow. *Ultrasound Obstet Gynecol* 1992; **2**: 266–271.
23. Odibo AO, Riddick C, Pare E, Stamilio DM, Macones GA. Cerebroplacental Doppler ratio and adverse perinatal outcomes in intrauterine growth restriction. *J Ultrasound Med* 2005; **24**: 1223–1228.
24. Arduini D, Rizzo G. Normal values of pulsatility index from fetal vessels – a cross-sectional study on 1556 healthy fetuses. *J Perinat Med* 1990; **18**: 165–172.
25. Baschat AA, Gembruch U. The cerebroplacental Doppler ratio revisited. *Ultrasound Obstet Gynecol* 2003; **21**: 124–127.
26. Kurmanavicius J, Florio I, Wisser J, Hebisch G, Zimmermann R, Muller R, Huch R, Huch A. Reference resistance indices of the umbilical, fetal middle cerebral and uterine arteries at 24–42 weeks of gestation. *Ultrasound Obstet Gynecol* 1997; **10**: 112–120.
27. Royston P, Wright EM. How to construct 'normal ranges' for fetal variables. *Ultrasound Obstet Gynecol* 1998; **11**: 30–38.
28. Altman DG, Chitty LS. Design and analysis of studies to derive charts of fetal size. *Ultrasound Obstet Gynecol* 1993; **3**: 378–384.
29. Johnsen SL, Rasmussen S, Sollien R, Kiserud T. Fetal age assessment based on ultrasound head biometry and the effect of maternal and fetal factors. *Acta Obstet Gynecol Scand* 2004; **83**: 716–723.
30. Gosling R, King D. Ultrasound angiology. In *Arteries and Veins*, Macus A, Adamson J (eds). Churchill-Livingstone: Edinburgh, 1975; 61–98.
31. Altman DG, Chitty LS. Charts of Fetal Size. 1. Methodology. *Br J Obstet Gynaecol* 1994; **101**: 29–34.
32. Detti L, Mari G, Akiyama M, Cosmi E, Moise KJ, Stefor T, Conaway M, Deter R. Longitudinal assessment of the middle cerebral artery peak systolic velocity in healthy fetuses and in fetuses at risk for anemia. *Am J Obstet Gynecol* 2002; **187**: 937–939.
33. Clerici G, Luzietti R, Cutuli A, Di Renzo GC. Cerebral hemodynamics and fetal behavioral states. *Ultrasound Obstet Gynecol* 2002; **19**: 340–343.
34. Abel DE, Grambow SC, Brancazio LR, Hertzberg BS. Ultrasound assessment of the fetal middle cerebral artery peak systolic velocity: a comparison of the near-field versus far-field vessel. *Am J Obstet Gynecol* 2003; **189**: 986–989.
35. Locci M, Nazzaro G, Deplacido G, Montemagno U. Fetal cerebral hemodynamic adaptation – a progressive mechanism – pulsed and color Doppler evaluation. *J Perinat Med* 1992; **20**: 337–343.
36. Hsieh YY, Chang CC, Tsai HD, Tsai CH. Longitudinal survey of blood flow at three different locations in the middle cerebral artery in normal fetuses. *Ultrasound Obstet Gynecol* 2001; **17**: 125–128.
37. Evans DH, Schlindwein FS, Levene MI. The relationship between time averaged intensity weighted mean velocity, and time averaged maximum velocity in neonatal cerebral arteries. *Ultrasound Med Biol* 1989; **15**: 429–435.
38. Bartha JL, Abdel-Fattah SA, Hunter A, Denbow M, Kyle P, Soothill PW. Optimal interval between middle cerebral artery velocity measurements when monitoring pregnancies complicated by red cell alloimmunization. *Fetal Diagn Ther* 2006; **21**: 22–25.

39. Mari G, Abuhamad AZ, Cosmi E, Segata M, Altaye M, Akiyama M. Middle cerebral artery peak systolic velocity – Technique and variability. *J Ultrasound Med* 2005; **24**: 425–430.
40. Acharya G, Wilsgaard T, Berntsen GKR, Maltau JM, Kiserud T. Reference ranges for serial measurements of umbilical artery Doppler indices in the second half of pregnancy. *Am J Obstet Gynecol* 2005; **192**: 937–944.
41. Arbeille P, Perrotin F, Salihagic A, Sthale H, Lansac J, Platt LD. Fetal Doppler hypoxic index for the prediction of abnormal fetal heart rate at delivery in chronic fetal distress. *Eur J Obstet Gynecol Reprod Biol* 2005; **121**: 171–177.
42. Skjaerven R, Gjessing HK, Bakketeig LS. Birthweight by gestational age in Norway. *Acta Obstet Gynecol Scand* 2000; **79**: 440–449.
43. Jacquemyn Y, Verdonk P. Doppler ultrasound of the feto-maternal circulation: a preliminary study on differences between ethnic groups. *Clin Exp Obstet Gynecol* 2001; **28**: 277–279.

SUPPLEMENTARY MATERIAL ON THE INTERNET

The following material is available from the Journal homepage:

http://www.interscience.wiley.com/jpages/0960-7692/suppmat (restricted access)

Figure S1 Raw data (566 observations) for the middle cerebral artery peak systolic blood velocity (PSV) in 161 low-risk pregnancies, illustrating the longitudinal variation in the population. Each line represents results from one fetus.

Figure S2 Individual observations ($n = 566$) of time-averaged maximum velocity (TAMXV) in the middle cerebral artery in 161 low-risk pregnancies, with fitted 5^{th}, 50^{th} and 95^{th} percentiles. Thin lines represent 95% confidence limits for these percentiles.

Table S1 Longitudinal reference ranges for the middle cerebral artery time-averaged maximum velocity (cm/s) based on 566 observations in 161 low-risk pregnancies.

Spreadsheet S1 Excel spreadsheet for calculating unconditional and conditional ranges for serial measurements of middle cerebral artery blood flow velocities and pulsatility index.

Spreadsheet S2 Excel spreadsheet for calculating unconditional and conditional ranges for serial measurements of cerebroplacental pulsatility ratio.

Appendix S1 Formulae for calculating conditional means, reference ranges and SDs for serial measurements of middle cerebral artery blood flow velocities and pulsatility index.

Appendix S2 Formulae for calculating conditional means, reference ranges and SD for serial measurements of umbilical artery blood flow velocities and pulsatility index and the cerebroplacental ratio.

